

HYPERSCANNING OF BRAIN-TO-BRAIN INTERACTIONS IN THE
PREFRONTAL CORTEX DURING A JOINT SENTENCE READING TASK: AN
OPTICAL BRAIN IMAGING STUDY

A THESIS SUBMITTED TO
THE GRADUATE SCHOOL OF INFORMATICS OF
THE MIDDLE EAST TECHNICAL UNIVERSITY
BY

ERDİNÇ İŞBİLİR

IN PARTIAL FULFILLMENT OF THE REQUIREMENTS FOR THE DEGREE
OF DOCTOR OF PHILOSOPHY
IN
THE DEPARTMENT OF COGNITIVE SCIENCE

SEPTEMBER 2016

**HYPERSCANNING OF BRAIN-TO-BRAIN INTERACTIONS IN THE
PREFRONTAL CORTEX DURING A JOINT SENTENCE READING TASK:
AN OPTICAL BRAIN IMAGING STUDY**

Submitted by ERDİNÇ İŞBİLİR in partial fulfillment of the requirements for the degree of **Doctor of Philosophy in The Department of Cognitive Science Middle East Technical University** by,

Prof. Dr. Nazife Baykal
Director, **Graduate School of Informatics**

Assist. Prof. Dr. Cengiz Acartürk
Head of Department, **Cognitive Science**

Assist. Prof. Dr. Murat Perit Çakır
Supervisor, **Cognitive Science**

Examining Committee Members:

Assist. Prof. Dr. Cengiz Acartürk
Cognitive Science, Middle East
Technical University

Assist. Prof. Dr. Murat Perit Çakır
Cognitive Science, Middle East Technical University

Assist. Prof. Dr. Nart Bedin Atalay
Psychology Department, TOBB ETÜ
Economy and Technology University

Prof. Dr. Kürşat Çağıltay
Computer Education and Instructional Technology,
Middle East Technical University

Assist. Prof. Dr. Murat Ulubay
Business School, Yıldırım Beyazıt
University

Date:

09.09.2016



I hereby declare that all information in this document has been obtained and presented in accordance with academic rules and ethical conduct. I also declare that, as required by these rules and conduct, I have fully cited and referenced all material and results that are not original to this work.

Name, Last name: Erdinç İşbilir

Signature : _____

ABSTRACT

HYPERSCANNING OF BRAIN-TO-BRAIN INTERACTIONS IN THE PREFRONTAL CORTEX DURING A JOINT SENTENCE READING TASK: AN OPTICAL BRAIN IMAGING STUDY

İşbilir, Erdinç

Ph.D., Department of Cognitive Sciences

Supervisor: Assist. Prof. Dr. Murat Perit Çakır

September 2016, 113 pages

A functioning and developing human society is possible due to successful communication and joint actions between the members of the group that constitute the society at large. Synchrony among members of a society is widespread and is seen in many distinct areas such as military parades and political activities as well as in the daily lives of people such as singing together, dancing and simply taking turns during a conversation. Although such synchronous behavior between people are central to their daily lives, the behavioral and neural correlates of such behavior have only recently been studied in the context of cognitive neuroscience. With the recent advent of the new neuroimaging methods such as functional near infrared spectroscopy (fNIRS) that are both portable and cheaper compared to more traditional methods such as fMRI, many researchers have started to investigate the neural correlates of social interactions in terms of synchronization of neural activations across the interlocutors' brains. In this regard, hyperscanning, which is defined as the simultaneous measurement of multiple people's brain activity, has emerged as a central method in social neuroscience studies. Motivated by these developments, in this study two speakers' brain activity at their prefrontal cortices were measured during a joint sentence reading task in Turkish in order to investigate brain-to-brain interactions in different behavioral coupling conditions. The results of this dissertation indicated that pairs showed different levels of behavioral synchrony in relation to different levels of auditory (self, both, other) and block conditions (match, mismatch). Moreover, in terms of brain-to-brain interactions the results indicated a significant coherence increase bilaterally in prefrontal cortex, especially in dorsolateral prefrontal cortex, dorsomedial prefrontal cortex and right-superior frontal cortex, which are regions implicated in related social neuroscience literature.

Keywords: brain-to-brain coupling, hyperscanning, fNIRS, two-person neuroscience, neurolinguistics.

ÖZ

HİPERTARAMA YÖNTEMİYLE ORTAK CÜMLE OKUMA GÖREVİNDE BEYİN-BEYİN ETKİLEŞİMLERİNİN ÖNBİYİN KORTEKSİNDE İNCELENMESİ: OPTİK BEYİN GÖRÜNTÜLEME ÇALIŞMASI

İşbilir, Erdinç

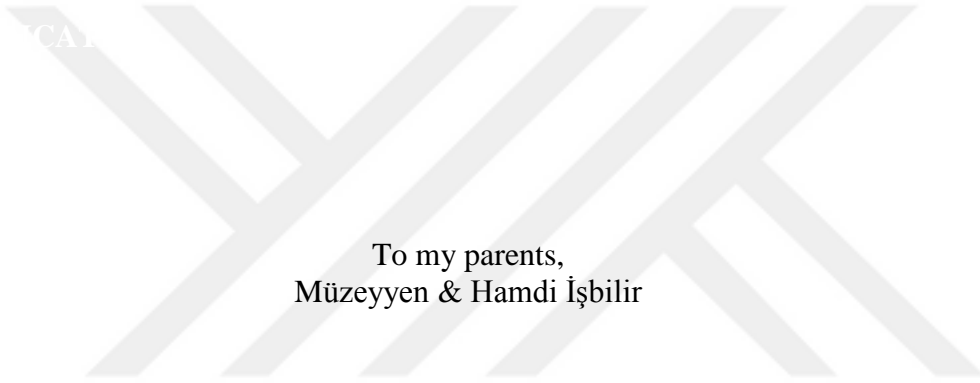
Doktora, Bilişsel Bilimler Bölümü

Tez Yöneticisi: Yrd. Doç. Dr. Murat Perit Çakır

Eylül 2016, 113 sayfa

Üretken ve gelişen bir toplumun ortaya çıkmasında o toplumu oluşturan bireylerin arasındaki başarılı iletişim ve ortak eylemler oldukça önemlidir. İnsanlar arasındaki eşgüdüm bir toplumun askeri ve politik alanları gibi farklı kademelerinin yanısıra insanların günlük hayatlarında birlikte söyledikleri şarkı, birlikte yaptıkları dans ve en basit örnek olarak karşılıklı olarak sırayla etkileşime girdikleri durumlar (ör. karşılıklı konuşma ve dinleme) gibi toplumsal etkileşimin farklı kademelerinde görülmektedir. İnsanlar arasındaki bu tür eşgüdüm davranışlarının günlük yaşamda merkezi bir yeri olmasına rağmen, bu eşgüdümün davranışsal ve sinirbilimsel temelleri bilişsel nörobilim bağlamında ancak yakın zamanda ele alınmaya başlamıştır. Geleneksel nörogörüntüleme yöntemlerinden fMRI ile karşılaştırıldığında daha ekonomik ve portatif olan işlevsel yakın kızılötesi tayföçümü (fNIRS) gibi yeni nörogörüntüleme yöntemlerinin yakın zamanda geliştirilmesiyle birçok araştırmacı sosyal etkileşim sırasında gerçekleşen eşgüdümün nöral izdüşümlerini araştırmaya başlamıştır. Bu bağlamda iki kişinin beyin aktivasyonlarının aynı anda ölçülmesi olarak tanımlanan hipertarama (ing. hyperscanning) yöntemi iki-kişilik sinirbilim çalışmalarında merkezi bir yöntem olarak öne sürülmüştür. Bu çalışmalar ışığında, bu doktora tezinde iki kişinin ön beyin bölgelerindeki aktivasyonlar kişilerin beyinleri arasındaki etkileşimlerin ve davranışsal eşgüdümün ortaya çıkarılması için ortak Türkçe cümle okuma görevlerinde ölçülmüştür. Bu çalışmanın sonuçları çalışmanın işitsel (kendi, her ikisi, diğeri) ve cümle durumları (aynı, farklı) ile uyumlu yönde davranışsal eşgüdüm gösterdiğini ortaya koymuştur. Ayrıca, beyinler arası etkileşim açısından bu çalışmanın sonuçları ön beyin korteksinde iki taraflı ve özellikle sosyal nörobilim çalışmalarında ortaya konulmuş dorsolateral prefrontal korteks, dorsomedial prefrontal korteks ve sağ-superior frontal korteks bölgelerinde uyumluluk artışı olduğunu göstermiştir.

Anahtar Sözcükler: beyinler arası eşleşme, hipertarama, fNIRS, iki-kişili sinirbilim, nörodilbilim.



To my parents,
Müzeyyen & Hamdi İşbilir

ACKNOWLEDGMENTS

There are many people that I would like to express my deepest gratitude for their support, guidance, encouragement and motivation throughout the years that lead to this dissertation. This thesis would not have been possible without their contributions.

First of all, I would like to express my deepest gratitude to my thesis supervisor Assist. Prof. Dr. Murat Perit akır. His guidance, encouragement, motivation, outstanding academic knowledge and support during all stages of my doctorate studies is an excellent example for a supervisor and one that I also would like to take as a role model and an ideal example for my personal as well as academic development. This dissertation from its conception as a research question to its current contribution to the literature was only possible with the productive discussions that I had with my supervisor, his contributions to all aspects of the research and his unique guidance through the difficulties of a dissertation study.

Besides my supervisor, I also would like to thank my thesis committee members Prof. Dr. Krřat ađiltay and Assist. Prof. Dr. Cengiz Acartrk for their valuable feedbacks, suggestions, insightful comments and continuous support in thesis committee meetings that significantly facilitated the scientific development of this dissertation. In addition, I also would like to thank the members of the thesis examining committee, Assist. Prof. Dr. Nart Bedin Atalay and Assist. Prof. Dr. Murat Ulubay, for their important questions, suggestions and support that significantly contributed to the final shape of this study.

In addition to my thesis supervisor, thesis committee and examining members, I would like to express my sincere thanks to Prof. Dr. Fred Cummins for his tremendous contributions to the technical phases of this study. His detailed explanations, guidance and sharing of his knowledge and data analysis algorithms were of great importance in shaping the scope of this dissertation.

I am also thankful to many friends of mine including Dr. Tuna akar for his invaluable help in all phases of this dissertation from basic setup of the experimental design to data analysis, Asiye ztrk for her help in finding participants for the study and ađatay Tařçı for solving hard problems in this dissertation by utilizing his excellent skills in programming.

Besides, I also would like to give my heartfelt thanks to my dearest friends řule Alıcı, Mehmet řen, Gzde Kaplan, Dr. Dekant Kıran, H. Aya Alan, Sinem Demirci, Dr. Deniz Kahrıman, Aykut Bulut, Semanur Kandil and Burak aylak for their friendship, patience, and support during the time that we spend together.

Finally, this dissertation was supported by TBTAK 3501 (Project No: 115E281).



TABLE OF CONTENTS

ABSTRACT	iv
ÖZ	v
DEDICATION	vi
ACKNOWLEDGMENTS.....	vii
TABLE OF CONTENTS.....	ix
LIST OF TABLES	xi
LIST OF FIGURES	xiii
LIST OF ABBREVIATIONS	xv
CHAPTERS	
1. INTRODUCTION	1
1.1. Research Problem, Questions and Hypotheses	3
1.1.1. Research Problem.....	3
1.1.2. Research Questions	4
1.1.3. Research Hypotheses	5
1.2. Scope of the Thesis.....	5
2. LITERATURE REVIEW	7
2.1. Research on Functional and Neuroanatomical Organization of Speech Comprehension and Production	7
2.2. Research on Brain-to-Brain Coupling Activations in Interaction Contexts.....	13
2.3. Hyperscanning of Joint Speech Processes.....	19
3. METHODOLOGY.....	21
3.1. Joint Sentence Reading Experimental Protocol	21
3.1.1. Participants.....	21
3.1.2. Auditory Feedback	21
3.1.3. Matching and Mismatching Sentences.....	21
3.1.4. Physical Conditions and Experimental Setup	22
3.1.5. Pre-task Baseline for Experimental Conditions	26
3.2. Quantitative Assessment of Performance by Dynamic Time Warping Analysis of Asynchrony	26
3.3. Qualitative Assessment of Performance through Asynchrony Ratings	28
3.4. fNIRS Hyperscanning	29
3.4.1. fNIRS Hyperscanning of Brain Activations	29
3.4.2. Functional Connectivity - Wavelet Transform Coherence (WTC).....	32
3.4.3. Calculation of Frequency from Period.....	33

3.4.4.	Validation of the coherence.....	35
3.6.	Summary of the Methodology.....	35
4.	RESULTS.....	37
4.1.	Behavioral Analysis Results.....	37
4.1.1.	Quantitative Assessment of Performance.....	37
4.1.2.	Qualitative Assessment of Performance.....	39
4.2.	Brain Activation Results.....	42
4.3.	Coherence Analysis.....	46
4.3.1.	HbR Coherence Analysis Results.....	47
4.3.2.	HbO Coherence Analysis Results.....	50
4.4.	Summary of the Results.....	52
	The results of could be summarized as follows:.....	52
5.	DISCUSSION.....	55
5.1.	Discussion of Behavioral Performance Analysis Results.....	55
5.1.1.	Discussion of Quantitative Assessment of Performance.....	55
5.1.2.	Discussion of Qualitative Assessment of Performance.....	58
5.2.	Discussion of Brain Activation Analysis Results.....	59
5.2.1.	Discussion of Group Brain Activation Results.....	59
5.3.	Discussion of Coherence Analysis Results.....	62
5.3.1.	Discussion of HbR and HbO Coherence Analysis Results.....	62
6.	CONCLUSIONS AND SUMMARY.....	67
6.1.	Conclusions and Summary of the Study.....	67
6.2.	Limitations of the Study.....	68
6.3.	Future Directions.....	69
	REFERENCES.....	71
	APPENDICES.....	79
	APPENDIX A - Joint Sentence Reading Task Blocks.....	79
	APPENDIX B - One Sample t-Tests for HbR and HbO Coherence Increase.....	85
	APPENDIX C - Ethical Approval Form.....	107
	APPENDIX D - CURRICULUM VITAE.....	109
	APPENDIX E - TEZ FOTOKOPİ İZİN FORMU.....	113

LIST OF TABLES

Table 1. Repeated measures ANOVA for quantitative assessment of performance..	38
Table 2. Repeated measures ANOVA for qualitative assessment of performance....	41
Table 3. Mean HbO activation levels in 16 optodes	44
Table 4. One-sample t-test for HbO in Both condition.....	85
Table 5. One-sample t-test for HbO in Other condition.....	86
Table 6. One-sample t-test for HbO in Self condition	86
Table 7. One-sample t-test for HbO in Silent condition	87
Table 8. One-sample t-test for HbO in Both-Match condition	87
Table 9. One-sample t-test for HbO in Both-Mismatch condition.....	88
Table 10. One-sample t-test for HbO in Other-Match condition.....	88
Table 11. One-sample t-test for HbO in Other-Mismatch condition	89
Table 12. One-sample t-test for HbO in Self-Match condition.....	89
Table 13. One-sample t-test for HbO in Self-Mismatch condition.....	90
Table 14. One-sample t-test for HbR in Both condition	91
Table 15. One-sample t-test for HbR in Other condition.....	91
Table 16. One-sample t-test for HbR in Self condition	92
Table 17. One-sample t-test for HbR in Silent condition.....	92
Table 18. One-sample t-test for HbR in Both-Match condition.....	93
Table 19. One-sample t-test for HbR in Both-Mismatch condition.....	93
Table 20. One-sample t-test for HbR in Other-Match condition	94
Table 21. One-sample t-test for HbR in Other-Mismatch condition	94
Table 22. One-sample t-test for HbR in Self-Match condition.....	95
Table 23. One-sample t-test for HbR in Both-Match condition.....	95
Table 24. One-sample t-test for HbO in Random Both condition	96
Table 25. One-sample t-test for HbO in Random Other condition	96
Table 26. One-sample t-test for HbO in Random Self condition.....	97
Table 27. One-sample t-test for HbO in Random Silent condition.....	97
Table 28. One-sample t-test for HbO in Random Both-Match condition.....	98
Table 29. One-sample t-test for HbO in Random Both-Mismatch condition	98
Table 30. One-sample t-test for HbO in Random Other-Match condition	99
Table 31. One-sample t-test for HbO in Random Other-Mismatch condition.....	99
Table 32. One-sample t-test for HbO in Random Self-Match condition	100
Table 33. One-sample t-test for HbO in Random Self-Mismatch condition	100
Table 34. One-sample t-test for HbR in Random Both condition.....	101
Table 35. One-sample t-test for HbR in Random Other condition	101
Table 36. One-sample t-test for HbR in Random Self condition.....	102
Table 37. One-sample t-test for HbR in Random Silent condition	102
Table 38. One-sample t-test for HbR in Random Both-Match condition	103
Table 39. One-sample t-test for HbR in Random Both-Mismatch condition	103
Table 40. One-sample t-test for HbR in Random Other-Match condition.....	104
Table 41. One-sample t-test for HbR in Random Other-Mismatch condition.....	104
Table 42. One-sample t-test for HbR in Random Self-Match condition	105
Table 43. One-sample t-test for HbR in Random Self-Mismatch condition	105



LIST OF FIGURES

Figure 1: Comparison of spatial and temporal sensitivities of non-invasive neuroimaging methods	9
Figure 2: The dual-stream model of the functional neuroanatomy of language	11
Figure 3: The cortical language circuit	12
Figure 4: Subdivisions in Broca's region.....	13
Figure 5: Photograph of the experimental setup	23
Figure 6: Schematics of the experimental setup	24
Figure 7: Experimental protocol	25
Figure 8: Standard Dynamic Time Warping path estimation (left)	27
Figure 9: Time aligned speech waveforms with associated warp curve.....	28
Figure 10: fNIRS devices and measurement locations	30
Figure 11: NIRS absorption pattern (left). fNIRS source-detector configuration and light path in neural tissue (right)	31
Figure 12: Wavelet transform coherence (WTC) analysis between two raw deoxy-Hb (HbR) signals	34
Figure 13: Quantitative assessment of performance	38
Figure 14: Line graph DTW Self, Both, Other	39
Figure 15: Qualitative assessment of performance	40
Figure 16: Line graph rating Self, Both, Other	42
Figure 17: Overall mean HbO concentration changes ($\mu\text{molar/Lt}$)	43
Figure 18: Mean HbO concentration changes ($\mu\text{molar/Lt}$) observed at each optode for the match and mismatch blocks.....	44
Figure 19: Mean HbO concentration changes ($\mu\text{molar/Lt}$) observed at Optode 2 and 4 for each auditory and block condition.....	45
Figure 20: Mean HbO concentration changes ($\mu\text{molar/Lt}$) observed at Optode 11...	46
Figure 21: FDR corrected t-maps for HbR coherence increase	48
Figure 22: FDR corrected t-maps for HbR coherence increase	49
Figure 23: FDR corrected t-maps for HbO coherence increase.....	50
Figure 24: FDR corrected t-maps for HbO coherence increase.....	51



LIST OF ABBREVIATIONS

DLPFC	Dorsolateral Prefrontal Cortex
DMPFC	Dorsomedial Prefrontal Cortex
DTW	Dynamic time Warping
ECoG	Electro-Corticography
EEG	Electro-Encephalography
fMRI	Functional Magnetic Resonance Imaging
fNIRS	Functional Near-Infrared Spectroscopy
IFG	Inferior Frontal Gyrus
IFC	Inferior Frontal Cortex
LFO	Low Frequency Oscillation
MEG	Magnetoencephalography
PET	Positron Emission Tomography
pMNS	Putative Mirror Neuron System
SFC	Superior Frontal Cortex
SPECT	Single-Positron Emission Computed Tomography
TRW	Temporal Receptive Window
VMPFC	Ventromedial Prefrontal Cortex
WTC	Wavelet Transform Coherence

CHAPTERS

CHAPTER 1

INTRODUCTION

People constantly engage in social interactions and synchronous actions with each other to accomplish tasks together in daily life. As evidenced in Cummins et al. (2016), synchronous behavior such as chanting, marching, singing and dancing are widespread in all aspects of the society such as military, political rallies and religious activities. However, little is known about the neural underpinnings of such a widespread and integral behavior to one's life. With the recent development of a variety of portable and relatively affordable neuroimaging modalities such as functional near infrared spectroscopy (fNIRS) that allow simultaneous measurement of cortical activity during mutual interactions, the researchers are nowadays in a better position to investigate the interactions between people's brains during such joint actions. Such efforts are geared towards revealing the nature of time-locked interrelationships among brain activations of two or more people in various social contexts.

Along these lines of research, Schilbach et al. (2013) argue for the development of a "two-person neuroscience" to allow for the investigation of real-time social interactions. However, the relevant research has only started to gain momentum in this new line of research and many areas of this two-person neuroscience remain as a "dark matter" as defined by Schilbach et al. (2013).

In an effort to charting the unknown territory of "dark matter" of two-person neuroscience, Liu and Pelowski (2014) argued for a clarification for the types of interactions between the participants. They define three main axes of interaction that affect humans when they interact with each other as (1) interaction structure (i.e. concurrent vs. turn-based), (2) goal structure (i.e., cooperative vs. competitive) and (3) task structure (i.e., independent vs. interdependent). Based on these three main axes, eight types of interactions in two-person neuroscience research (e.g., concurrent independent cooperation, turn-based interdependent competition, etc.) could be defined. As the researchers point out, these different types of interactions between participants might involve distinct neural mechanisms and might require careful separation of brain-to-brain coupling results.

In this regard, simultaneous measurement of the participants' brain activity in such interactive contexts is becoming an increasingly important and relevant methodological approach in social neuroscience research. Montague et al. (2002) first coined the term hyperscanning for simultaneous measurements of two or more people's brain activations. In this way, the researchers would be able to identify and study the dynamically unfolding neural activity relevant to social interactions. Hyperscanning could be defined as an integral method to study simultaneous brain activations between individuals in a socially relevant joint activity context. Hyperscanning has also been employed as the main method in this dissertation in the form of functional near-infrared spectroscopy (fNIRS) hyperscanning by simultaneously measuring two people's brain hemodynamics while performing a joint speech task.

Several researchers have emphasized that language-based communication constitutes an important aspect of two-person neuroscience (e.g., Stephens et al., 2010; Jiang et al., 2012), and they argued that language is an important mediator of interaction dynamics and the level of neural synchrony between the two interlocutors' brains. Moreover, human social interaction and joint behavior is mostly in the form of linguistic interaction and therefore, investigation of coupling relationships among multiple brains in the context of linguistic communication is a relevant and important undertaking in this line of research. Accordingly, the general purpose of this dissertation is to help illuminate a portion of this "dark matter" defined by Schilbach et al. (2013) and to contribute to the knowledge and identification of neural correlates in terms of brain activations of two people who are engaged with a joint read aloud task.

As mentioned previously, the measurement of simultaneous brain activations of two or more people (i.e., hyperscanning) in interactive contexts is useful in identifying dynamical aspects of people's brain activations during successful communication or joint actions. Such dynamical neural activations between the participants' brains are quantified by a measure called "coherence". Coherence is defined as a degree of synchrony measured between the brain activation signals recorded simultaneously from two people. In the related literature, coherence is defined and calculated as a form of correlation between two time-series signals in the time and frequency domains. Throughout this dissertation, the term coherence will be used to indicate the correlation as calculated by such methods between two brain activation signals. In the recent literature of hyperscanning, the coherence term is also used interchangeably with other terms such as inter-personal neural synchronization (INS), coupling, brain-to-brain interaction/coupling and synchrony. In this dissertation, the coherence term will be adopted and used mainly to indicate the measurement of the brain signals of interacting people, together with occasional use of other terms such as brain-to-brain coupling and synchronization to mean the same measure of similarity between brain signals of interacting participants.

Along similar lines with this dissertation, there are recent studies in the related two-person neuroscience literature that investigate social interactions among speakers during simultaneous reading of sentences (Cummins et al., 2013), game-based interactions during competitive, cooperative and individual conditions (e.g., Cui et al., 2012, Liu et al., 2016), face-to-face communications (e.g., Jiang et al., 2012, Osaka et al., 2015) and speaker-listener interactions (Silbert et al., 2014, Jasmin et al., 2016) to identify and study the inter-personal neural synchronization among the participants during coordinated motor, decision making and natural communication (in English and Chinese) tasks. However, some of these studies did not employ hyperscanning for the joint reading tasks where brain imaging data was collected for only one of the speakers (Jasmin et al., 2016). Moreover, studies that employed hyperscanning included primarily joint motor actions during game-based interaction (Cui et al., 2012). There is a single hyperscanning study focusing on comparing the level of neural coupling between turn by turn conversation and single turn monologue for dyads, which only focuses on the language regions in the left frontal, temporal and parietal cortices, without any consideration for the homologues of these regions in the right hemisphere (Jiang et al., 2012).

Consequently, the purpose of this dissertation is to investigate behavioral synchronization and simultaneous brain activations in the prefrontal cortex of two people during joint sentence reading task of Turkish sentences. This dissertation employs similar research methodology as in Cummins et al., (2013) in presenting Turkish sentences to the joint reading aloud task, and in addition introduces hyperscanning of the participants' brain activations during such communicative conditions. To the best of our knowledge, this is the first study employing the hyperscanning method for a joint sentence reading task in Turkish that focuses on bilateral neural activity and coherence increase patterns in the participants' prefrontal cortices.

1.1. Research Problem, Questions and Hypotheses

1.1.1. Research Problem

In this dissertation, the research problem is to explore brain-to-brain interactions between the participants' prefrontal cortex (PFC) activations during joint sentence reading task with experimental conditions of auditory feedback type (i.e., self, other and both) and sentence type (i.e., matching and mismatching sentences).

The brain activations of participants in these conditions will be recorded with two functional near infrared spectroscopy (fNIRS) devices. The pair of signals obtained from the participants will be analyzed using wavelet transform coherence (WTC) method to quantify the level of coherence between the brains of the participants during the conditions of the study. In addition, the recordings of the participants' joint reading aloud of Turkish sentences will be quantified by using a dynamic time

warping (DTW) algorithm as well as a subjective rating method to measure the level of asynchrony between the participants' sentence reading performances.

1.1.2. Research Questions

The research questions and related hypotheses to be investigated in this dissertation are as follows:

Research Question 1. Specifically, the behavioral synchronization observed during joint sentence reading in English and Mandarin Chinese (Cummins, et al., 2013) will be investigated for simultaneous reading aloud of Turkish sentences. The strength of the behavioral coupling during joint sentence reading task will be manipulated similar to the study by Cummins et al., (2013) in which the participants will be subjected to different auditory conditions (i.e., self, other, and both) and block conditions (i.e., match and mismatch). In this regard, the first research question is formulated as:

RQ1. What are the effects of the manipulation of the experimental conditions (i.e., auditory (self, both, other) and block (match, mismatch) conditions) on the participants' behavioral synchronization during joint sentence reading task?

This research question will investigate the behavioral synchrony between the participants during a joint sentence reading task. Joint actions and ability to coordinate behaviors during similar tasks have been investigated in a variety of studies (Cummins et al., 2013, Stephens et al., 2010, Silbert et al., 2014). These studies showed that during social interaction conditions, people demonstrate joint behaviors as well as coupled brain activations. Similarly, in this dissertation, investigation of the participants' behavioral synchronization during joint sentence reading tasks would contribute to the literature of joint actions as well as demonstrate behavioral synchronizations and manipulation of such synchronization through experimental conditions for joint reading of Turkish sentences.

Research Question 2. In addition to the behavioral synchronization of the participants during joint sentence reading task, the second research question will investigate the neural correlates of brain-to-brain interactions in the prefrontal cortices of the participants during such synchronizations. Therefore, the second research question is formulated as:

RQ2. What are the effects of degree of behavioral coupling between the participants during auditory (i.e., self, other, and both) and block (i.e., match and mismatch) conditions on the degree of brain-to-brain interactions observed at the prefrontal cortices of the participant pairs?

In this regard, the second research question will add to the hyperscanning literature of joint actions and social interactions in the context of joint linguistic interaction in

the form of reading aloud sentences. Hyperscanning of people's brain activations during naturalistic social interaction environments is a recently developing research area in cognitive neuroscience. Instead of measuring single participants' brain activations, hyperscanning allowed researchers to investigate simultaneous brain activation during such interactive contexts. There are several recent studies that make use of hyperscanning techniques to define social interactions in terms of interpersonal coherence between the participants' brains (Cui et al., 2012, Jiang et al., 2012, Osaka et al., 2015). Along the similar lines, the second research question of this dissertation will extend the behavioral investigation of synchronization to brain-to-brain interactions between the participants during the experimental conditions.

1.1.3. Research Hypotheses

The research hypotheses to be investigated in this dissertation are as follows:

Research Hypothesis 1a. The participant pairs' behavioral synchrony will be lower in the Self condition than Both and Other conditions.

Research Hypothesis 1b. The participant pairs will exhibit higher behavioral synchrony (as measured by lower dynamic time warping scores and higher qualitative performance ratings) while reading matching sentences but not during mismatching sentences.

Research Hypothesis 2a. The participant pairs' brain-to-brain synchrony will be the least in the Self condition than Both and Other conditions.

Research Hypothesis 2b. The participant pair's brain-to-brain synchrony will be higher in matching sentences as compared to mismatching sentences.

1.2. Scope of the Thesis

The scope of this dissertation was to investigate behavioral synchrony as well as brain-to-brain interactions between people in the context of a joint sentence reading task. The experimental task included Turkish sentences selected from METU Turkish Corpus. The participants were required to jointly read aloud the sentences presented in the LCD monitors in front of them. However, other linguistic considerations such as neural and behavioral aspects of speech production and comprehension processes were not investigated as part of this dissertation.

A variety of methods were employed in this dissertation for quantitative and qualitative assessment of behavioral synchrony as well as for quantifying brain-to-brain interactions. Behavioral synchrony between the participants during joint sentence reading task was measured by a quantitative method called Dynamic Time Warping (DTW) which finds the optimum warping path between two time-aligned speech signals. In addition to DTW method, ratings of sentences as part of a

qualitative method were also used. In terms of brain-to-brain interactions, hyperscanning of prefrontal cortex activations of the participants' during joint sentence reading task was employed in order to quantify the degree of inter-personal neural synchronization by a method called Wavelet Transform Coherence (WTC) that computes coherence between the brain signals simultaneously recorded from the participants. In summary, the scope of this dissertation was to investigate behavioral as well as brain-to-brain interactions during a joint sentence reading task which is also a recently developing research area in social neuroscience studies.



CHAPTER 2

LITERATURE REVIEW

The review of related literature is organized in three main sections. In the first section, related neurolinguistics research about functional and neuroanatomical correlates of speech comprehension and production will be provided. In the next section, related literature on the brain-to-brain coupling activation in interaction contexts will be reviewed. Finally, in the third section the recently proliferating body of literature on hyperscanning in social neuroscience, which focus on brain-to-brain coupling between two or more participants during joint activities will be introduced and reviewed.

2.1. Research on Functional and Neuroanatomical Organization of Speech Comprehension and Production

There is a great body of research in neurolinguistics on functional and neuroanatomical organization of speech comprehension and speech production networks. These neurolinguistics research are of particular interest and will be foundational in identifying the relevant neural networks and activation patterns in the prefrontal cortex during joint sentence reading tasks investigated in this dissertation.

Research on functional and neuroanatomical organization of speech comprehension and production is an important and well established research avenue in the cognitive neuroscience. The relevant research is also closely important in people's daily lives and interactions with each other since successful social interactions require people to understand the actions and perceptions of others. In order to provide a comprehensive literature review on the functional and neuroanatomical organization of speech comprehension and production as well as to introduce the body of hyperscanning studies in social neuroscience with details on the relevant neuroimaging methodologies, a short review on a variety of neuroimaging techniques available to the researchers, their advantages and disadvantages and relevant research methods implemented using these neuroimaging modalities will be reviewed.

In the related literature of neuroimaging, brain activations during speech comprehension and production and brain-to-brain couplings of socially interacting people in the hyperscanning literature were recorded by a variety of non-invasive

brain imaging techniques such as functional near-infrared spectroscopy (fNIRS) (Cui et al., 2012), functional magnetic resonance imaging (fMRI) (Montague et al., 2012), magnetoencephalography (MEG) (Baess et al., 2012) and electroencephalography (EEG) (Dumas et al., 2010). When a comparison between several brain monitoring techniques such as MEG/EEG, PET (positron emission tomography), SPECT (single-positron emission computed tomography), fMRI and fNIRS is made, it is evident that each technique has its advantages and disadvantages in terms of their temporal and spatial resolution as well as the physical constraints imposed on the participants that have important implications for the experimental designs of the relevant studies. In terms of technological specifications of these imaging modalities, MEG/EEG focus on the electrical fields/potentials generated by neural populations, and offer the highest temporal sensitivity in the order of milliseconds as compared to other imaging modalities. Despite its high temporal resolution, EEG is relatively weak in spatial sensitivity due to the complexities involved with the propagation of electric potentials in the brain. Since electric field properties are less affected by neural tissue, MEG excels on both temporal and spatial resolution, but it's the least cost-effective option that also requires a facility that can shield the sensors from the earth's magnetic field. However, EEG/MEG studies have played a significant role in our current understanding of linguistic processing within the brain at various timescales.

On the other hand, fMRI, PET and SPECT are strong in spatial sensitivity that can detect hemodynamic activity in millimeter cube voxels in the brain, but they are relatively weak in temporal sensitivity due to their operating principle that relies on hemodynamic coupling between blood flow and neural activity. Neurons require energy to get activated, which requires the metabolization of glucose with the oxygen transported by the blood cells. fMRI, PET, SPECT and fNIR monitor the oxygen transportation process in the capillaries for imaging purposes, which is an indirect and slower method as compared to direct recording of electrical firings of nerve cells in the brain. Moreover, fMRI and MEG are bulky and they fill an entire room that require high maintenance rates and costs. MEG in this case represents the ultimate example for high maintenance costs and the difficulty for conducting an MEG study since it requires constant replacement of hard-to-obtain liquid helium for cooling down the superconducting circuits in the machine as well as near perfect isolation from the Earth's magnetic field. The level of noise in the MRI machine and the confined position in which the recordings have to be made for fMRI, SPECT and PET provide further constraints on the experiments that can be run with these modalities. Finally, PET requires the injection of radioactive tracers in the blood-stream and SPECT uses high energy wavelengths, making them more suitable for medical applications rather than imaging studies with healthy populations.

Motivated by these shortcomings, researchers increasingly make use of other neuroimaging techniques that have acceptable levels on both the temporal and spatial resolution for their research. One of such technique is a relatively recent and non-

invasive functional near infrared spectroscopy (fNIRS) that takes advantage of the coupling between hemodynamic response and brain activity and could provide a reliable measurement of changes in blood oxygenation concentrations due to the synaptic activity of the neurons with relatively good spatial resolution (Figure 1). More precisely, fNIRS takes advantage of the optical properties of hemoglobin molecules that play a key role in oxygen transportation for the monitoring of neural activity. fNIRS offers higher temporal resolution (e.g. 2-10Hz) as compared to fMRI, PET, SPECT methods, and better spatial resolution (e.g. $\sim 1 \text{ cm}^3$) as compared to EEG. However, fNIRS is limited in terms of its penetration depth into the tissue due to its optical nature, which limits its access to cortical regions close to the scalp.

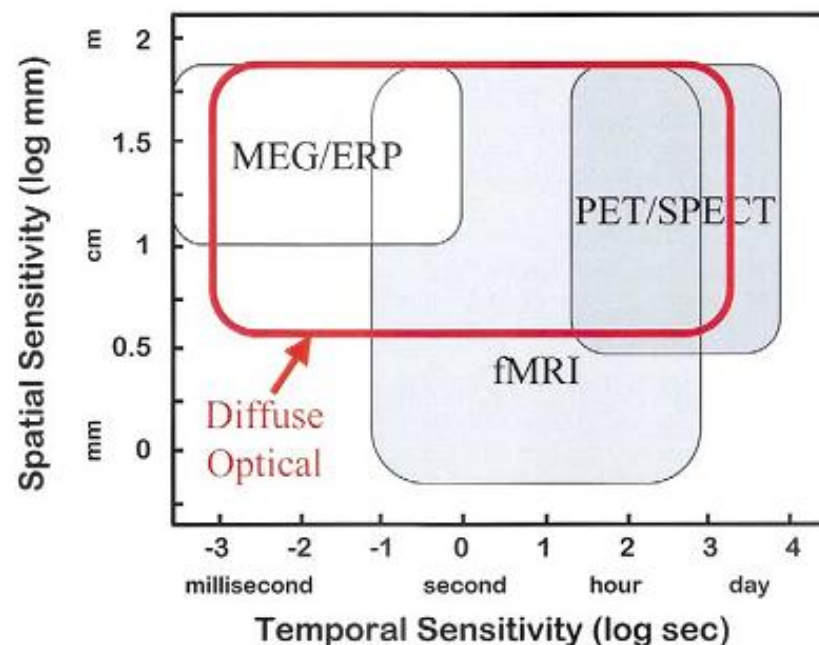


Figure 1: Comparison of spatial and temporal sensitivities of non-invasive neuroimaging methods Adapted from Gary Strangman, David A. Boas, and Jeffrey P. Sutton (2002). Non-Invasive Neuroimaging Using Near-Infrared Light. *Biological Psychiatry*, 52, 679-693.

Accordingly, among several non-invasive brain monitoring techniques that make use of coupling between brain activity and hemodynamics, fNIRS has been the preferred method for brain monitoring for an increasing number of researchers due to its low-cost, reliability, portability, robustness and ease of implementation.

In terms of related literature on neurolinguistics that investigate the functional and anatomical organization of human speech production and comprehension, early research in neurolinguistics was summarized by Stemmer and Whitaker (1998) in “Handbook of Neurolinguistics” which covers a range of topics within neurolinguistics from the history of neurolinguistics to the clinical and experimental

methods. In the handbook, the historical developments in linguistics research, anatomical as well as functional identification and lateralization of language related areas such as the left hemisphere and the Broca's area are given. The related theories on hemispheric lateralization, unity of language through interhemispheric interaction and the results of experimental neurolinguistics that indicate Broca's area and its right hemisphere homologue for language-specific tasks will provide the theoretical framework for this dissertation.

Scott and Johnsrude (2003) provided a categorization of the neuroanatomical and functional organization of speech perception. The researchers argue for multiple, parallel and hierarchically organized processing pathways of speech input based on studies of anatomical and functional organization of non-human primate auditory cortical system. Functional and neuroanatomical studies also indicate that human auditory cortex have multiple streams of processing starting from the primary auditory core. These streams of processing include ventrolateral and dorsolateral frontal cortices among other regions where acoustic-phonetic cues are mapped onto lexical representations and articulatory-gestural representations of speech acts are processed. Scott and Johnsrude (2003) also indicate that in terms of classical neuroanatomy of speech, multiple processing streams account of speech expands the roles of Broca's (which comprises prefrontal and premotor areas) and Wernicke's areas (which comprises parts of the temporal-parietal cortex) as output and input systems. The multiple processing account argued by Scott and Johnsrude (2003) shows that prefrontal cortex is involved in speech processing especially in the Broca's area.

In a review article summarizing the anatomy and function of Broca's area, Nishitani, Schürmann, Amunts, and Hari (2005) pointed out that Broca's region has its right-hemisphere homologue also identified by Brodmann's cytoarchitectonic areas (BA) 44 and 45. Functionally, in terms of language and speech processing, Broca's area is left lateralized, however the researchers indicate that it is less clear whether Broca's area is asymmetric in other language related functions. Based on their review of relevant evidence, Nishitani et al. (2005) concluded that Broca's area has a central role as a coordinator of time sensitive perceptual and motor functions for verbal and non-verbal communication. Thus, investigation of prefrontal cortex for a language related task in this dissertation will allow the researchers to describe the bilateral activation patterns in the prefrontal cortex and parts of Broca's area in single versus simultaneous speech conditions.

In this regard, several researchers proposed models to describe the neuroanatomical and functional organization of speech processing. Among these models, Hickok and Poeppel (2007) proposed a dual-stream model of the functional anatomy of language based on neuroimaging data. In their model, the researchers identify two pathways (i.e., dorsal and ventral) for speech processing where dorsal pathway is left-lateralized, have connections with frontal cortex and underlies speech perception

while ventral pathway is bilateral and performs mapping from sound to meaning with different computational organizations across both hemispheres (Figure 2).

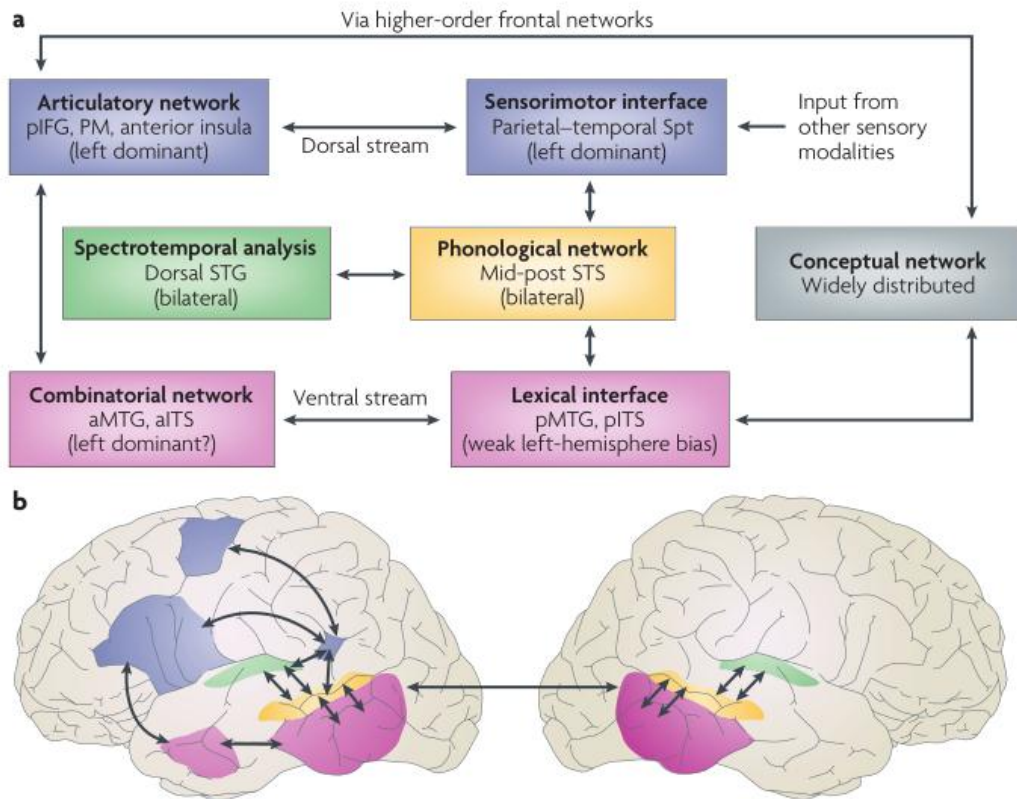


Figure 2: The dual-stream model of the functional neuroanatomy of language
Adapted from Hickok, G., & Poeppel, D. (2007). The cortical organization of speech processing. *Nature Reviews Neuroscience*, 8(5), 393-402.

In another study, Friederici (2012) proposed a model for the language circuitry in the cortex to account for the functional neuroanatomy of different computational steps from auditory perception to comprehension. In this model, structural and functional distinctions were proposed between the dorsal and ventral pathways of speech comprehension. The model details the dorsal and ventral pathways anatomically and functionally to account for the recent evidence that these pathways engage in more than one function. In particular, the model distinguishes two dorsal pathways that are structurally and functionally different from each other. One pathway maps from the auditory cortex to the pre-motor cortex, and the other projects from the temporal cortex to Brodmann Area (BA) 44, which is a part of Broca's area. In addition, the ventral pathway also consists of two streams of structures and together with the dorsal pathway, the ventral pathway encodes for syntactic structure building and sound-to-meaning mapping (Figure 3).

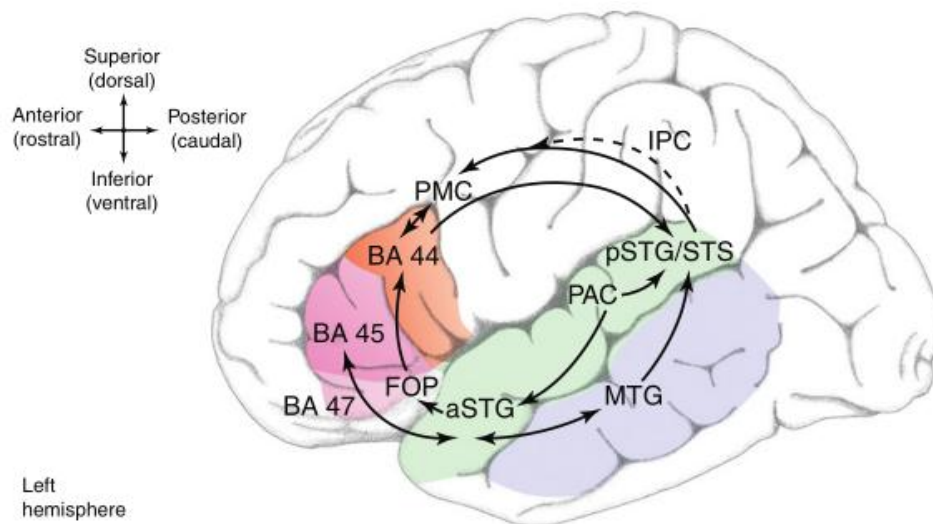


Figure 3: The cortical language circuit

Adapted from Friederici, A. D. (2012). The cortical language circuit: from auditory perception to sentence comprehension. *Trends in cognitive sciences*, 16(5), 262-268.

Based on recent evidence in neurolinguistics, Poeppel (2014) argued that the neurobiological research should develop a computational neurobiology of language which takes computational and representational primitives as the primary research focus. Poeppel (2014) stated that classical neurolinguistics theories of speech are no longer adequate to account for the variety and the detail of speech production and comprehension, as well as for the recent functional and anatomical evidence of cortical networks realizing these linguistic processes. In this regard, for example, Broca's area has been identified to have at least 10 different sub-regions rather than being a single area. It is estimated that each of these anatomical sub-regions performs at least one type of computation necessary for speech processing, amounting to an underestimated number of 10 computations performed by Broca's area (Figure 4).

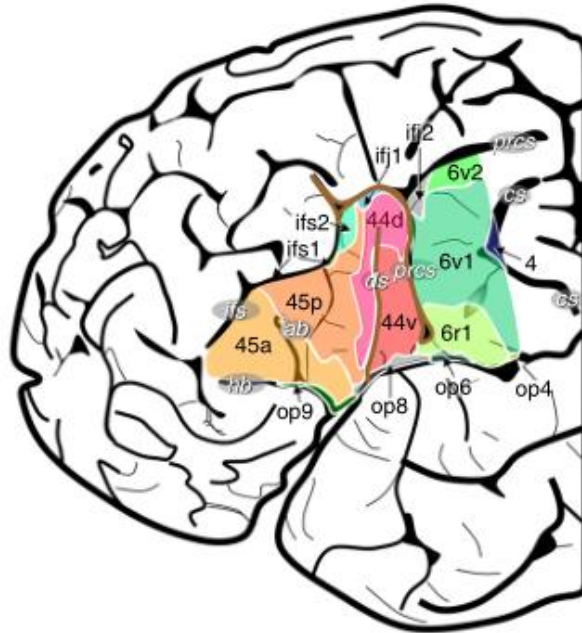


Figure 4: Subdivisions in Broca's region

Adapted from Amunts, K., Lenzen, M., Schleicher A., Morosan, P., Palomero-Gallagher, N. and Zilles, K. (2010). Broca's region: Novel organizational principles and multiple receptor mapping. *PLOS Biology*, 8(9).

Poepfel (2014) also proposes a temporal account of speech processing based on recent studies on cortical oscillations in speech related tasks. In this temporal account, the computational aspects of natural speech are undertaken by the intrinsic cortical oscillations to parse the continuous speech signal. The model was also supported by a magnetoencephalography (MEG) study (Doelling et al., 2014) where auditory cortex activations showed close alignment with the stimulus and an electrocorticography (ECoG) study (Golumbic et al., 2013) where participants attended different speech streams and the results indicated that the brain activity dynamically entrains to the ongoing speech streams by means of high- and low-frequency amplitude fluctuations.

2.2. Research on Brain-to-Brain Coupling Activations in Interaction Contexts

Many researchers argued for a transformation of research focus from single-subject measurements of brain activations to a multi-brain frame of reference. In this respect, hyperscanning allows simultaneous recording of the participants' brain activations in socially relevant contexts. Montague et al. (2002) argued that hyperscanning has many advantages in social exchange situations over single brain measurements such as measuring the dynamical neural activity related to social exchanges between interacting brains. In their study, the researchers argued that measuring participants' brain activations synchronously is a useful method for the investigation of social

contexts. The researchers argue that synchronous measurement of participants' brain activity is necessary since it would be difficult to correlate brain activations of participants with definite behavioral markers in asynchronous measurements of brain activations. Therefore, simultaneous measurement of brain activations of participants in a social interaction situation is an important methodology in revealing the structure of social interactions and their neural correlates.

Recently, many researchers studied brain-brain interactions between participants while they engage in a social interaction such as collaboration in problem solving and joint action. In the study by Hasson, Ghazanfar, Galantucci, Garrod and Keysers (2012), the researchers argued that cognition emerges in an interpersonal space and in many cases neural processes occurring in one brain are coupled to neural processes occurring in another brain through transmission of signals from one brain to another in a social interaction medium. In such cases, the joint behaviors of individuals can be observed which would not emerge in contexts where individuals were in isolation. In this perspective, in addition to using near-infrared spectroscopy technology in measuring single subjects' brain activations in cognitive tasks, researchers recently implemented near-infrared spectroscopy in simultaneously measuring brain activations of two people collaborating on cognitive tasks such as problem solving.

In the study by Funane et al. (2011), simultaneous near-infrared spectroscopy (NIRS) was used to measure the activity of two people's prefrontal cortices during a cooperative task. In their study, researchers used a wireless near-infrared system. The participants were told to count 10 seconds in their mind after an auditory cue and to press a button when they finished counting. In addition, the participants were required to adjust their button presses to make them as synchronized as possible. In the experimental condition, the auditory cue was removed thus requiring participants to produce the time interval as synchronized as possible with each other. The results of the study indicated that the spatiotemporal coherence of the brain activations of the participants were observed in medial prefrontal cortex (mPFC) which is a region of the brain activated in tasks that require integration of working memory with attention resource allocation and in processes when people think about other people's intentions. In this study, it is concluded that NIRS hyperscanning can be used to evaluate human interaction (Funane et al., 2011).

In another study by Holper, Scholkmann, and Wolf (2012), the researchers investigated brain activations of participants engaged in paced finger-tapping task (PFT) in imitation conditions as compared to control conditions. Wireless fNIRS was used to record hemodynamic response of the participants' premotor cortices (PMC) during imitation condition. In the imitation condition a model and an imitator were recorded while tapping in synchrony with an auditory pacer followed by tapping without auditory stimulus. In the control condition, the participants performed the same task as in imitation condition but alone. The functional connectivity between

brains measured by using wavelet transform coherence (WTC) indicated that imitation condition revealed higher coherence than control condition, in the imitation condition the coherence was higher for self-paced than stimulus-paced condition. Granger-causality (G-causality) analysis indicated that in imitation condition G-causality was larger than in control condition and in the imitation condition the model's signal G-caused the imitator's signal. The study showed that fNIRS is an appropriate tool for simultaneous measurement of activation patterns of the interacting brains which is not detectable using single-subject experiments (Holper et al., 2012).

In a similar study by Cui, Bryant, and Reiss (2012), the researchers simultaneously measured brain activity of two people using NIRS while they played a computer-based cooperation game. The researchers indicated that their study was the first in the literature of hyperscanning in which the participants' brain activations were measured with NIRS. In this study, pairs of participants completed four separate computer-based tasks. These tasks were cooperation, competition, single 1 and single 2. In the cooperation task, pairs of participants responded the "go" signal simultaneously. They both earned a point when the difference between their response times was below a threshold. The task also indicated which participant was faster. The competition task was similar to the cooperation task except that the pairs of participants were instructed to respond faster than their partner to earn points. The participant responded faster than his/her partner earned a point while the participant who responded slower lost a point. In addition, the participants who responded before the "go" signal lost a point. The feedback screen was also similar to that of cooperation task indicating which participant win or lost and which participant was faster or slower. In single 1 task, the task was similar to the cooperation task except that the first participant responded while the other passively observed the screen. Single 2 task was similar to Single 1 task except that the second participant responded in this task and the first participant passively observed the screen. The researchers found that the coherence between the participants' signals in their right superior frontal cortices was higher in cooperation than competition condition and increased coherence was associated with better cooperation performance. The increase in coherence compared to competition, single 1 and single 2 tasks was significant in cooperation task. In addition, the results indicated that learning improved participants' cooperation and coherence in their superior frontal cortices.

In the study by Jiang et al. (2012), the researchers investigated the neural mechanism of face-to-face communication in comparison to other types of communication. The participants were in four task periods: face-to-face dialog (f2f_d), face-to-face monologue (f2f_m), back-to-back dialog (b2b_d), and back-to-back monologue (b2b_m). ETG-4000 optical tomography system (Hitachi Medical Company) was used to monitor the participants' hemodynamic response in frontal, temporal, parietal and dorsal lateral prefrontal cortices. Based on the modified Beer-Lambert Law, oxyhemoglobin and deoxyhemoglobin concentration changes for each channel were

recorded but only oxyhemoglobin concentration (HbO) was used for analyses. The coherence between the participants' brain activations were calculated by wavelet transform coherence (WTC). The results showed a significant increase in neural synchronization between the participants during face-to-face dialogue compared to other conditions and random pairings. The coherence increase was found in left IFC which was in agreement with previous evidence that showed activation in left IFC during communication events.

In terms of coherence between two brains, Osaka et al. (2015) examined neural synchronization between two people while they sing or hum together. The researchers employed fNIRS to record the participant pairs' brain activations while they sat face-to-face (FtF) or face-to-wall (FtW) and they sing or hum together and alone in counterbalanced experimental conditions. Wavelet transform coherence analysis was used between the oxy-Hb signals of two participants to determine the inter-brain synchronization between the participants' brains and anatomical regions of such synchronization. The results of this study showed that an increased neural synchronization in the left inferior cortex for cooperative singing or humming regardless of FtF or FtW compared with singing or humming alone. Moreover, right IFC showed an increase in synchronization for humming only. The results are important since they show that interpersonal neural synchronization can be found in IFC which also include Brodmann areas 44 and 45.

In terms of joint task performance, Dommer, Jäger, Scholkmann, Wolf, and Holper (2012) used functional near-infrared spectroscopy in their study to measure brain signals of pairs playing joint n-back task as compared to single players. Functional connectivity of the paired players' brains was evaluated using wavelet transform coherence (WTC). In the experimental condition, the participants performed an n-back task. In this study, the researchers used a dual n-back task introduced by Jaeggi et al. (2008) in which two independent sequences were presented simultaneously and the participants were required to remember and to respond the stimuli appeared n-stimuli before. In this study, the two stimuli were colored visual squares appearing independently in a 3x3 grid. The participants of pairs were assigned the color of the squares and were required to give their responses by a keyboard. In the single player case, the single player received only one color stimulus and performed the n-back task. The results of the study showed that there was a significant increase in between-brain coherence as compared to baseline condition in heart rate (HR) frequency and in low frequency oscillations (LFOs) as well as average hemodynamic responses in total hemoglobin concentration (HbT) in paired players were larger than that of single players and as compared to a rest period and baseline condition in joint group tasks. This study indicated that fNIRS is a suitable tool for investigating simultaneous brain activations. In addition, using between-brain connectivity analysis provides insight into interpersonal activation patterns not detectable by measuring single participants.

Related to joint activity, Stephens, Silbert, and Hasson (2010) investigated a speaker-listener pair in terms of neural correlates of successful communication. The researchers used fMRI to record brain activity of the speaker and listeners. The speaker's spatiotemporal brain activity was used to model the listeners' brain activity. In addition, the listeners' comprehension of the story told by the speaker was measured by a multiple choice questionnaire. The speaker's and the listeners' brain activations were measured asynchronously. The speaker told a 15-min long unrehearsed real-life story in the fMRI and the speaker's voice was recorded by an fMRI compatible microphone. The same procedure was repeated by a Russian speaker telling an unrehearsed real-life story. After the speaker's story was recorded, the listeners listened to the audio recording of the story. None of the listeners knew Russian. The results of the study indicated that the speaker's and the listeners' brain activity was spatially and temporally coupled for the story in English. Moreover, this coupling disappeared when the speaker and the listeners fail to communicate such as in Russian speaker's case. On average, the brain activations of listeners were similar to the brain activations of the speakers with a delay. The researchers also found areas that showed anticipatory responses. In this perspective, the results also showed that the understanding of the story by the listeners were greater when there were more anticipatory responses in the listeners' brain activations. These results provide an insight into the mechanism by which brains convey information during interactive alignment between pairs.

In another line of research, Hasson et al. (2008) and Honey et al. (2012) demonstrated that neural circuits differ in their properties of accumulating information over time. Neural assemblies near sensory regions are modulated by instantaneous physical parameters (e.g., acoustics of a word) and are defined as having short temporal receptive windows" (TRWs) while higher order perceptual and cognitive cortices are modulated by the information accumulated over longer periods of time are defined as having "long TRWs". In addition, in the study by Honey et al. (2012) the researchers recorded electrocorticographic (ECoG) signals from the participants watching intact and scrambled movies. The results indicated that within sensory regions fluctuations of high frequency power followed low-level properties of the intact and scrambled movies. On the other hand, for higher order regions the fluctuations were more reliable for the intact movie than the scrambled movie.

In a similar study by Lerner et al. (2011), the researchers mapped TRWs in auditory and language areas while the participants listened to a real-life story scrambled at different levels such as words, sentences and paragraphs. The results indicated a hierarchical organization of TRWs in the cortex. The early auditory areas were responsive to momentary input and brain activations were reliable for all scrambling levels. In areas with intermediate TRWs, the brain responses were more reliable for scrambled story at the sentence level or higher levels. The longest TRWs were found in parietal and frontal areas (e.g., precuneus and mPFC) and these areas responded

only to the paragraphs in a meaningful sequence. These results suggest that longer TRWs could be related to the information accumulation and processing over long timescales in higher cortical regions.

In the study by Schippers et al. (2010), the researchers investigated information flow from one brain to another during gestural communication. The participants were allowed to play the game of charades while the gesturer's and the guesser's brain activities were recorded by fMRI. The putative mirror neuron system (pMNS) and the ventromedial prefrontal cortex (vmPFC) are important brain regions that are active in social interactions. The pMNS is suggested to resonate with the actions of others while the vmPFC is involved in mentalizing (i.e., reflecting on other people's thoughts and beliefs). In their study, the researchers used Granger causality mapping to identify the direction of influence between brains of the participants. The results showed that the guesser's brain activity in pMNS and vmPFC mirrors the temporal structure of the brain activity of the gesturer in these regions. These results allow researchers to design more ecologically valid experiments in social neuroscience as well as to understand the brain activations and to identify neural mechanisms in participants engaging in social interactions.

In a similar study in line with the research questions of this dissertation, Jasmin et al. (2016) investigated joint speech and its neural correlates in a non-hyperscanning fMRI study. In the study, the researchers investigated the brain activations of a single participant in a joint sentence reading task during six experimental conditions such as synchronous live (Synch_Live) where the researcher and the participant synchronously read sentences, synchronous recorded (Synch_Rec) where the participant jointly read the researcher's pre-recorded sentence and different live (Diff_Live) where the researcher and the participant jointly read different sentences. In addition to these experimental conditions, the researchers also implemented control conditions in which the participant did not speak simultaneously with the experimenter. These control conditions were Listen_Alone where the participant only listened a pre-recorded speech of the researcher reading a model sentence, Speak_Alone where the participant spoke the model sentence on their own and Rest where no stimulus was presented. The results of this study indicated that synchronous speaking elicited more activation than solo speaking and listening in temporal plane and superior temporal gyrus with activations in inferior parietal cortex in the right hemisphere as well as an activation in the right homologue of Broca's area in the right inferior frontal gyrus. In terms of behavioral analyses, the participant's and the experimenter's wav file was analyzed by dynamic time warping algorithm in order to determine the synchrony between the recorded speeches. The participants' and the researcher's speech were more closely synchronized during live trial than prerecorded ones. An important finding in this study was that during synchronous speech production, right IFG which is a right homologue of Broca's area (in the left-IFG) is activated. In the related literature, speech is generally investigated with single participants that show left PFC activations however, in this

study it was found that synchronous speech activates right hemisphere regions in rIFG, temporal cortex (STG/IPL, motor cortex) and parietal cortex (somatosensory cortex).

In summary, there are many recent research that make use of near-infrared spectroscopy as a brain-imaging tool and to measure brain-to-brain coupling relations in collaborative environments in which two participants interact in verbal or non-verbal contexts. Moreover, similar to a neuron's receptive field, a hierarchical organization of temporal response windows that are sensitive to different timescales of information and specific regions such as pMNS and vmPFC involved in social interactions are defined in the organization of human cortex and argued to be important for the brain activations of interacting participants. Lastly, one recent study that investigated behavioral and neural correlated of joint speech of sentences with live and recorded conditions showed that synchronous activity in the context of joint reading aloud of sentences recruits brain regions especially in the right hemisphere that have not been previously associated with speech production.

In this regard, in the related literature language specific regions and functional connections between these regions were studied with single participants. However, these studies did not fully capture brain activations during real-time dialogue with a live speaker or joint conditions such as synchronous speech with a live speaker. Recently, studies that investigated joint speech paradigms in a more ecologically valid condition that more closely reflected human linguistic interaction gained more attention in neurolinguistics literature. Therefore, recent studies that simultaneously investigated the participants' brain activations were reviewed in the following section.

2.3. Hyperscanning of Joint Speech Processes

In terms of brain-brain coupling during live verbal communication, Spiegelhalder et al. (2014) investigated the brain activity of close friends while they were talking about autobiographical life events by simultaneously recording the brain activations of participant pairs using two fMRI machines. In this study, the experimental protocol consisted of three conditions. In two of the conditions, each participant spoke in turn about a real life event while the other was listening, and in the third condition both of the participants imagined an event. The researchers investigated inter-individual neural coupling by analyzing time courses of the brain activations of interacting participants during experimental conditions. The researchers found that listening was related to bilateral activation of the auditory cortex and speaking was related to the activation of the areas related to language and speech production. In terms of coupling analysis, the time course of neural activity in talking-related areas was found to be coupled to the time course of neural activity in the auditory cortex.

This study implemented a novel methodology by fMRI hyperscanning of verbally interacting pairs, but as the researchers indicated, even though this study did not require hyperscanning and could be conducted by using pseudo-hyperscanning, inter-individual coupling during live verbal communication was justified by using neuroimaging methods.

In another study by Silbert, Honey, Simony, Poeppel and Hasson (2014), the researchers investigated the coupling of neural systems during production and comprehension of naturalistic speech between speakers and listeners. In this study, the researchers implemented fMRI to identify the neural responses during production and comprehension of complex real-life speech between speakers and listeners. This study did not use hyperscanning, but the speaker's brain activation was recorded first during speaking a 15-min long real-life story, then 11 listeners' brain activations were scanned while they were listening to the recorded speech. The results of the study indicated that production of speech is not left-lateralized but an extensive bilateral network is activated, and this activation pattern also overlaps with the comprehension system. In addition, the researchers analyzed time courses of neural activity during production and comprehension of the same speech and identified neural coupling between the speakers' and the listeners' brain activity in linguistic as well as extra-linguistic areas including medial and prefrontal cortices.

In conclusion, recent research on functional and neuroanatomical organization of speech perception and comprehension demonstrated that speech production and comprehension networks are overlapping and distributed bilaterally in an extensive network, unlike the implicated brain locations in classical theories of speech processing. In addition, for the investigation of brain-to-brain coupling between interacting participants in joint use of language, hyperscanning methods to quantify such coupling is justified in recent neurolinguistics and two-person neuroscience literature. However, currently there is a need for further studies that investigate joint actions specifically in the context of linguistic interactions. Further research in these lines would help establish neural and behavioral correlates of joint linguistic interaction in a close-to-real life situation. In light of these considerations, in this dissertation, two people's prefrontal cortex activations were measured by fNIRS hyperscanning during joint reading of Turkish sentences in an effort to explore the activation and coherence patterns across the participants' prefrontal cortices in joint speech conditions. The research questions in this dissertation would contribute to the investigation of to the existing literature of coordinated, joint behaviors as well as to the hyperscanning research in the context of linguistic interactions. In addition, the research questions would also contribute to and fill the gap in hyperscanning of joint sentence reading contexts.

CHAPTER 3

METHODOLOGY

3.1. Joint Sentence Reading Experimental Protocol

In this chapter, the experimental protocol of the joint sentence reading is described in detail.

3.1.1. *Participants*

The participants of this study were 35 male-male pairs (70 participants in total) with no neurological/psychiatric disorders, normal or corrected-to-normal vision and hearing. Before the study, the participants completed the Edinburgh Handedness Inventory (Oldfield, 1971). All of the participants were right-handed. The random sampling method was used in which the participants were randomly selected in the public university where the research was conducted.

3.1.2. *Auditory Feedback*

In this study, the researcher setup audio equipment (audio mixers, headphones, and microphones) in order to modulate the direction of the auditory feedback available to each co-speaker. Similar to Cummins et al. (2013) where they implemented three levels of auditory linkage between the participants, the researcher investigated three levels of auditory feedback, which were referred as Self, Both and Other conditions. In the Self condition, the speaker's own speech was only relayed to the same speaker's headphone. In the Both condition, the speaker's own speech was relayed to the other speaker as well as to himself at the same volume level. Finally, in the Other condition, the headphones relayed only the co-speaker's speech to the other speaker.

3.1.3. *Matching and Mismatching Sentences*

The experimental protocol included matching and mismatching Turkish sentences. The sentences were selected from the METU Turkish Corpus (Say et al., 2004). All selected sentences have the Subject-Object-Verb (S-O-V) structure (Appendix A). The matching sentences were identical to each other while the mismatching sentences differed by one lexical item in the middle position of the sentences. A software program named "Wuggy" (Erten, Bozsahin & Zeyrek, 2014) was used for the generation of pseudo-words used in mismatching sentences. Orthographic Levenshtein distance 20 (OLD20) is obtained by taking the average of the 20 closest words in the unit of Levenshtein distance (LD) (Yarkoni et al., 2008). LD is a continuous metric that indicates the minimum number of insertions, deletions or

substitutions required for turning one string into another (Levenshtein, 1966). OLD20 values are indicative of response times such that words having lower OLD20 values are recognized better and responded faster than the words having higher OLD20 values (Yarkoni et al., 2008). In order to compute OLD20 values, Wuggy was used and the difference score (OLD20_diff) is reported for each pseudo-word generated. Accordingly, the researcher chose pseudo-words that have the smallest OLD20_diff scores.

Examples of matching and mismatching sentences:

Matching sentence: “*Defalarca tırmanılan, sonra kayarak inilen **tepeler** bir anda yerlerini geniş bir düzlüğe bıraktı.*”

Mismatching sentence: “*Defalarca tırmanılan, sonra kayarak inilen **meceler** bir anda yerlerini geniş bir düzlüğe bıraktı.*”

In the example given above, two sentences are identical except the words “tepeler – meceler”. In this example, one of the participants is presented with the matching sentence that includes the regular word “tepeler” and the other is presented with the mismatching sentence that includes the non-word “meceler”.

3.1.4. Physical Conditions and Experimental Setup

In this study, the participants were invited in a secluded, dimly lit room. The experimental setup consisted of two desktop computers with LCD monitors, two fNIR 1000 Devices connected to each of these desktop computers, an audio setup including one Behringer Xenyx 802 Premium 8-input 2-Bus mixer with Xenyx mic preamps and British EQs, one Behringer Xenyx 1002FX mixer, two Behringer Ultravoice XM8500 microphones, two XLR 3-pin microphone cables, mono 1/4” cables, RCA to 1/4” adaptors, RCA to Line-in cables, two Sony MDRZX300/BLK Stereo headphones, 3.5mm TRS to 1/4” TRS adaptors, and microphone holders/tripods. In addition to this audio setup, the participants’ voice was recorded on a MacBookPro 15” Late 2011 computer running Audacity® and GarageBand® software programs.

After the participants admitted to the room, they sat back to back. An LCD monitor was placed in front of each participant in order to display the directions of the study and present stimuli to the participants. The keyboards were used to input participant information to the computer as well as to record participants’ keypresses during the experiment. In addition to the LCD monitor and a keyboard, each participant had also a microphone placed in front of them. The participants wore headphones for the duration of the study. The microphones recorded the participants’ speech during the time of the study and the headphones relayed the participants’ speech to one another according to the auditory condition the researcher implemented (i.e., self, both, other). (Figure 5) and (Figure 6).

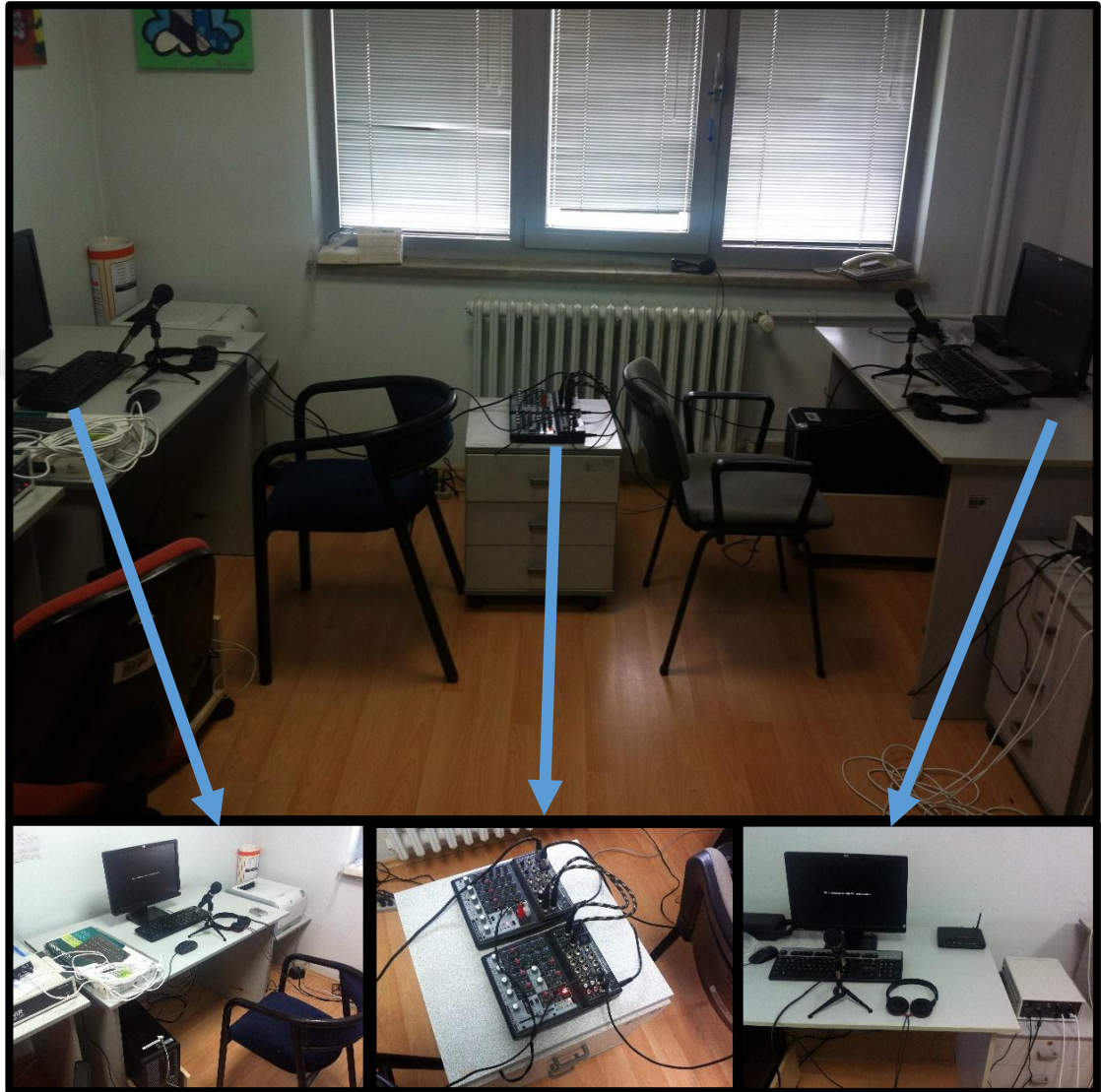


Figure 5: Photograph of the experimental setup

The participants sat back to back facing two LCD monitors, keyboards and microphones in front of them. Audio mixers are in between the participants and fNIR Devices are next to each computer (Upper). The participants are seated back to back in front of the stimulus displays. The participants wore headphones during the experiment (bottom left, bottom right). The researcher manipulated audio conditions and recorded the participants' speech with audio mixers (middle).

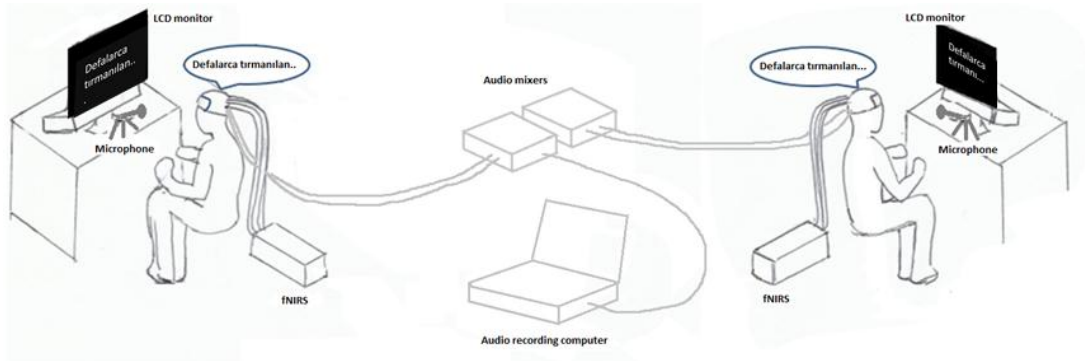


Figure 6: Schematics of the experimental setup

The experimental protocol included silent reading practice, silent reading and practice sentences as well as the main experiment. The participants completed silent reading practice, silent reading and practice sentences simultaneously before the start of the main experiment. In silent reading practice, both of the participants silently read a total of three sentences simultaneously as part of the procedure for getting familiar to the experimental conditions. Then, in the silent reading condition, the participants silently read a total of 7 sentences one of which is a mismatch sentence (Appendix A). In the practice sentences block, the participants started reading aloud five practice sentences simultaneously. These sentences were not reused in the experimental blocks. In the main experiment, the pairs of participants read 9 blocks of 7 sentences each. The number of matching and mismatching sentences in the experimental protocol was similar to the ratio of the number of matching and mismatching sentences in Cummins et al.'s (2013) study, such that there were a total of 6 mismatching sentences in a total of 9 experimental blocks (i.e., mismatching sentences in blocks 2, 3, 4 and 6, 7, 8) (Figure 7).

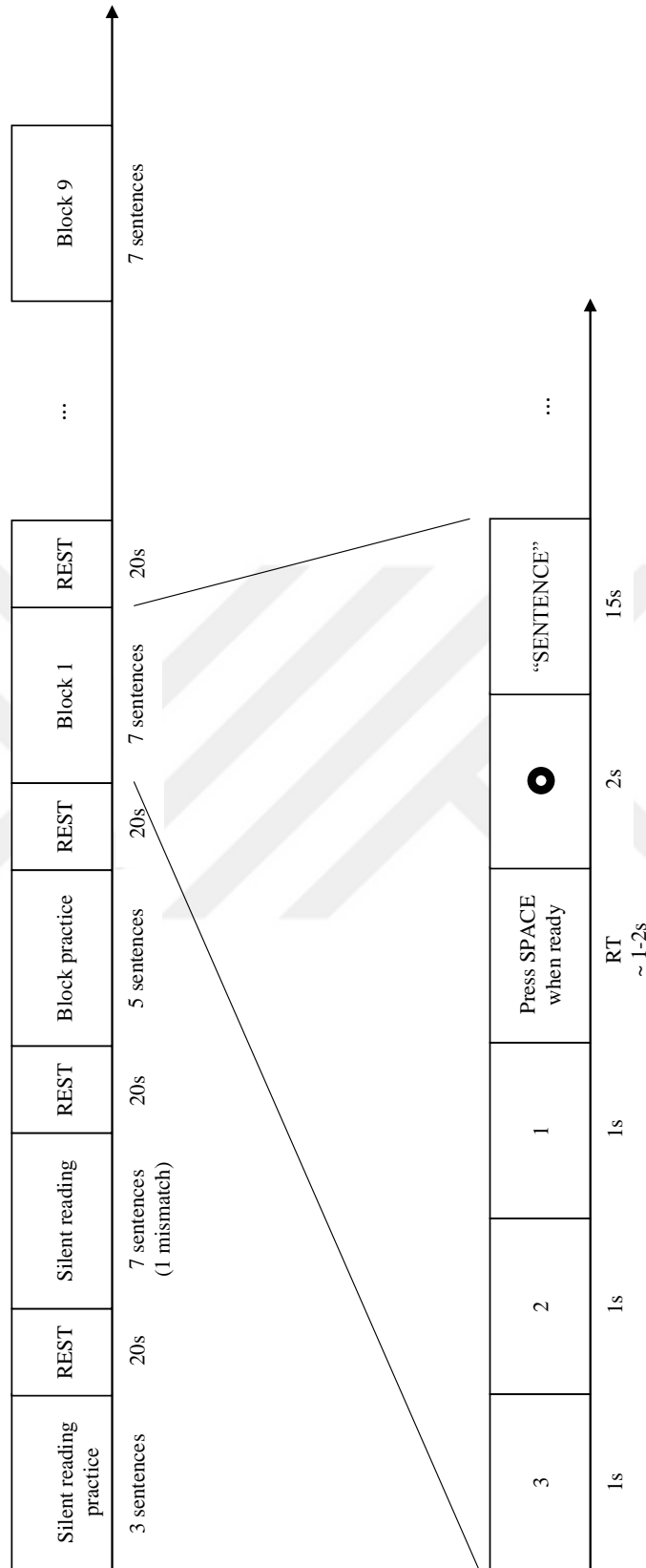


Figure 7: Experimental protocol

In this experimental design, two sentences in each block were repeated similar to Cummins et al. (2013) however, all of the sentences were used for quantitative asynchrony measurement. The participants read five matching sentences together as a practice before the actual data collection procedure. Then, in each block the participants jointly read aloud 7 sentences. In blocks 2-4 and 6-8, one participant of each pair was presented with a mismatching sentence where there was a pseudo-word (i.e., a pronounceable non-word) in the middle of the sentence. The presentation of the mismatching sentences was dispersed such that participants were not able to predict when mismatching sentences will come. Open Sesame (Mathôt et al., 2012) was used for the generation and presentation of experimental trials. During the experiment, the presentations of the target sentence on both participants' screens were automatically synchronized with the help of a custom TCP/IP based coordination script implemented in Python. The script also triggered two time-synchronization markers for the fNIRS recorders, to enable synchronized data acquisition from two participants.

3.1.5. Pre-task Baseline for Experimental Conditions

Before the experimental condition, participants completed silent reading practice and practice blocks in order to get familiar with the main experiment. In addition, before each block in the experimental condition, there was a 20 sec fixation period implemented as a REST condition. Within each block, before the sentence was displayed, a countdown was displayed on the screen as 3...2...1 followed by a text reading as 'SPACE'. Participants were instructed to press the SPACE key on their keyboards when prompted after the countdown. This step was added to help participants initiate sentence reading in a coordinated manner. The rest periods served as a baseline where the participants wait for the main experimental blocks.

3.2. Quantitative Assessment of Performance by Dynamic Time Warping Analysis of Asynchrony

Participants' speech waveforms were analyzed for an estimate of asynchrony using a method called dynamic time warping (DTW). Dynamic time warping algorithm was initially developed by Sakoe and Chiba (1978) for speech recognition. DTW is a well-known methodology for measuring the similarity between two time-series signals.

In this dissertation, dynamic time warping algorithm developed by Cummins, Li and Wang (2013) (MATLAB script) was used to quantitatively measure the asynchrony between the speech performance of two participants. In order to measure the asynchrony between the two speech waveforms, the pair's speech was exported as a WAV file for each participant. Cummins (2007) identified that shared pauses in the speech inflates estimated asynchrony. Therefore, only the voiced parts of the speech are extracted from the exported WAV files. Voiced parts of the standard file were identified by using the "ToPointProcess" function provided by the Praat software,

with sex-dependent parameters (Male: 75 to 350 Hz). The resulting PPFILe represented only the voiced parts of the speech signal. Each PPFILe has a header of information that consisted of 6 lines. These headers are removed by a custom Perl script by Cummins.

The dynamic time warping algorithm first converts speech waveforms that are aligned in real time to Mel Frequency Cepstral Coefficients (i.e., MFCC vectors). Then, the dynamic time warping algorithm warps one utterance onto the other to find a best fit between the two speech waveforms. The resulting warping curve is defined as the minimum cost path between the two speech waveforms (Figure 8).

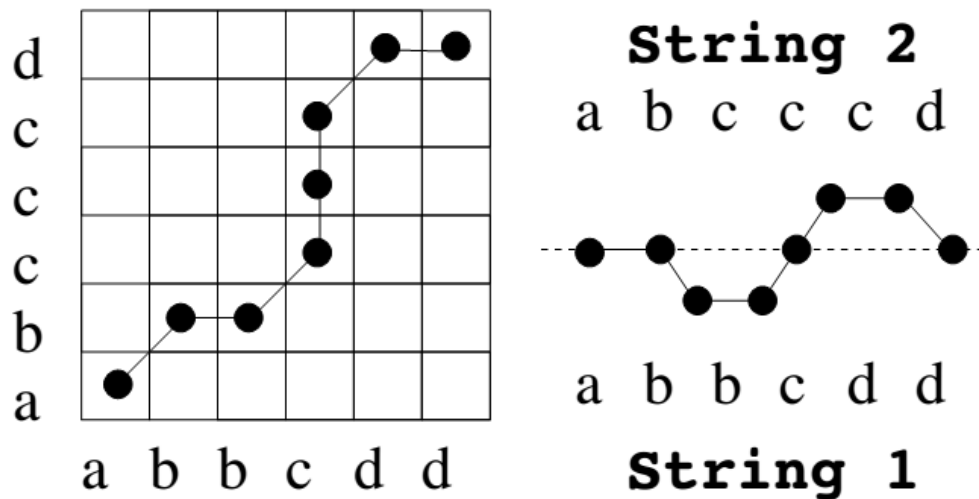


Figure 8: Standard Dynamic Time Warping path estimation (left)
 The resulting warping curve is used in estimating the degree of asynchrony between two strings of MFCC vectors (right). Adapted from Fred Cummins (2007).

The area under the warp curve is used as an estimate of asynchrony between the two speech waveforms. As the area under the warp path gets larger, the asynchrony between the two speeches becomes bigger.

Since dynamic time warping uses one speech waveform as a template to warp the other onto, and since the voiced parts of the speech is determined with respect to the template signal, this analysis was performed twice for each of the signals being templates. The resulting DTW scores were averaged to get a mean asynchrony score (Figure 9).

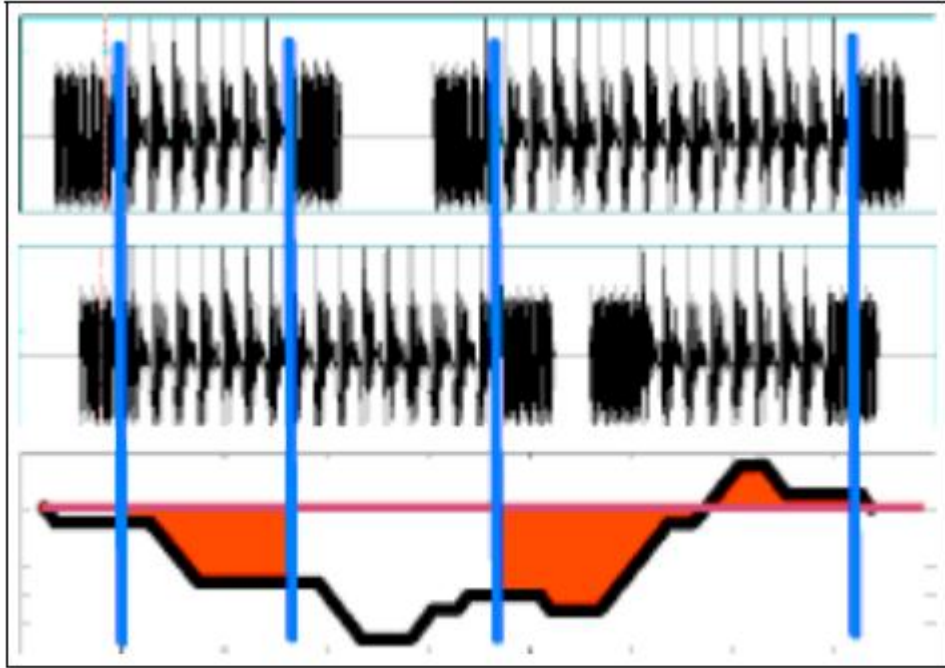


Figure 9: Time aligned speech waveforms with associated warp curve
 The area under the curve is represented with red and used to calculate the asynchrony between the signals. Adapted from Fred Cummins (2007).

3.3. Qualitative Assessment of Performance through Asynchrony Ratings

The DTW analysis is followed up with a qualitative evaluation of each pair's joint read aloud performance during the experiment. For each sentence uttered by the participants within each block, a rating between 1 and 5 was assigned to rate the level of perceived synchrony in their joint read aloud performance, where lower and higher ratings indicated poor and good performance respectively. Raters were instructed to consider specific factors while assigning their ratings, such as whether one partner was noticeably slower than the other, and whether they were able to pronounce each word in the sentence in an intelligible manner. Raters were also allowed to use half-way marks such as 3.5 or 4.5 as they see fit.

A reliability analysis was conducted over a sample of speech audio files obtained from 2 pair's 63 performances. As part of a reliability trial these files were independently rated by three raters. The raters used a custom developed graphical user interface that allowed them to play/re-play a sound file in the sample to store their ratings. The sound files were presented in a random order without providing any information about the experimental conditions. A Krippendorff's alpha statistic was computed by using the KALPHA script (Hayes & Krippendorff, 2007) in SPSS

to measure the level of agreement among the coders. An alpha of 0.69 was obtained among 3 raters, which suggests sufficient level of inter-rater reliability (Krippendorff, 2004). The rest of the voice recordings in the dataset is split into 3 equal parts and individually rated by one of three raters.

3.4. fNIRS Hyperscanning

In parallel with audio recordings of the participant pairs' speech, the hemodynamic changes in the participants' prefrontal cortices (PFC) were recorded simultaneously during the experiment by using two fNIRS devices. The experimental setup for the fNIR based neurophysiological measurements and data analysis methods are further explained in the following sections.

3.4.1. fNIRS Hyperscanning of Brain Activations

During the experiment the hemodynamic activity at the prefrontal cortex of each participant was measured with a continuous wave functional near-infrared spectroscopy (fNIRS) system developed at Drexel University (Philadelphia, PA), manufactured and supplied by fNIRS Devices LLC (Potomac, MD; www.fnirdevices.com) that is capable of measuring oxyhemoglobin and deoxyhemoglobin concentration changes (i.e., ΔHbO ($\mu\text{molar/Lt}$) and ΔHbR ($\mu\text{molar/Lt}$), respectively) in all optodes of the fNIRS sensor probe.

The system is composed of three modules: a flexible headpiece (sensor pad), which holds 4 light sources and 10 detectors to obtain oxygenation measures at 16 optodes on the prefrontal cortex; a control box for hardware management; and a computer that runs the COBI Studio software (Ayaz et al., 2011) for data acquisition (Figure 10). The sensor has a source-detector separation of 2.5 cm, which allows for approximately 1.25 cm penetration depth. This system can monitor changes in relative concentrations of oxy- and deoxy-hemoglobin at a temporal resolution of 2 Hz. The locations of 16 regions on the cortical surface monitored by fNIRS are displayed in Figure 10, which also correspond to Brodmann areas 9, 10, 44 and 45.

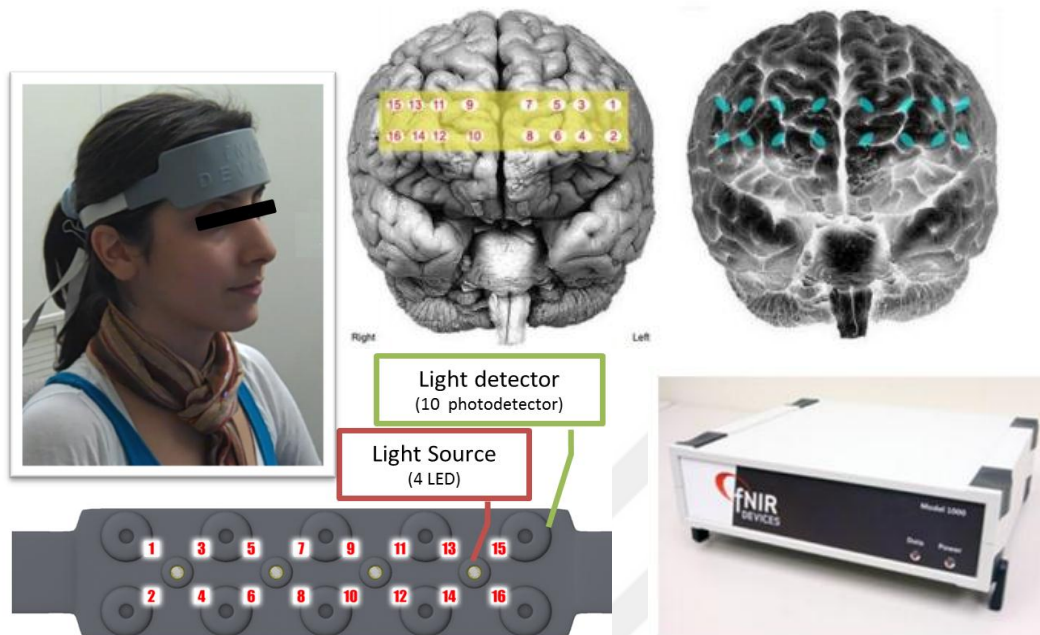


Figure 10: fNIRS devices and measurement locations
 fNIRS sensor (top left), projection of measurement locations (optodes) on brain surface image (top right), optodes identified on fNIRS sensor (bottom left) and fNIR Devices 1000 (bottom right)

fNIRS is a neuroimaging modality that enables continuous, noninvasive, and portable monitoring of changes in blood oxygenation and blood volume related to human brain function. Neuronal activity is determined with respect to the changes in oxygenation since variation in cerebral hemodynamics are related to functional brain activity through a mechanism known as neurovascular coupling (Obrig et al., 2000). Over the last decade, studies in the laboratory have established that fNIRS spectroscopy provides a veridical measure of oxygenation and blood flow in the brain (Bunce et al., 2006). fNIRS is not only non-invasive, safe, affordable and portable, it also provides a balance between temporal and spatial resolution which makes fNIRS a viable option for *in-the field* neuroimaging.

fNIRS technology uses specific wavelengths of light, introduced at the scalp, to enable the non-invasive measurement of changes in the relative ratios of deoxygenated hemoglobin (deoxy-Hb or HbR) and oxygenated hemoglobin (oxy-Hb or HbO₂) in the capillary beds during brain activity. fNIRS consists of near infra-red light sources and detectors that receive light after it has interacted with the tissue. Near-infrared light is known to diffuse through the intact scalp and skull, which makes it suitable for tracing relative changes in the concentration of specific chromophores in the neural tissue with non-invasive, spectroscopic methods (Jobsis, 1977). Whereas most biological tissue (including water) are relatively transparent to

light in the near infrared range between 700 to 900 nm, hemoglobin is a strong absorber of light waves in this range of the spectrum. Within 700 to 900 nm, oxy and deoxy-hemoglobin are among the highest absorbers of infra-red light. This provides an optical window into neural tissue where one can approximate relative changes in the concentration of oxy and deoxy-hemoglobin based on how infra-red light is attenuated in neural tissue.

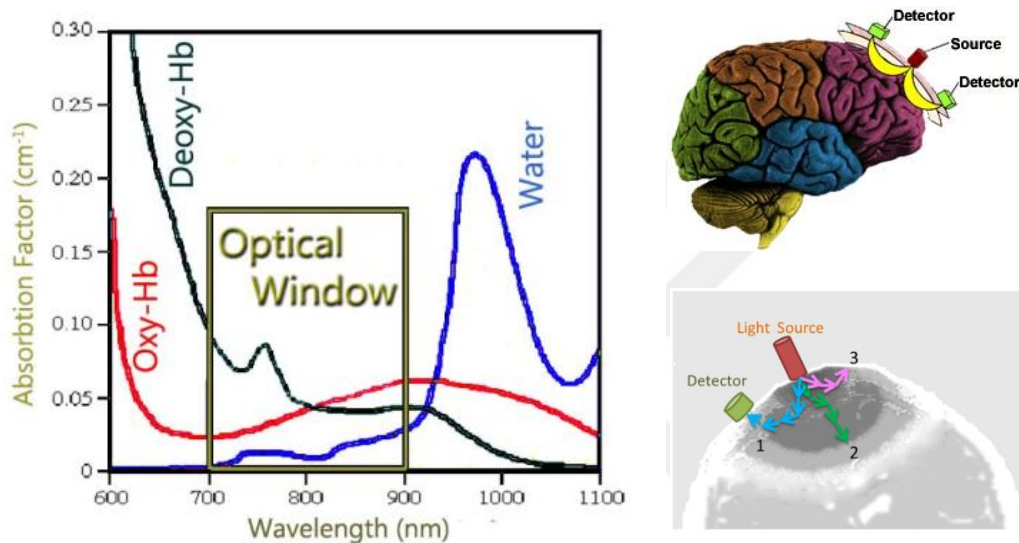


Figure 11: NIRS absorption pattern (left). fNIRS source-detector configuration and light path in neural tissue (right)

The banana shaped path which includes the photons scattered back to the photo-detector (top right). Representative paths (bottom right), enumerated as 2 and 3 correspond to photons absorbed by the tissue and scattered out of the scalp without reaching the detector, respectively. Adapted from Hasan Ayaz (2012).

Photons that enter tissue undergo two different types of interaction: absorption and scattering (Obrig et al., 2000). Two chromophores, oxy- and deoxy-Hb, are strongly linked to tissue oxygenation and metabolism. The absorption spectra of oxy- and deoxy-Hb remain significantly different from each other allowing spectroscopic separation of these compounds to be possible by using only a few sample wavelengths. Once photons are introduced into the human head, they are either scattered by extra- and intracellular boundaries of different layers of the head (skin, skull, cerebrospinal fluid, brain, etc.) or absorbed mainly by oxy- and deoxy-Hb. A photo-detector placed on the skin surface at a certain distance from the light source can collect the photons that are scattered and thus have travelled along a “banana shaped path” from the source to the detector, which carry important information about the optical properties of the diffused neural tissue (Figure 11). This raw light attenuation information is then converted into tissue oxygenation measures that

quantify the relative changes in the presence of oxy- and deoxy-hemoglobin within the banana shaped path by using a method called modified Beer Lambert law (Cope et al., 1988).

3.4.2. Functional Connectivity - Wavelet Transform Coherence (WTC)

Wavelet transform coherence (WTC) is used to evaluate functional connectivity between two brains of simultaneously speaking pairs. Wavelet transform coherence (also wavelet coherence) has been used in many areas ranging from image compression and storage of fingerprints to the analysis of oscillations in glacier movements and weather systems in geophysics. Wavelet transform coherence is a method to measure the cross-correlation between two time-series signals by decomposing the time series signal in a frequency-time space (Torrence & Compo, 1998). The wavelet coherence can be interpreted as the local squared correlation coefficient in the time-scale plane. In this regard, wavelet transform coherence is able to identify significant coherence between two brains in a pair of subjects.

In this respect, the coherence calculated by WTC analysis is an extension of Pearson correlation coefficient. However, unlike Pearson correlation coefficient, coherence in WTC is evaluated as a local correlation (i.e., time-locked) between two time-series signals as a function of frequency, and is therefore more suitable for the analysis of coordination or coupling between two hemodynamic signals in the context of brain-to-brain interactions.

In order to calculate wavelet coherence, the wavelet coherence MATLAB® package provided by Grinsted et al. (2004) on the authors' webpage (<http://noc.ac.uk/using-science/crosswavelet-wavelet-coherence>) was used in this study. In WTC analysis, a wavelet is used to decompose the original time-series data in time and frequency domains. A wavelet is a function with a mean of zero. In this analysis, Morlet wavelet was employed to analyze fNIRS signals. A Morlet wavelet is described by the following formula:

$$\psi_0(\mu) = \pi^{\left(\frac{-1}{4}\right)} e^{(j\omega_0\mu)} e^{\left(\frac{-1}{2}\mu^2\right)}$$

where ω_0 is the dimensionless frequency and μ is the dimensionless time.

In WTC analysis, 2D graphs of coherence between the two signals were generated. In these WTC graphs, the horizontal axis indicates the time course of the experiment (i.e., data points in WTC graphs) and the vertical axis indicates different periods (or frequencies) in the signal. The graph shows high coherence regions in red and low coherence regions in blue color. These high coherence regions were determined by Monte Carlo significance test with 95% confidence interval (significance level 0.05). Significant high coherence regions were indicated with a black contour line around the region. Another property of the WTC graph is that, the cone of influence (COI) is

depicted on the graph as a transparent white region of cone. Since wavelet-transform coherence deals with finite-length time series, the wavelet transform would produce errors at the beginning and end points of a signal. The cone of influence indicates these border effects.

3.4.3. Calculation of Frequency from Period

In this dissertation, the brain signals of the participants were recorded by fNIR Imager 1000 device which has a sampling rate of 2 Hz. Therefore, frequency (f) to be calculated from period for the WTC graphs is given by the following formula:

$$f = 1 / \left(\frac{\text{period}}{\text{sampling frequency}} \right)$$

According to this formula the period axis in the WTC graphs can be converted to frequencies as follows:

Period:	[2	4	8	16	32	64	128	256]
Freq.:	[1	0.5	0.25	0.125	0.0625	0.03125	0.015625	0.0078125]

In the wavelet transform coherence graphs, periods 2-4 (1 Hz – 0.5 Hz) corresponds to heart rate of the participants. In addition, periods 4-8 (0.5 Hz – 0.25 Hz) were attributable to respiration of the participants. Physiological signals such as heart rate (over 0.5 Hz) and respiration (over 0.2 Hz) are at higher frequency ranges than hemodynamic responses (Ayaz et al. 2011) and therefore were ignored in wavelet coherence analysis.

Time-synchronized HbO and HbR signals were fed into the MATLAB® function developed by Grinsted et al. (2004) to compute the frequency-time plots and WTC measures for each pair. The data was collected at 2Hz by fNIR Devices 1000 and each task block for read aloud epochs consisted of 7 trials. Each trial (reading aloud a sentence) lasted for (20+RT)s. RT is the reaction time of the participants to press SPACE key on the keyboard when they are ready and the time for the computers to get synchronized and display the next sentence to be read aloud on the screen. RT was between ~1-2s and thus period of each trial was between ~21-22s.

In the Figure 12 below, a wavelet transform coherence graph is plotted between the two participants' deoxy-hemoglobin signals from optode 13 in the pre-frontal cortex. The coherence value is computed between 0 and 1 and is shown as a color legend in the graph. Monte Carlo significance tests indicate significant coherence regions (i.e., red regions in the WTC graph) by encircling these regions with a black contour line. The period band of interest was shown as a white region between period 32s and period 64s in the WTC graph. The significant wavelet coherence values in this study

are found in this band (from period 32s to 64s or frequency 0.0635Hz to 0.03125Hz) since periods 32s-64s region corresponds to 16s – 32s trial time (due to 2Hz data collection frequency) and thus includes the period of the blocks (~ 21-22 s) in joint sentence reading task.

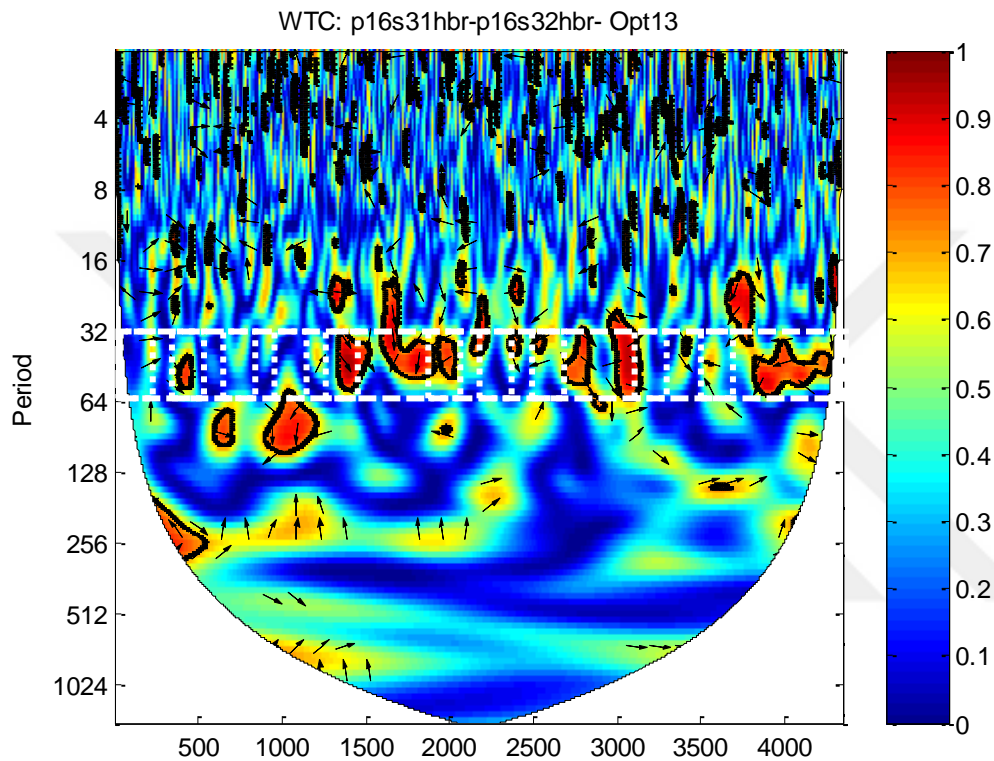


Figure 12: Wavelet transform coherence (WTC) analysis between two raw deoxy-Hb (HbR) signals from optode 13 of the 1st participant and the raw deoxy-Hb (HbR) signal from optode 13 of the 2nd participant in pair 16. The coherence value is between 0 and 1. High coherence is indicated by red regions in the graph.

The WTC values for the data epochs for the rest and task periods were extracted from the continuous data using time synchronization markers, which were automatically triggered in a synchronized manner by both partner’s computers as they were presented each sentence. These time synchronization markers defined the white colored regions of windowed areas in the WTC graph from which significant coherence values are extracted.

The WTC measure for each block is then subtracted from the WTC measure corresponding to the rest period to calculate mean coherence increase measure for each block. The coherence increase measures are then converted into z-scores using the Fisher-transform. One sample t-tests were conducted for each condition to detect

optodes that exhibit non-zero coherence values. Since multiple t-tests were conducted for match/mismatch and self/both/other/silent conditions, a False Discovery Rate (FDR) correction (Benjamini & Hochberg, 1995) was applied to control family-wise error rate. The FDR corrected t-test results were then used to produce t-maps with spline smoothing in the fNIRSoft software to visualize locations of strong coherence over the prefrontal cortex.

3.4.4. Validation of the coherence

In order to verify that the coherence increase between the participants was due to the task conditions and is not independent of the experimental conditions, the researchers randomly paired the data from each participant such that the participants in these new pairs had not communicated previously and were from totally different pairs who did not interact with each other. Then, wavelet transform coherence analysis was performed on these randomly matched pairs. This method of random matching of participants served as a control condition in order to compare the coherence increase between the participants during different experimental conditions with respect to the random matching condition.

3.5. Ethics Committee Approval

The participants for this dissertation were recruited from a public university. The experimental procedures did not involve any harm to the participants. The participation was entirely on voluntary basis and the participants could leave the study in case they need to do so. All the procedures and experimental protocols were approved by the METU Applied Ethics Committee.

3.6. Summary of the Methodology

In this dissertation, several methods were used to investigate the peoples' behavioral and brain-to-brain interactions during joint reading of Turkish sentences in different experimental conditions such as auditory (self, both, other) and block (match, mismatch) conditions. In order to investigate the behavioral synchrony and brain-to-brain interactions, the participants were invited to the experiment room where they sat back-to-back. In the room, auditory and brain activations of the participants' PFC were recorded by audio setup and fNIR devices, respectively. The behavioral synchrony of the participants was measured both quantitatively and qualitatively. For the quantitative measurement, dynamic time warping (DTW) algorithm was used. DTW measures the asynchrony between two speech signals by warping one speech onto the other and computing the resulting warp path and area under the warp curve as a measure of the asynchrony. For the qualitative measurement, three raters rated the participants' speech between 1 and 5. Poor synchrony between the participants was rated 1 while good performance was rated 5. The raters also used half-way points such as 1.5 and 4.5. The ratings were then cubic transformed for a more symmetric distribution of the scores. The scores from quantitative and qualitative

measurement methods were subjected to a 3x2 repeated measures ANOVA in order to determine significant main effects and interactions.

In addition to behavioral measurements, prefrontal cortex activations of the participants were simultaneously measured by fNIR devices during joint sentence reading task. The brain-to-brain interactions were quantified by wavelet transform coherence (WTC) method that calculates the coherence between two brain signals. Coherence increase was computed as the difference between the coherence in the task block and the coherence in the rest before the task such that the coherence in the rest block was subtracted from the coherence in the task block (Coherence increase = Block coherence – Rest coherence). Moreover, the participants were randomly matched as a control condition. Random matching of the participants allowed the researcher to compare the coherence increase in the experimental conditions and validate the coherence increase as due to the manipulation of experimental factors rather than by chance coherence.

CHAPTER 4

RESULTS

In this chapter, the results of the joint sentence reading study are described. The results are organized under three main categories as behavioral analysis, brain activation and coherence analysis results. For behavioral analysis results quantitative and qualitative assessments of joint reading performance are reported. For brain activation results, the participants' prefrontal cortex activations as described by the changes in the relative concentrations of oxy-hemoglobin (HbO) within each 16 optodes in auditory (i.e., self, both, other) and block (i.e., match, mismatch) conditions during joint sentence reading conditions are reported. Finally, for the coherence analysis, brain-to-brain interactions as defined by the coherence values obtained from wavelet transform coherence analysis based on oxy-hemoglobin (HbO) and deoxy-hemoglobin (HbR) results are reported.

4.1. Behavioral Analysis Results

4.1.1. Quantitative Assessment of Performance

A 3x2 repeated measures ANOVA was conducted where auditory condition (both, self, other) and the block type (match, mismatch) were within-subjects independent variables and the mean asynchrony scores obtained from the DTW algorithm was the dependent variable. The data met the sphericity assumption, so no corrections were applied, $W(2)=.78$, $p>.05$. The ANOVA results suggested a significant main effect of auditory condition, $F(2, 42) = 15.23$, $p<.001$, partial $\eta^2=.42$, as well as a significant main effect of block type $F(1, 21) = 17.39$, $p<.001$, partial $\eta^2=.45$. No significant interaction was observed. Sidak corrected post-hoc tests showed that the Other ($M=321.85$, $SE=5.60$) condition elicited significantly higher mean asynchrony values as compared to Both ($M=309.40$, $SE=5.63$, $MD=12.45$, $p<.001$) and Self ($M=298.89$, $SE=5.97$, $MD=22.96$, $p<.05$) conditions. Moreover, the asynchrony level observed in the Both condition was significantly higher than the Self condition, $MD=10.51$, $p<.01$. Finally, the match blocks ($M=306.99$, $SE=5.58$) received significantly lower asynchrony values than the mismatch blocks ($M=313.11$, $SE=4.92$), $MD=-6.11$, $p<.001$ (Table 1) (Figure 13) (Figure 14).

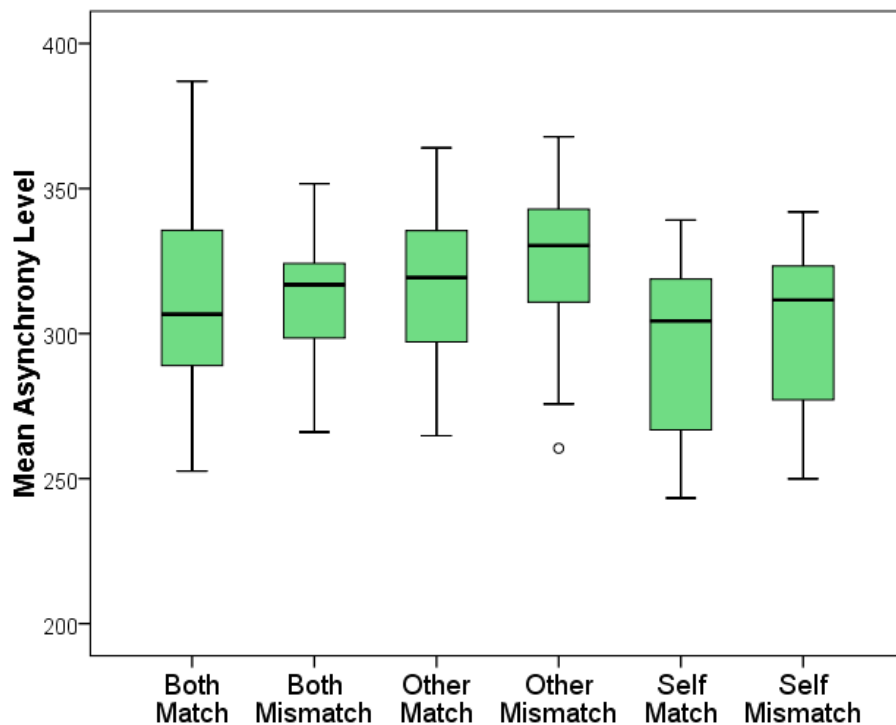


Figure 13: Quantitative assessment of performance

Table 1. Repeated measures ANOVA for quantitative assessment of performance

	Sum of Squares	df	Mean Square	F	p	η^2
Auditory Condition	11622.6	2	5811.28	15.229	< .001	0.420
Residual	16026.6	42	381.59			
Block Type	1233.4	1	1233.43	17.394	< .001	0.453
Residual	1489.2	21	70.91			
Auditory Condition * Block Type	259.5	2	129.74	0.670	0.517	0.031
Residual	8138.7	42	193.78			

Note. Type III Sum of Squares

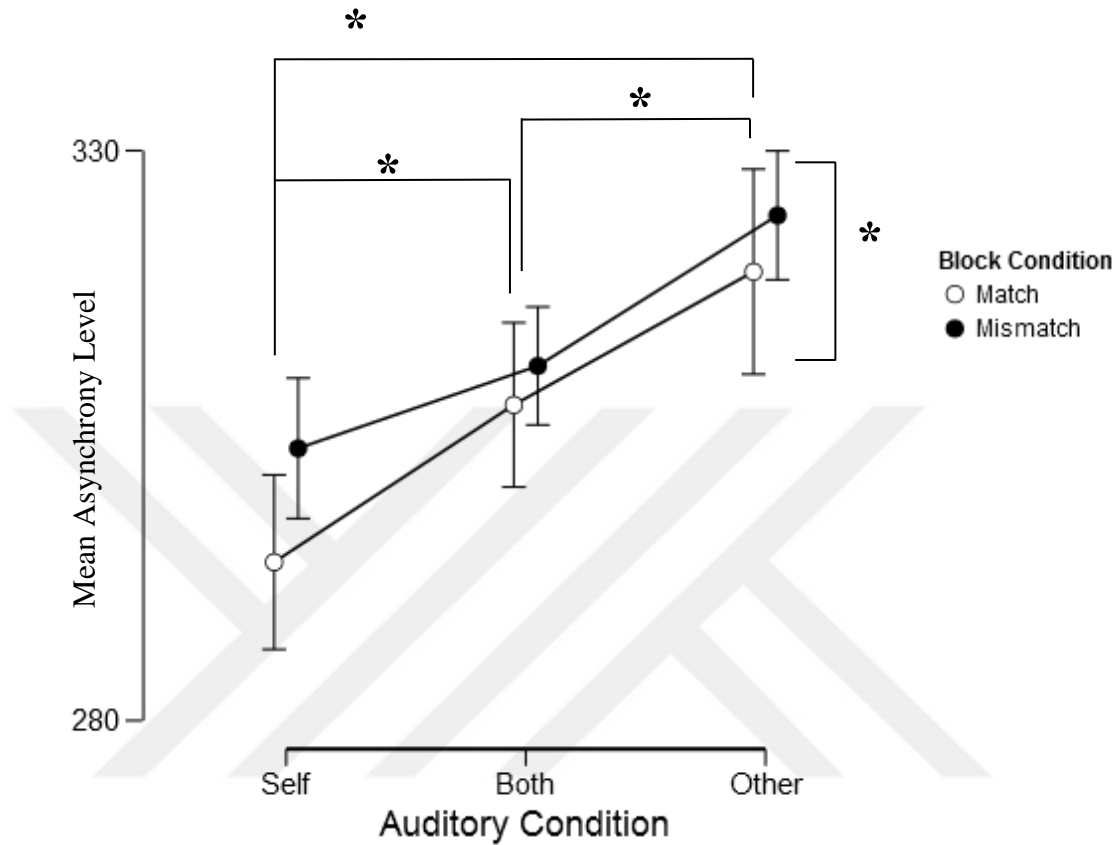


Figure 14: Line graph DTW Self, Both, Other

4.1.2. Qualitative Assessment of Performance

The DTW analysis is followed up with a qualitative evaluation of each pair's read aloud performance during the experiment. For each sentence uttered by the participants within each block, a rating between 1 and 5 was assigned to rate the level of perceived synchrony in their joint read aloud performance, where lower and higher ratings indicated poor and good performance respectively. Raters were instructed to consider specific factors while assigning their ratings, such as whether one partner was noticeably slower than the other, and whether they were able to pronounce each word in the sentence in an intelligible manner. Raters were also allowed to use half-way marks such as 3.5 or 4.5 as they see fit.

A reliability analysis was conducted over a sample of speech audio files obtained from 2 pair's 63 performances. As part of a reliability trial these files were independently rated by three raters. The raters used a custom developed graphical user interface that allowed them to play/re-play a sound file in the sample to store their ratings. The sound files were presented in a random order without providing any information about the experimental conditions. A Krippendorff's alpha statistic

was computed by using the KALPHA script (Hayes & Krippendorff, 2007) in SPSS version 23.0 to measure the level of agreement among the coders. An alpha of 0.69 was obtained among 3 raters, which suggests sufficient level of inter-rater reliability was obtained (Krippendorff, 2004). The rest of the voice recordings in the dataset is split into 3 equal parts and individually rated by one of three raters.

The pairs read aloud 7 sentences in each block. The mean of the ratings for these 7 sentences were considered as the overall rating of that block. The blocks were then organized under 6 categories corresponding to each auditory and block type combination. The distributions of ratings for each experiment condition exhibited a left-skewed distribution. A cubic transformation was applied to obtain a more symmetric distribution suitable for the use of parametric tests. The boxplot in Figure 15 shows the distribution of the ratings after the cubic transformation.

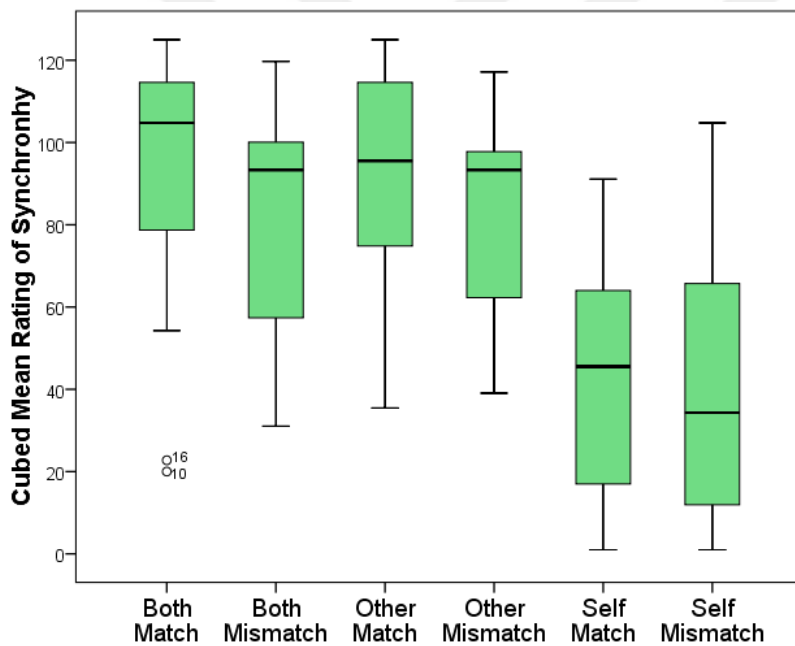


Figure 15: Qualitative assessment of performance

A 3x2 repeated measures ANOVA was conducted where auditory condition (both, self, other) and the block type (match, mismatch) were within-subjects independent variables and the cubed ratings were the dependent variable. A Huynh-Feldt correction was applied since the auditory condition variable violated sphericity, $W(2)=.65$, $p<.01$, $H-F=.77$. The ANOVA results suggested a significant main effect of auditory condition, $F(1.55, 43.35) = 78.53$, $p<.001$, partial $\eta^2=.73$, as well as a significant main effect of block type $F(1.0, 28.0) = 14.31$, $p<.01$, partial $\eta^2=.34$. The interaction was not significant. Sidak corrected post-hoc tests showed that Both ($M=87.23$, $SE=4.63$) and Other ($M=87.05$, $SE=4.08$) conditions elicited significantly

higher ratings as compared to the Self ($M=41.59$, $SE=5.07$) condition, $MD=45.64$, $p<.001$ and $MD=45.45$, $p<.001$ respectively. Moreover, the match blocks ($M=76.26$, $SE=4.00$) received significantly higher ratings than the mismatch blocks ($M=67.66$, $SE=4.17$), $MD=8.60$, $p<.01$ (Table 2) (Figure 16).

Table 2. Repeated measures ANOVA for qualitative assessment of performance

	Sphericity Correction	Sum of Squares	df	Mean Square	F	p	η^2
Auditory Condition	Huynh-Feldt	80211.9 ^a	1.548 ^a	51804.5 ^a	78.534 ^a	< .001 ^a	0.737
Residual	Huynh-Feldt	28598.2	43.354	659.6			
Block Type	Huynh-Feldt	3215.1	1.000	3215.1	14.312	< .001	0.338
Residual	Huynh-Feldt	6289.9	28.000	224.6			
Auditory Condition	* Huynh-Feldt	881.0	2.000	440.5	1.790	0.176	0.060
Block Type							
Residual	Huynh-Feldt	13778.8	56.000	246.1			

Note. Type III Sum of Squares

^a Mauchly's test of sphericity indicates that the assumption of sphericity is violated ($p < .05$).

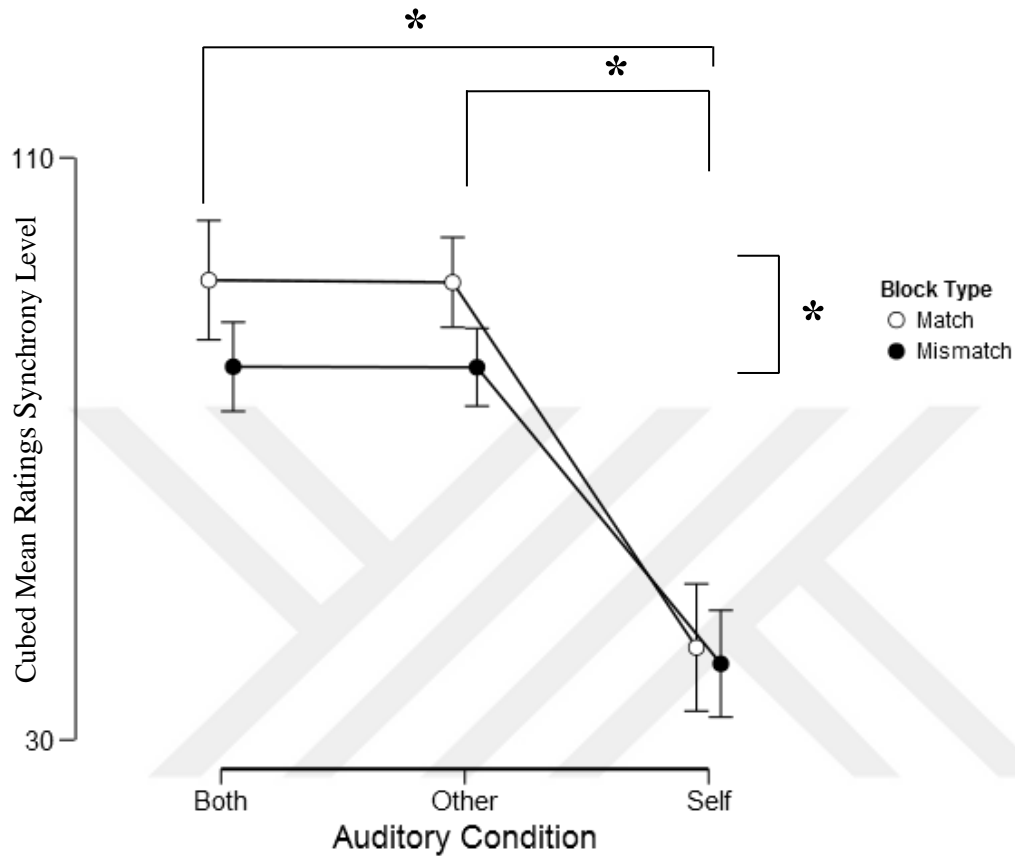


Figure 16: Line graph rating Self, Both, Other

4.2. Brain Activation Results

During the experiment brain activity measures were obtained from 16 locations distributed over each participant's prefrontal cortex. Raw fNIR data (16 optodes \times 2 wavelengths) were first checked for signal quality. Saturated channels (if any), in which light intensity at the detector was higher than the analog-to-digital converter limit were excluded. Artifacts due to motion are detected and excluded by applying the sliding windows motion artifact filter (Ayaz et al., 2010). The remaining raw fNIR signals were low-pass filtered with a finite impulse response, linear phase filter with order 20 and cut-off frequency of 0.1 Hz to attenuate the high frequency noise due to respiration and cardiac cycle effects (Izetoglu et al., 2005). fNIR data epochs for the rest and task periods were extracted from the continuous data using time synchronization markers, which were automatically triggered in a synchronized manner by both partner's computers as they were presented each sentence. Changes in the relative concentrations of oxy-hemoglobin (HbO) and deoxy-hemoglobin (HbR) within each 16 optodes were calculated using the modified Beer-Lambert Law

for task periods with respect to rest periods at the beginning of each trial with fNIRSoft (Ayaz, 2010).

The level of hemodynamic response elicited by each experimental condition was assessed through 3x2 repeated measures ANOVAs over the mean HbO concentration change observed across the 16 optodes. We chose to focus on HbO as it highly correlates with the fMRI's BOLD signal, so as to discuss the findings of the study in relation to relevant fMRI studies (Cui et al., 2011; Sato et al., 2013).

Figure 17 below shows the mean HbO concentration change observed during all joint speech conditions at all 16 measurement locations. Highest levels of activity were observed at optode 3 over left dIPFC (close to the Broca's region), optode 4 in the left inferior frontal gyrus, optode 6 in the left dmPFC, optode 9 in the right frontopolar region, optode 11 in the right dmPFC and optode 13 in the right dIPFC (close to the right homologue of Broca's region).

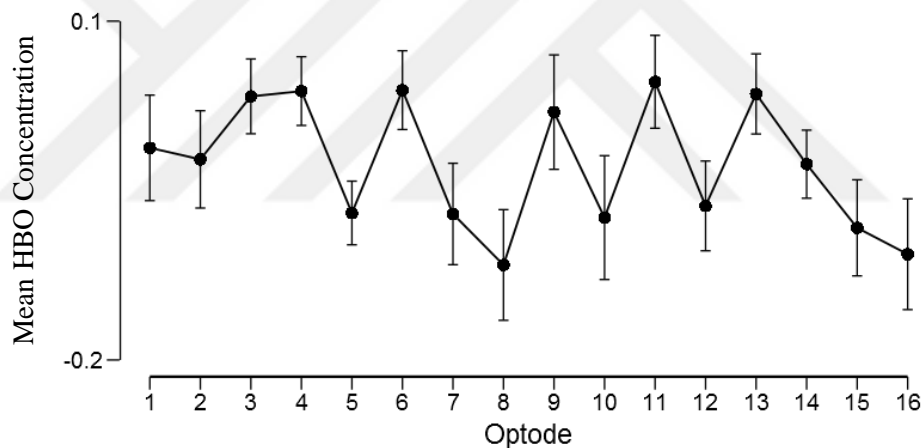


Figure 17: Overall mean HbO concentration changes ($\mu\text{molar/Lt}$) observed at each optode. The whiskers indicate standard error of the mean.

A main effect of block type (match vs mismatch) was observed at all locations except optodes 10 and 14. Significantly higher mean HbO levels were observed during match blocks as compared to mismatch blocks (Table 3). (Figure 18).

Table 3. Mean HbO activation levels in 16 optodes

	F	df	Sig. (2-tailed)	partial η^2
Optode 1	9.25	(1,23)	.006*	.29
Optode 2	8.82	(1,46)	.005*	.16
Optode 3	5.56	(1,47)	.023*	.11
Optode 4	8.97	(1,39)	.005*	.19
Optode 5	9.71	(1,38)	.003*	.20
Optode 6	8.98	(1,40)	.005*	.18
Optode 7	18.20	(1,33)	.000*	.36
Optode 8	5.84	(1,32)	.022*	.15
Optode 9	6.94	(1,28)	.014*	.20
Optode 10	2.62	(1,32)	.115 ^{ns}	.08
Optode 11	21.86	(1,34)	.000*	.39
Optode 12	4.33	(1,32)	.046*	.12
Optode 13	5.89	(1,36)	.020*	.14
Optode 14	1.52	(1,30)	.228 ^{ns}	.05
Optode 15	9.36	(1,49)	.004*	.16
Optode 16	7.71	(1,41)	.008*	.16

* : significant ($p < .05$), ns: non-significant

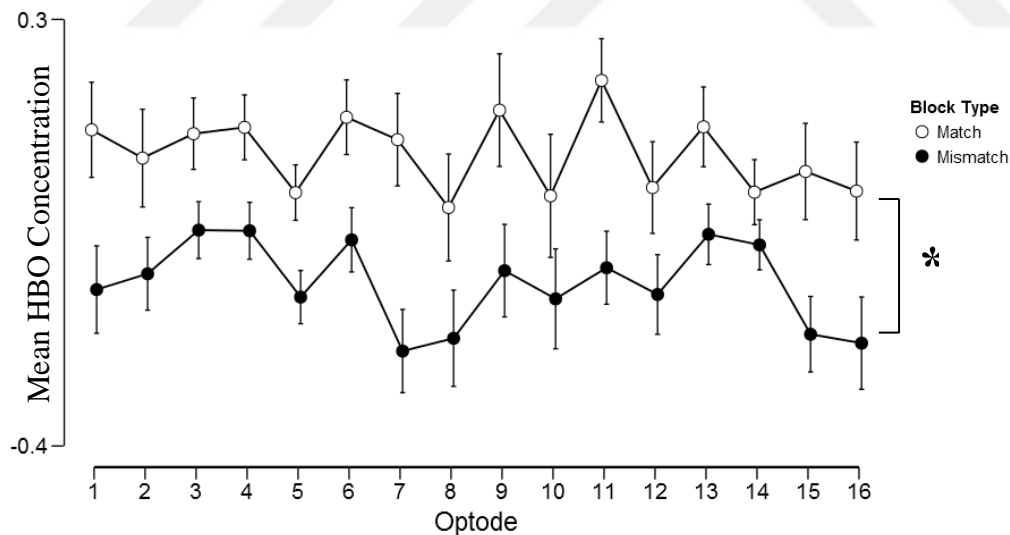


Figure 18: Mean HbO concentration changes ($\mu\text{molar/Lt}$) observed at each optode for the match and mismatch blocks

The whiskers indicate standard error of the mean.

A main effect of auditory condition was observed only in optode 2 ($F(2,92)=7.83$, $p < .01$, partial $\eta^2=.15$), which monitors a region within left inferior frontal gyrus. No interaction was observed between block type and auditory condition at optode 2. Sidak corrected pairwise comparisons indicated the Other condition elicited higher

mean HbO levels as compared to Self ($MD=.216, p=0.51$) and Both ($MD=.34, p<.01$) conditions. A similar trend across levels of the auditory condition was observed in optode 4, which was only marginally significant ($F(2,78)=3.03, p=0.54$, partial $\eta^2=.07$). A Sidak corrected post-hoc comparison suggested that this was due to the higher mean HbO observed in the Other condition as compared to the Both condition, $MD=.17, p<.05$ (Figure 19).

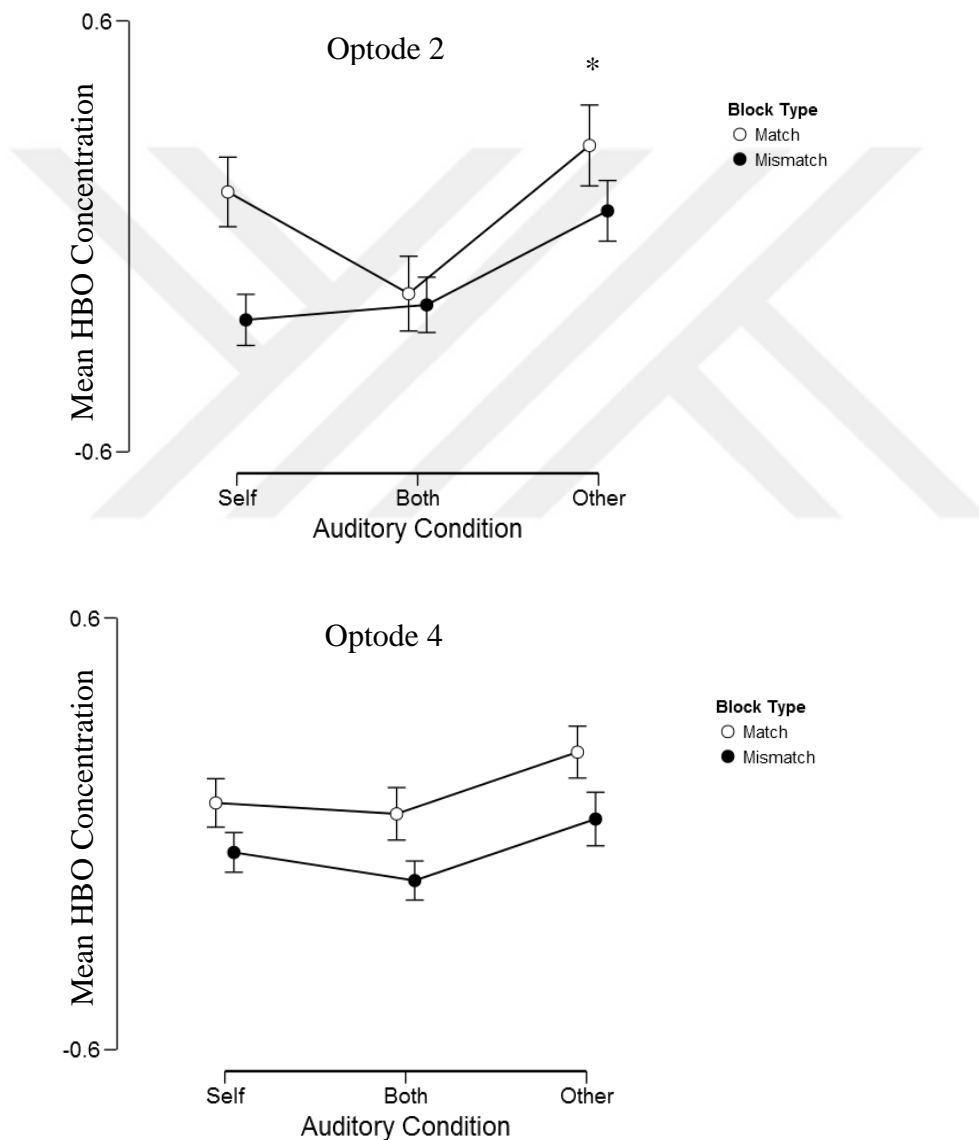


Figure 19: Mean HbO concentration changes ($\mu\text{molar/Lt}$) observed at Optode 2 and 4 for each auditory and block condition. The whiskers indicate standard error of the mean.

The interaction between the levels of auditory condition and the block types did not reach significance in 15 out of 16 optodes. A marginally significant interaction was observed at optode 11, $F(2,68)=2.83$, $p=0.066$, partial $\eta^2=.08$ (Figure 20).

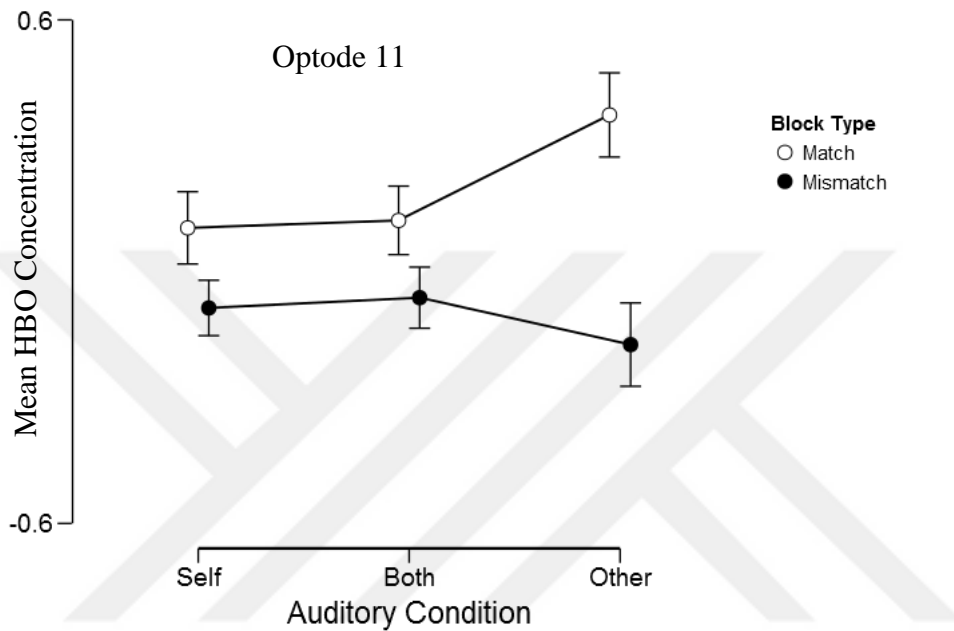


Figure 20: Mean HbO concentration changes ($\mu\text{molar/Lt}$) observed at Optode 11 showed an interaction between auditory conditions and block types. The whiskers indicate standard error of the mean.

4.3. Coherence Analysis

Coherence analysis was conducted over Wavelet Transform Coherence (WTC) measures computed for each pair's HbO and HbR signals. For this purpose, the HbO and HbR signals were computed from raw NIR signals by applying the Modified Beer Lambert Law in reference to the baseline measures obtained before the experiment. The raw NIR measures were qualitatively checked for signal quality and the presence of artifacts. Problematic cases due to excessive motion and saturated channels were excluded from analysis. WTC measures were computed in MATLAB® by using the WTC script developed by Grinsted et al. (2004).

Wavelet Transform Coherence method, which is a method to define the local correlation between two time-series signals in the time frequency domain, was originally used in the Geosciences field by Grinsted et al. (2004) to investigate the relationship between Arctic Oscillation Index and sea ice in the Baltic region. Recently, WTC method was applied to the analysis of NIRS data by Cui et al. (2012)

and Jiang et al. (2012) to quantify brain-to-brain interactions (i.e., inter-brain coherence/synchronization) during cooperative vs. competitive and face-to-face vs. face-blocked communication conditions. Similarly, WTC method was used in this study to measure the degree of coherence between the HbO and HbR concentration changes of both partners during each experimental condition. For this purpose, HbO and HbR signals were computed with respect to the eyes-closed rest period recorded at the beginning of the experiment. Since WTC separates different frequency bands from each other, high frequency noise due to heartbeat and respiration can be separated from other frequencies of interest in which the task is performed. For that reason, no pre-processing steps such as low pass filtering or de-trending were performed on the raw NIR signals and the HbO/HbR signals.

Since the data was collected at 2Hz by fNIR Devices 1000 and each trial for reading-aloud in experiment blocks lasted approximately ~21-22 seconds, the period range of interest in the frequency band for the WTC graph was chosen between 32s to 64s (16s – 32s trial period). Within the time boundary of each block, the values in this frequency band were averaged to obtain the WTC value for the corresponding block. The WTC measure for each block is then subtracted from the WTC measure corresponding to the rest period to calculate mean coherence increase measure for each block. The coherence increase measures are then converted into z-scores using the Fisher-transform. One sample t-tests were conducted for each condition to detect optodes that exhibit non-zero coherence increase values. Since multiple t-tests were conducted for match/mismatch and self/both/other/silent conditions, a False Discovery Rate (FDR) correction (Benjamini & Hochberg, 1995) was applied to control family-wise error rate. The FDR corrected t-test results were then used to produce t-maps with spline smoothing in the fNIRSoft software to visualize locations of strong coherence over the prefrontal cortex.

In the related literature NIRS coherence analysis has been conducted over HbO (Cui et al., 2012; Jiang et al., 2012) and HbT (Holper et al., 2012) signals and interpreted in a similar manner, which are known to correlate with the fMRI BOLD signal (Sato et al., 2013) and the total blood flow (Izzetoglu et al., 2005), respectively. In addition to this, HbR changes can serve as another measure sensitive to neural activity (Yamamoto & Kato, 2002). For these reasons, we conducted coherence analysis over HbO and HbR measures.

4.3.1. HbR Coherence Analysis Results

Figure 21 shows the HbR coherence increase values observed in the prefrontal cortex during both, other, self and silent conditions. The HbR coherence increase is stronger in the right dorsolateral and right superior frontal cortices. In the self condition a stronger HbR coherence increase trend was observed in the left dorsolateral and left dorsomedial prefrontal cortices as compared to both and other cases. The silent condition elicits the lowest level of coherence increase as expected. Participants were reading sentences that are shown at the same time silently in this condition, which

seems to elicit some significant coherence increase around the right inferior frontal gyrus.

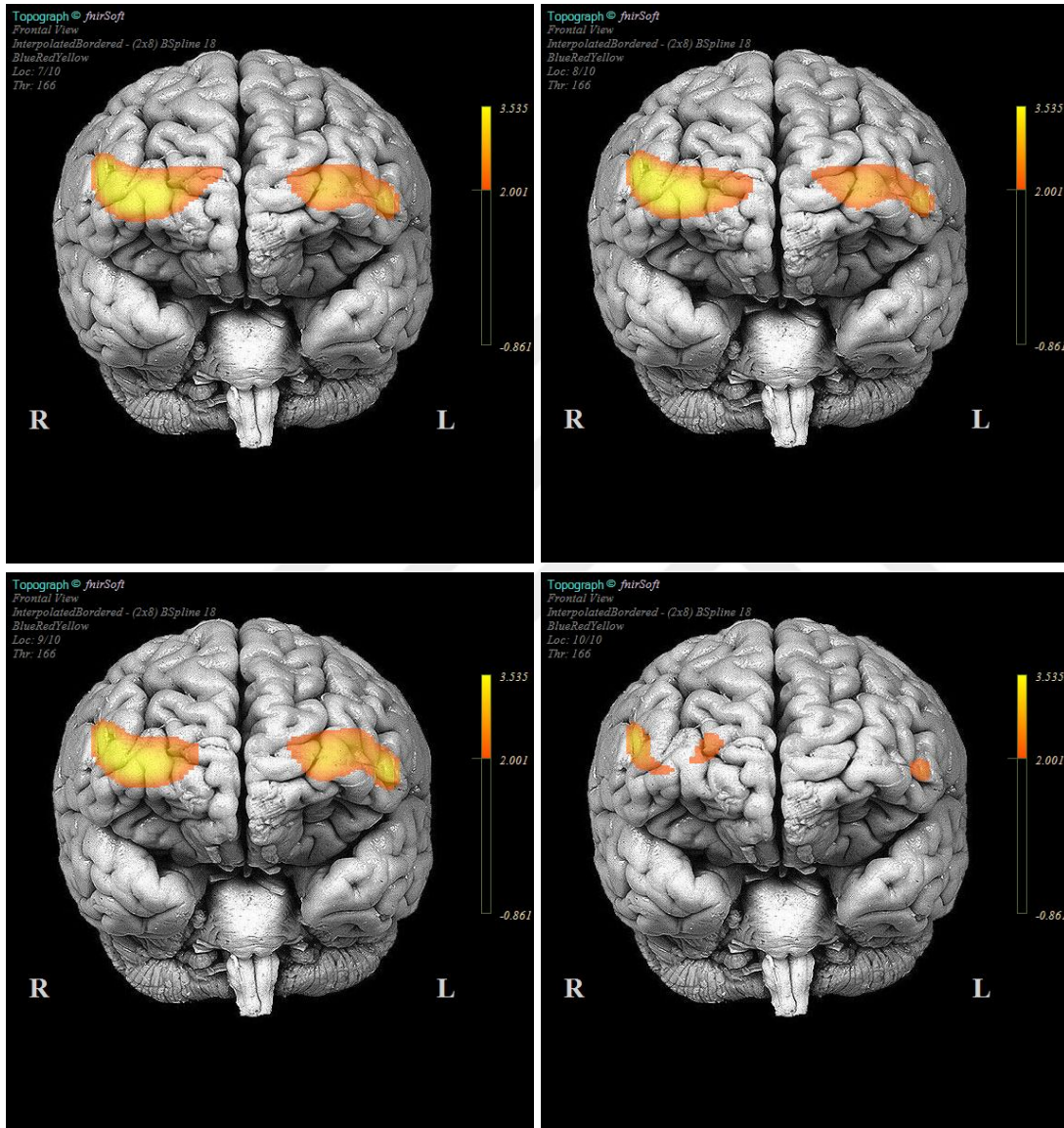


Figure 21: FDR corrected t-maps for HbR coherence increase measures observed at both (top-left), other (top-right), self (bottom-left) and silent (bottom-right) conditions.

Figure 22 shows the HbR coherence increase values observed in the prefrontal cortex during both, other and self conditions by distinguishing match cases from mismatch cases. In the mismatch blocks there was one sentence that included a non-word, which was found to disrupt the joint speech of the pairs in most cases as indicated by the behavioral analysis. The coherence trends look similar across matching and

mismatching conditions, except the both condition where the mismatch case elicited less coherence in the left-dIPFC and right-dmPFC regions as compared to the match case.

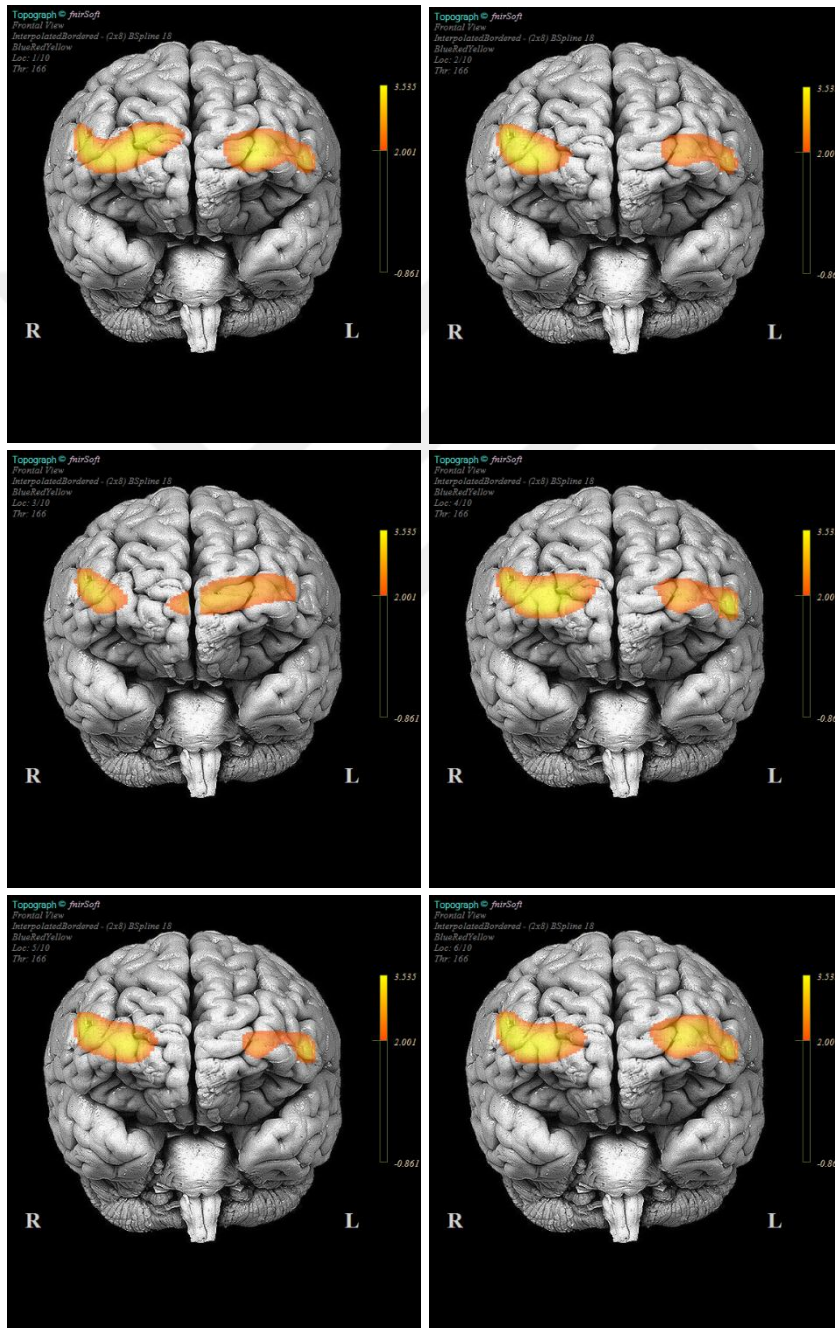


Figure 22: FDR corrected t-maps for HbR coherence increase measures obtained for the both-match (top-left), both-mismatch (top-right), other-match (middle-left), other-mismatch (middle-right), self-match (bottom-left) and self-mismatch (bottom-right) cases.

4.3.2. HbO Coherence Analysis Results

Figure 23 shows the HbO coherence increase values observed in the prefrontal cortex during both, other, self and silent conditions. In contrast to HbR t-maps, we observed a lower level of coherence among HbO signals. Right-dIPFC and partly the right superior PFC showed the highest coherence in the both condition. Right-dIPFC region exhibited high degree of coherence in other and self conditions, whereas almost no coherence pattern was observed during the silent condition.

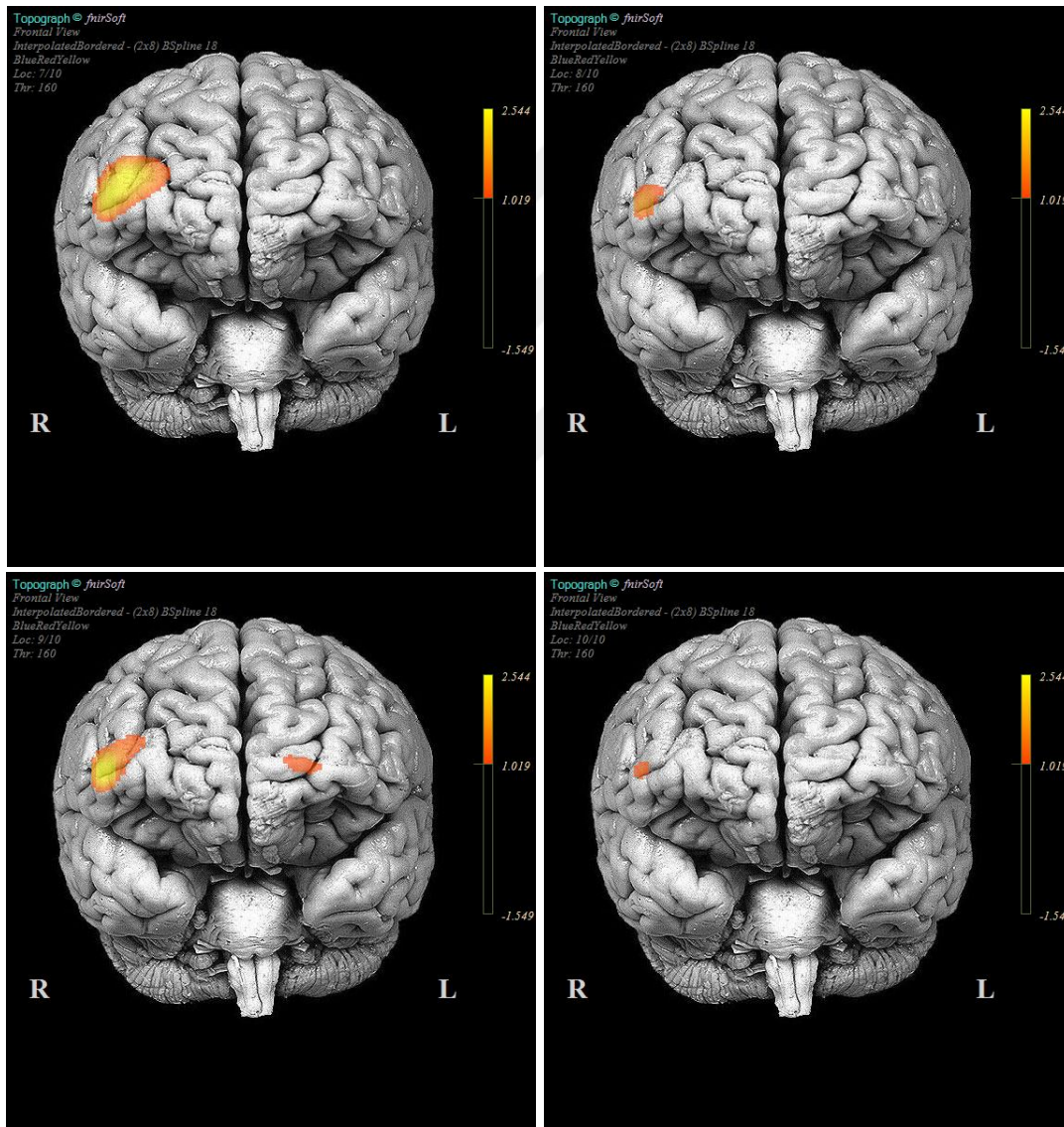


Figure 23: FDR corrected t-maps for HbO coherence increase measures observed at both (top-left), other (top-right), self (bottom-left) and silent (bottom-right) conditions.

Figure 24 shows the HbO coherence increase values observed in the prefrontal cortex during both, other and self conditions by distinguishing match cases from mismatch cases.

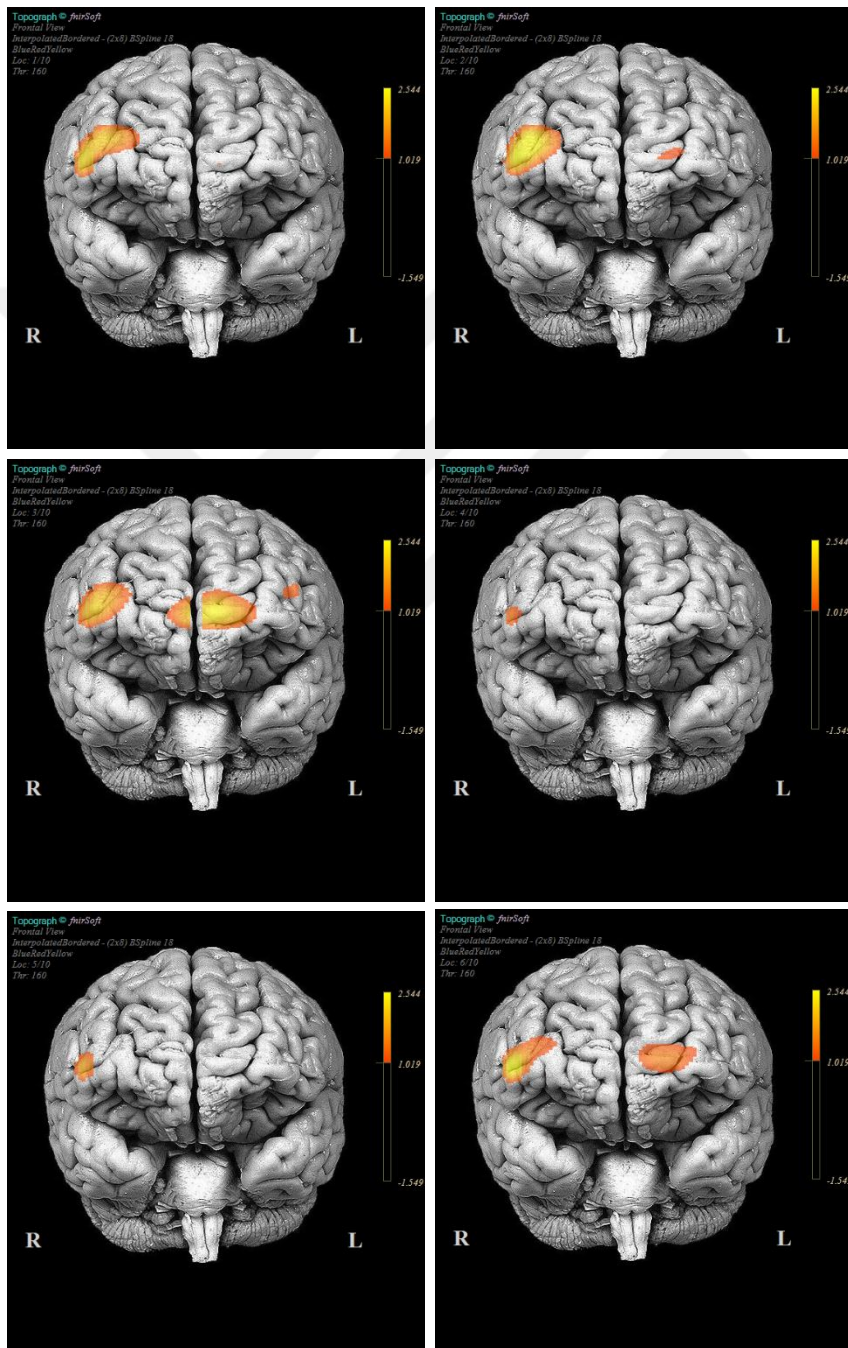


Figure 24: FDR corrected t-maps for HbO coherence increase measures obtained for the both-match (top-left), both-mismatch (top-right), other-match (middle-left), other-mismatch (middle-right), self-match (bottom-left) and self-mismatch (bottom-right) cases.

Overall, the degree of HbO coherence increase is weaker than the coherence increase t-maps for HbR. Right-dIPFC also exhibits significant level of coherence in almost all cases. The match/mismatch distinction seemed to make the largest difference in the other condition, where the match case is accompanied with increased HbO coherence around left frontopolar regions implicated in theory of mind studies. Coherence is almost diminished in the mismatch case for the other condition. These results support our hypothesis of coherence increase in accordance with auditory condition (i.e., self, both, other in increasing order) and the effect of mismatch conditions to disrupt the coherence most in the other condition.

4.4. Summary of the Results

The results of could be summarized as follows:

- Quantitative assessment of performance by dynamic time warping (DTW) suggested a significant main effect of auditory condition, $F(2, 42) = 15.23$, $p < .001$, partial $\eta^2 = .42$, as well as a significant main effect of block type $F(1, 21) = 17.39$, $p < .001$, partial $\eta^2 = .45$. Other ($M=321.85$, $SE=5.60$) condition elicited significantly higher mean asynchrony values as compared to Both ($M=309.40$, $SE=5.63$, $MD=12.45$, $p < .001$) and Self ($M=298.89$, $SE=5.97$, $MD=22.96$, $p < .05$) conditions. Moreover, the asynchrony level observed in the Both condition was significantly higher than the Self condition, $MD=10.51$, $p < .01$. Finally, the match blocks ($M=306.99$, $SE=5.58$) received significantly lower asynchrony values than the mismatch blocks ($M=313.11$, $SE=4.92$), $MD=-6.11$, $p < .001$.
- Qualitative assessment of performance by rating speech audio files suggested a significant main effect of auditory condition, $F(1.55, 43.35) = 78.53$, $p < .001$, partial $\eta^2 = .73$, as well as a significant main effect of block type $F(1.0, 28.0) = 14.31$, $p < .01$, partial $\eta^2 = .34$. Both ($M=87.23$, $SE=4.63$) and Other ($M=87.05$, $SE=4.08$) conditions elicited significantly higher ratings as compared to the Self ($M=41.59$, $SE=5.07$) condition, $MD=45.64$, $p < .001$ and $MD=45.45$, $p < .001$ respectively. Moreover, the match blocks ($M=76.26$, $SE=4.00$) received significantly higher ratings than the mismatch blocks ($M=67.66$, $SE=4.17$), $MD=8.60$, $p < .01$.
- Brain activation results in terms of mean HbO concentration change were observed during all joint speech conditions at all 16 measurement locations. Highest levels of activity were observed at optode 3 over left dIPFC (close to the Broca's region), optode 4 in the left inferior frontal gyrus, optode 6 in the left dmPFC, optode 9 in the right frontopolar region, optode 11 in the right dmPFC and optode 13 in the right dIPFC (close to the right homologue of Broca's region). A main effect of block type (match vs mismatch) was observed at all locations except optodes 10 and 14. Significantly higher mean

HbO levels were observed during match blocks as compared to mismatch blocks. A main effect of auditory condition was observed only in optode 2 ($F(2,92)=7.83$, $p<.01$, partial $\eta^2=.15$), which monitors a region within left inferior frontal gyrus.

- Brain coherence analyses were conducted by Wavelet Transform Coherence (WTC) method. The HbR coherence increase is stronger in the right dorsolateral and right superior frontal cortices. In the self condition a stronger HbR coherence increase trend was observed in the left dorsolateral and left dorsomedial prefrontal cortices as compared to both and other cases. The silent condition elicits the lowest level of coherence increase as expected. Both mismatch condition elicited less coherence in the left-dlPFC and right-dmPFC regions as compared to the both match condition. The degree of HbO coherence increase is weaker than the coherence increase t-maps for HbR. Right-dlPFC also exhibits significant level of coherence in almost all cases. The match/mismatch distinction makes the largest difference in the other condition, where the match case is accompanied with increased HbO coherence around left frontopolar regions implicated in theory of mind studies compared to mismatch case. A particularly important observation made in this dissertation is the significant coherence increase patterns in the right dlPFC and right superior PFC observed during both and other conditions, where participants exhibited higher levels of behavioral synchrony.



CHAPTER 5

DISCUSSION

In this chapter, the results of the hyperscanning of brain-to-brain interactions during a joint sentence reading task in the prefrontal cortex will be discussed. This chapter is organized under three main titles as Discussion of Behavioral Performance Analysis Result, Discussion of Brain Activation Analysis Results and Discussion of Coherence Analysis Results with subtitles for each of the main categories. For the discussion of behavioral performance analysis, there are two subtitles as Discussion of Qualitative Assessment of Performance and Discussion of Quantitative Assessment of Performance where dynamic time warping results and interrater reliability ratings are compared and discussed, respectively. For Discussion of Brain Activation Analysis Results, there are one subtitle as Discussion of Group Brain Activation Results, where the participants' brain activations in terms of HbO levels ($\mu\text{molar/Lt}$) are compared within each optode for three auditory (i.e., self, both, other) and two block (i.e., match, mismatch) conditions. For Discussion of Coherence Analysis Results, there is one subtitle as Discussion of HbR and HbO Coherence Results where the wavelet transform coherence values that indicate brain-to-brain coherence are discussed.

5.1. Discussion of Behavioral Performance Analysis Results

5.1.1. Discussion of Quantitative Assessment of Performance

The participant pairs' read aloud performances during joint sentence reading task were measured by a method called Dynamic Time Warping (DTW). This method works by warping one speech waveform onto the other to find the optimum warp path between the two time-aligned signals. Then, the area under the warp curve is calculated and is used as a measure of the asynchrony between the two signals such that as the warp area is larger, the asynchrony between the two signals is bigger.

In this study, the participants' speech during read aloud conditions were extracted and were subjected to DTW analysis. A 3x2 repeated measures ANOVA with auditory condition (self, both, other) and the block type (match, mismatch) was performed. The results suggested a significant main effect of auditory condition and a significant main effect of block type. There was no interaction effect. The direction of the significant main effect of auditory condition indicated that Other condition elicited higher mean asynchrony values than Both and Self conditions. In addition,

the asynchrony values of Both condition was significantly higher than the asynchrony of Self condition. In the related literature and in our hypotheses, the degree of synchrony between the participants is defined as a function of the strength of coupling between participants. In the study by Cummins et al. (2013), an analogy between the coupling among participants and three-legged race is made. In the three-legged race, the middle legs of the participants are tied to each other and they are required a run along a path with coupled legs. In this analogy, the participants' legs are physically coupled to each other and if the coupling is a little bit loose then the participants' movements could be less synchronized since this would allow them a space to be more independent of their partners. On the other hand, when the middle legs are tightly coupled, then they would demonstrate a more synchronized behavior during the race. In a similar manner, the coupling between the participants in joint sentence reading task was established by manipulating the strength of the co-speaker's voice available to the other participant. In this case, Self condition is predicted to elicit highest level of asynchrony, followed by Both and Other conditions in decreasing order of asynchrony, respectively (i.e., tighter auditory coupling between the participants). In the study by Cummins et al. (2013), Self condition elicited lowest level of asynchrony between the participants followed by Both and Other conditions for English and Mandarin Chinese. There was no significant difference between Both and Other conditions for English.

Based on these findings in the literature, the research hypothesis in this study regarding auditory coupling between the participants was that Self condition would provide the least coupling between the participants as compared to Both and Other conditions. In this regard, the participant pairs' behavioral synchrony as measured by the DTW will be the least in Self condition than Both and Other conditions.

However, the results of this study did not support our hypothesis in terms of auditory coupling conditions. On the contrary, Other condition elicited significantly higher levels of asynchrony than Both and Self conditions. In addition, Both condition elicited significantly higher levels of asynchrony than Self condition. These unexpected results could have arisen due to various factors related with the audio recording hardware and software setup, and the effect of such factors on the DTW algorithm. Firstly, in order to record as well as relay the participants' speech to their co-speaker, the gains of the microphone's and the main output volume for the relayed sound to the headphones were set to relatively high values such that the microphones could pick up many sounds in the experiment room. Therefore, even though the headphones provided isolation from the environmental sounds and relayed the co-speaker's speech to the participant, the participants' speech could have been heard through airborne sound, bone conductance and proprioception during auditory conditions.

Moreover, the dynamic time warping algorithm computes the warping curve between two speech waveforms by taking into account only the voiced parts of the speech. In

this regard, the DTW algorithm could not have taken specific factors into account as close as to a human ear, such as whether one partner was noticeably slower than the other, and whether they were able to pronounce each word in the sentence in an intelligible manner. Consequently, these conditions might have contributed to the contradictory results of the DTW values in terms of auditory conditions.

In the related literature regarding the quantitative assessment of performance by using dynamic time warping was employed by Cummins et al. (2013). In their study, the researchers investigated English and Mandarin Chinese. The findings of Cummins et al. (2013) showed that self, both and other conditions elicit similar asynchrony levels across both languages (i.e., self has the highest asynchrony level than both and other conditions). In addition, in English mismatch sentences resulted in complete cessation of the coupled speech while in Mandarin Chinese this effect was less as observed in the fewer speech errors by Chinese speakers during mismatch sentences. The results of the DTW algorithm in Turkish showed significant differences between self, both and other conditions in the opposite direction (i.e., self has the lowest level of asynchrony as compared to both and other conditions). These diverse findings in the related literature requires further investigation of the effects of auditory conditions in different experimental conditions (i.e., different language, sentence type) as well as verification of the results given by the dynamic time warping algorithm by other comparable methodologies. In this way, the observed directions of effects could be explained with more confidence based on the specification of the algorithm, the language used or the sentences implemented in the experimental conditions to measure asynchrony.

Another result of the quantitative assessment of performance by DTW was that the results suggested a significant main effect of block type (match, mismatch). The direction of this effect was that match blocks received significantly lower asynchrony values than the mismatch blocks. In the study by Cummins et al. (2013), another interpretation of the three-legged race metaphor was that successful pairs demonstrate greater synchrony but they are also susceptible to small disruptions that break their coordination. In this study, the hypothesis about block type was also similar to the to the study by Cummins et al. (2013) such that the asynchrony score would be less in matching block as compared to mismatching blocks. The results of this study are in agreement with the hypothesis and Cummins et al.'s (2013) findings. In this case, the participants had several difficulties associated with mismatching blocks ranging from brief cessation of the speech to complete dissolution of the coupled reading due to the presence of a single mismatching lexical item in such sentences. In terms of the asynchrony values of the DTW algorithm, matching blocks generated less asynchrony as compared to mismatching blocks. In this particular case, the DTW algorithm was able to distinguish between the different block types (match, mismatch).

The method and the results of the dynamic time warping could be investigated in further studies that take into account of the environmental conditions such as auditory setup, placement of participants, and properties of the experiment room as well as the details of the dynamic time warping algorithm, configurations of recording devices and related software in order to design well-controlled experimental conditions.

5.1.2. Discussion of Qualitative Assessment of Performance

In addition to quantitative analysis of read aloud performance, each sentence uttered by the participants was rated between 1 and 5 according to the level of perceived synchrony. Raters were instructed to consider specific factors while assigning their ratings, such as whether one partner was noticeably slower than the other, and whether they were able to pronounce each word in the sentence in an intelligible manner. In addition, the raters were allowed to use half-way marks such as 3.5 and 4.5 as they see appropriate.

A Krippendorff's reliability analysis was applied to the ratings and an alpha of 0.69 was obtained among 3 raters, which suggests sufficient level of inter-rater reliability was obtained (Krippendorff, 2004).

In each block the pairs read aloud 7 sentences and the mean of the ratings for these 7 sentences were considered as the overall rating of that block. A cubic transformation was applied to obtain a more symmetric distribution suitable for the use of parametric tests. A 3x2 repeated measures ANOVA with auditory condition (self, both, other) and the block type (match, mismatch) was performed. The results suggested a significant main effect of auditory condition and a significant main effect of block type. There was no interaction effect. The direction of the significant main effect of auditory condition showed that Both and Other conditions elicited significantly higher ratings as compared to Self condition. Moreover, in terms of block type, match blocks received significantly higher ratings than mismatch blocks.

Based on the findings in the literature, specifically in the study by Cummins et al. (2013), the ratings of participants' joint speech performance in this study are in agreement with the expected results. In this case, qualitative analysis of participants' speech confirms both of the research hypotheses of this study, such that Self condition provided the least synchronous conditions as compared to Both and Other conditions, as well as matching blocks were rated with higher levels of synchrony than mismatching blocks.

The difference for the auditory condition (self, both, other) between the quantitative assessment of read aloud performance by using dynamic time warping algorithm and qualitative assessment of performance by rating the participants' utterances of each sentence from each joint reading block could be attributed to the specifics of the DTW algorithm in correctly distinguishing between Self, Both and Other conditions.

In this regard, as previously mentioned, due to the way the speech signals were recorded in the experiment setup, the correct identification of speech variations in specific conditions could be better captured by the human ear than the dynamic time warping algorithm, and the results from an inter-rater analysis could be more suitable than DTW algorithm to the conditions of this study. However, the qualitative analysis results also suggest that the experiment succeeded in producing conditions that differed in terms of the level of synchronization in speech performance.

5.2. Discussion of Brain Activation Analysis Results

5.2.1. Discussion of Group Brain Activation Results

The group brain activation results were reported based on the level of hemodynamic response elicited by each experimental condition. Mean HbO concentration change observed during all joint speech conditions indicated highest levels of activity at optode 3 over left dorsolateral prefrontal cortex (dlPFC) (close to the Broca's region), optode 4 in the left inferior frontal cortex (left IFC), optode 6 in the left dorsomedial prefrontal cortex (dmPFC), optode 9 in the dmPFC and right frontopolar region, optode 11 in the right dmPFC and optode 13 in the right dlPFC (close to the right homologue of Broca's region).

In terms of the high levels of HbO concentration change observed at these brain regions, several studies in the related literature corroborate with these observations. For the high levels of activation observed at optode 3 over left dlPFC which is close to the Broca's region and optode 13 in the right dlPFC which is close to the right homologue of Broca's region, it is established in the neurolinguistics research and through results of experimental neurolinguistics, Broca's region and its right hemispheric homologue are an integral functional and anatomical location for the language-specific tasks.

In terms of the anatomy and function of Broca's area, Nishitani, Schürmann, Amunts, and Hari (2005) in their review article, demonstrate that Broca's region has its right-hemisphere analog also identified by Brodmann's cytoarchitectonic areas (BA) 44 and 45. Functionally, in terms of language and speech, Broca's area is left lateralized however the researchers indicate that it is less clear whether Broca's area is asymmetric in other language related functions. In addition, Nishitani et al. (2005) conclude from the research reviewed that Broca's area has a central role as a coordinator of time sensitive perceptual and motor functions for verbal and non-verbal communication. In light of such relevant research, the high levels of activity observed at optode 3 and optode 13 could be explained by the fact that in this study, the participants simultaneously read aloud sentences during auditory and block experimental conditions which elicit activations in Broca's region and its right hemisphere homologue.

For the high levels of activation observed at optode 4 in the left inferior frontal cortex, there are several studies in the related literature that could be given as a reference. In the study by Belin et al. (2004), they have developed a model of voice perception in which right and left inferior prefrontal cortical regions are identified as important regions in vocal information processing. In addition, Jiang et al. (2012), in their study investigated inter-brain coherence during face-to-face communication between participants. The researchers also used HbO concentration change for the analyses. The results showed a significant increase in neural synchronization between the participants during face-to-face dialogue compared to other conditions and random pairings in left IFC. Osaka et al. (2015) examined neural synchronization between two people while they sing or hum together during face-to-face (FtF) or face-to-wall (FtW) conditions. They have also used HbO signals for the calculation of inter-brain synchronization. Their results showed that an increased neural synchronization in the left inferior cortex for cooperative singing or humming regardless of FtF or FtW compared with singing or humming alone. Moreover, the researchers also identified right IFC for an increase in synchronization for humming only. These results are important since they show that interpersonal neural synchronization can be found in IFC which also include Brodmann areas 44 and 45. For the current study, increased HbO activity in the optode 4 in the left inferior frontal cortex could be regarded as a neural marker that shows increased activity in cooperative conditions between participants.

For the high levels of activation observed at optode 6 in the left dmPFC, optode 9 in the mPFC and optode 11 in the right dmPFC, there are several studies in the related literature that refer to medial frontal cortex (MFC), mPFC and dmPFC activations during social cognition contexts. In this regard, Amodio et al. (2006) identified medial frontal cortex activation as a general area in different aspects of social cognitive processing. In their review, the researchers indicated that medial frontal cortex is activated for a number of social cognition conditions such as mentalizing, action monitoring and social semantic knowledge about others and self. In addition, Stephens et al. (2010), in their study, investigated speaker-listener neural coupling during verbal communication. They have found widespread coupling across regions of listeners and the speaker's brains including low-level auditory cortex, linguistic and extra-linguistic areas. One of the regions that activated during successful speaker-listener coupling was mPFC. In another study, Hensel et al. (2013) identified dmPFC activation during explicit social judgments on vocal stimuli. The researchers report that mediation of attentional resources during social reasoning is executed within the dmPFC. Finally, the researchers reported that dmPFC is activated during high-level integration of knowledge about oneself and others. For the current study, the participants jointly read aloud sentences in different auditory conditions (self, both, other) as well as different block conditions (match, mismatch) that could likely contribute to bilateral dmPFC activations observed in optode 6, optode 9 and optode 11.

In terms of the activation observed in optode 9 which is also in the frontopolar region, a relevant study by Nozawa et al. (2016) that investigated group verbal communication in terms of cooperative word chain generation in which they measured interpersonal neural synchronization in the frontopolar cortex of the participants showed that unstructured group communication enhanced interpersonal neural synchronization measures in the frontopolar region. Frontopolar region (BA 10) has been identified as an important region that activates in social interactions for successful communication, understanding of others' mental states, desires and beliefs as well as for multi-task coordination (Amodio et al., 2006, Stephens et al., 2010). In this regard, the brain activation of the participants observed in optode 9 in this dissertation are in line with the related literature of functional and anatomical regions implicated in the social interactions as well as recent hyperscanning studies.

In addition to the high HbO concentration levels observed during all joint speech conditions across optodes in the prefrontal cortex, 3x2 repeated measures ANOVAs over the mean HbO concentration change across the 16 optodes indicated significant activations in optodes during auditory (self, both, other) and block (match, mismatch) conditions. Specifically, a main effect of block type (match vs mismatch) was observed at all locations except optodes 10 and 14. The direction of the effect was that significantly higher mean HbO levels were observed during match blocks as compared to mismatch blocks. Such high HbO levels during match blocks may be due to the sustained effort for maintaining joint speech, which is distorted in the mismatch cases that often resulted in poor coupling and disengagement from the reading task as evidenced in lower behavioral performance scores as well as higher dynamic time warping asynchrony values.

Moreover, a main effect of auditory condition was observed in optode 2 which is in a region within left inferior frontal gyrus and dorsolateral PFC. No interaction was observed between block type and auditory condition at optode 2. Sidak corrected pairwise comparisons indicated that the Other condition elicited higher mean HbO levels as compared to Self and Both conditions. A similar trend across levels of the auditory condition was observed in optode 4 in the left IFC, which was only marginally significant. A Sidak corrected post-hoc comparison suggested that this was due to the higher mean HbO observed in the Other condition as compared to the Both condition.

Both of these regions (i.e., optode 2 and optode4) are located within left dlPFC, which is often associated with working memory management during speech processing and production. The increased activity in the Other condition may have differed from the other two joint speech conditions (i.e., self, both) due to the increased processing demand in that situation since in the Other condition both of the participants hear their co-speaker's voice in their headphones that task the working memory capacity of the participants as well as the Other condition could selectively

activate inferior frontal cortex which is important in social cognition especially in self-other distinction.

5.3. Discussion of Coherence Analysis Results

In addition to the higher levels of HbO activations observed in optodes in the PFC of the participants during experimental conditions, brain-to-brain interactions as measured by wavelet transform coherence (WTC) method was implemented in order to capture inter-personal neural synchronization (i.e., coherence) between the participants' brain activations. The results of the wavelet transform coherence analysis of HbR and HbO coherence increase values will be discussed in the following section.

5.3.1. Discussion of HbR and HbO Coherence Analysis Results

The results of the HbR coherence increase values observed in the prefrontal cortex during both, other, self and silent conditions indicated bilateral coherence increase in the prefrontal cortex such that HbR coherence increase was observed in left- and right-dorsolateral prefrontal cortex (left- and right-dlPFC), left- and right- inferior frontal gyrus (left- and right-IFG), left- and right-dorsomedial prefrontal cortex (left- and right-dmPFC) and right superior frontal cortex (right-SFC). In addition, HbR coherence increase is stronger in the right dorsolateral and right superior frontal cortices. In terms of auditory conditions (self, both, other), in the self condition a stronger HbR coherence increase trend was observed in the left dorsolateral and left dorsomedial prefrontal cortices as compared to both and other cases. The silent condition elicits the lowest level of coherence increase as expected since the participants were reading sentences that are shown at the same time silently in this condition.

In terms of block conditions (match, mismatch), the HbR coherence increase showed that the coherence trends look similar across matching and mismatching conditions across left- and right-PFC, except both condition where the mismatch case elicited less coherence in the left-dlPFC and right-dmPFC regions as compared to the match case.

The results of the HbO coherence increase values observed in the prefrontal cortex during both, other, self and silent conditions indicated a lower level of coherence as compared to HbR coherence increase values. According to the HbO coherence increase results, right-dlPFC and partly the right superior PFC showed the highest coherence in the both condition. In addition, right-dlPFC region exhibited high degree of coherence in other and self conditions, whereas almost no coherence pattern was observed during the silent condition. In the HbO coherence increase, match/mismatch distinction is observed mostly in the other condition, where the

match case is accompanied with increased HbO coherence around left frontopolar regions implicated in theory of mind (ToM) studies. Coherence is almost diminished in the mismatch case for the other condition. These patterns for the HbO coherence increase in the PFC of the participants are also similar to the HbR coherence increase which suggest a similar interpretation of the HbO coherence increase in the PFC in relation to the relevant literature. As in the HbR silent condition, no coherence pattern was observed during the HbO silent condition.

The HbR coherence increase during auditory and block conditions observed in the PFC of the participants' brains could be interpreted in reference to similar studies that employed hyperscanning as well as non-hyperscanning methods in the related literature. In the study by Dommer et al. (2012), the researchers investigated inter-personal coherence measured in terms of wavelet transform coherence between total hemoglobin (HbT) signals in the left-PFC of the participants during a joint and a single playing of n-back task. The researchers found that the interpersonal coherence in the left-PFC increased in the joint conditions as compared to single task condition. In another study by Cui et al. (2012), the researchers investigated the inter-personal coherence between the participants' brain activations during a cooperation task that involved a simultaneous button press in response to a "Go" signal. The researchers found that the coherence between the participants' signals in their right superior frontal cortices (right-SFC) was higher in cooperation than competition condition and increased coherence was associated with better cooperation performance. The increase in coherence compared to competition and single tasks was significant in cooperation condition. In a similar study, in terms of coherence between two participants' brain activations, Osaka et al. (2015) examined neural synchronization between two people while they sing or hum together or alone while they sat face-to-face (FtF) or face-to-wall (FtW) in a counterbalanced experimental condition. The researchers employed HbO signals for wavelet transform coherence analysis. The results of the study showed that an increased neural synchronization in the left inferior cortex (left-IFC) for cooperative singing or humming regardless of FtF or FtW conditions compared with singing or humming alone. Moreover, right-IFC showed an increase in synchronization for humming only. The results are important since they show that interpersonal neural synchronization can be found in IFC which also include Brodmann areas (BA) 44 and 45 which is right hemisphere homologue of Broca's region. In a related study by Liu et al. (2016), two people played Jenga® game during cooperative and obstructive conditions while their right PFC activations were recorded by fNIRS hyperscanning. The study revealed strong inter-brain neural synchrony in middle and superior frontal gyrus (BA8) as well as in dorsomedial prefrontal cortex (dmPFC) in Brodmann Area 9 (BA9) area especially in cooperative conditions. These findings indicate BA9 is an important region implicated in theory-of-mind (ToM) during cooperative social interactions. dmPFC is a region identified in functional neuroanatomical literature as a region sensitive to the intention of another individual in social conditions (Behrens et al., 2008). In this regard, left- and

right- dmPFC activations observed in HbR coherence increase indicate social information processing. In the current study, stronger HbR coherence increase observed in left-dlPFC and left-dmPFC in self condition could be related to the increased demands for the coupling through jointly reading aloud sentences that could have tasked left-dlPFC in sustaining joint speech coupled with the partner as well as left-dmPFC for allocation of attentional resources for the processing of ongoing social information regarding the co-speaker.

In the related literature, Tang et al. (2016) investigated interpersonal brain synchronization using fNIRS hyperscanning during an economic exchange condition by means of a modified ultimatum game where the participants could interact with each other in face-to-face or face-blocked conditions. The pairs' brain activations were measured from right temporo-parietal junction (rTPJ) and right-dlPFC. The researchers found a greater inter-personal brain synchronization in rTPJ and an increase (non-significant) in coherence in the right-dlPFC during face-to-face communication between pairs of participants. Even though the results in Tang et al. (2016) study for the activation of right-dlPFC did not reach significance, in our study right-dlPFC demonstrated strong HbR coherence increase. These findings suggest that right-dlPFC is activated during a task that facilitates inter-personal synchronization among the participants. In this regard, the task implemented by Tang et al. (2016) was mostly based on predicting the participant's action and making decisions about action outcomes in an economic setting. On the contrary, in this dissertation, the participant pairs continuously and jointly read aloud sentences during different experiment conditions which could be interpreted as a task that affords stronger mutual activation in right-dlPFC that contributes to the observed coherence.

Finally, along the lines of this dissertation a similar study by Jasmin et al. (2016) on the cohesion and joint speech of participants investigated the neural activity using fMRI measurements of single subject's brain activations (i.e., non-hyperscanning) while participants spoke simultaneously with another person. In this study, the researchers contrasted several experimental conditions such as Synch_Live, Synch_Rec, Diff_Live, Listen_Alone, Speak_Alone and Rest in a counterbalanced design in order to identify activated brain regions specific to joint speech with a person (i.e., Synch_Live) compared to joint speech with a recording (i.e., Synch_Rec). The results indicated the greater activation across regions including bilateral superior temporal gyrus (STG) than solo speaking and listening conditions. An important finding relevant for this dissertation was that right-IFG was significantly active in the Synch_Live condition which was not active in the Synch_Rec condition. In Jasmin et al.'s (2016) study, they identified activity in the right-IFG as a neural marker during joint speech. Jasmin et al. (2016) suggested that since rIFG is also activated to the perceived ownership of a stimulus such as one's own face or voice, rIFG could also be an important region in processing self-other

distinctions. In this dissertation, rIFG showed activation and coherence increase across all conditions but was not selective of auditory or block conditions.

In relation to the related literature that was described previously, the findings of the current study such that the significant HbR coherence increase in the left- and right-dmPFC, left- and right-dIPFC, left- and right-IFG as well as right-SFC and significant HbO coherence increase in right-dIPFC and partly in right-SFC are in good agreement with the findings reported in the related literature that suggest interpersonal coherence increase in the dmPFC, dIPFC and right-SFC regions.





CHAPTER 6

CONCLUSIONS AND SUMMARY

6.1. Conclusions and Summary of the Study

In this dissertation, behavioral synchrony, brain activations and brain-to-brain interactions between two people during a joint sentence reading task in the auditory and block experimental conditions were investigated. The behavioral results as measured by the synchrony between the joint speech performances of participant pairs indicated significant main effects of auditory and block conditions, which suggests that manipulation of parameters of a coupling medium such as auditory conditions or task stimuli (i.e., block conditions) affects the degree of behavioral synchrony between the interacting participants. The brain activation results indicated that the joint sentence reading task resulted in activations in many of the brain regions including left- and right-dorsolateral prefrontal cortex, left-inferior frontal gyrus, right frontopolar region and right-dorsomedial prefrontal cortex. The activation of these brain regions are well supported in the social neuroscience and neurolinguistics literature. In addition to the brain activation results, in this dissertation the brain-to-brain interactions between the participant pairs as measured by wavelet transform coherence showed bilateral coherence increase in the prefrontal cortex during task blocks but not during silent conditions. The brain regions that showed coherence increase over the prefrontal cortex were left- and right-dorsolateral prefrontal cortex, left- and right-inferior frontal gyrus, left- and right-dorsomedial prefrontal cortex, and right-superior frontal cortex. The degree of brain-to-brain interactions (i.e., coherence increase) showed some variation across auditory and block conditions of the experiment such that in the Self condition, coherence increase was stronger in left-dIPFC and left-dmPFC, whereas during Both and Mismatching condition less coherence was observed as compared to Both and Matching condition in the left-dIPFC and right-dmPFC. Moreover, in Other and Matching case increased coherence in the left frontopolar region was observed as compared to Other and Mismatch condition. These results suggest that the experimental conditions succeeded in establishing and manipulation of coherence between the specific brain regions of the participants as expected from relevant social neuroscience studies.

A particularly important observation made in this dissertation is the significant coherence increase patterns in the right dIPFC and right superior PFC observed during both and other conditions, where participants exhibited higher levels of behavioral synchrony. A similar pattern was observed at the right superior PFC by

Cui et al. (2012) during a task that required coordinated key presses in a game, which suggests that the increase in coherence in this location could be related to the synchronization of motor circuits subserving the joint read aloud performance. The increased coherence in right homologue of Broca's area seems to be particularly important for the achievement of joint speech performance. The fMRI study by Jasmin et al. (2016) hinted at the possible role of this region in synchronized speech, but did not explore the brain-to-brain coupling aspects since only one participant could be scanned in their experiment at a time. Another related NIRS hyperscanning study by Jiang et al. (2012) focused on coherence changes during face to face dialogue and monologue conditions, but completely focused on the language regions localized on the left hemisphere. The results of this study suggests that the right hemisphere also plays a key role in linguistic processes like joint reading, which motivates further questions about the role played by these regions in the achievement of coordination and turn organization during conversation.

The significant findings of this dissertation regarding the behavioral and brain-to-brain synchronization between people during a joint sentence reading task have important implications in cognitive science. First, the main research question of this study was to investigate whether behavioral synchronization between people has also neural correlates that could be observed in right and left hemispheres of the prefrontal cortex as suggested by the related literature. The activation of the right prefrontal cortex specific to joint actions suggests researchers that several brain regions and activation patterns that include right superior frontal, right dorsolateral and right inferior frontal cortices are essential in establishing and managing joint actions between people. Second, although people in daily life do not engage in joint reading and are required to synchronize with each other during such tasks, the observation of behavioral synchronization and brain-to-brain coherence between people suggests that the synchronization among people develops in an emergent fashion in tasks that normally do not require synchronized behavior. In this regard, these findings indicate that the processes that underlie joint actions requires further research to better understand the cognitive foundations of joint actions in terms of behavioral synchronization, brain activations and brain-to-brain coherence.

6.2. Limitations of the Study

This dissertation had some limitations in terms of its experimental design. Firstly, in the beginning of the experiment, the participants were presented with a silent block in which they silently read sentences. However, these silent blocks were not counterbalanced with joint reading blocks, which prevented the researcher to make a conclusive comparison among these conditions in terms of the neural activity elicited by silent and joint conditions. Since the coherence increase analyses were based on one sample t-tests where separate t-maps were constructed for silent and joint conditions, useful comparisons could still be made between silent and joint cases in terms of coherence patterns. Moreover, we did not have a true individual case where

participants read sentences in complete isolation. This condition could have effects on inter-personal synchronization.

Another limitation of this dissertation could be stated such that there was not a control case which would force participants to read completely different sentences to hamper the coordination between them. However, the contrasts between three auditory conditions as well as having matching and mismatching sentences still allowed us to explore brain-to-brain synchronization patterns modulated by different levels of joint reading performance.

6.3. Future Directions

In this dissertation, joint reading of sentences during different experimental conditions were investigated. The reason for using sentences instead of longer episodes of interaction in which participants engage in speaking and listening full paragraphs or real life stories in the experimental conditions was that the researcher tried to implement a more controlled approach to hyperscanning of joint actions in the context of joint sentence reading in which dimensions of the experiment would be relatively smaller and thus would allow the researcher for easy manipulation of experimental conditions as well as to make an informed interpretation of the results based on current state of the art in the related literature. Therefore, the activations and coherence findings of this study in relation to the right prefrontal cortex which is related to the joint actions as well as middle prefrontal cortex which is related to theory of mind regions established the precursor for future studies that comprises of tasks that are communicative action and dialogic by nature.

In this line of research, future studies could also investigate free forms of conversation such as participants engaging in a dialogue or listening to longer stories that allow the researcher to investigate real life social interactions in the context of hyperscanning. These studies are the next step to take and they would contribute to the rapidly developing research area of hyperscanning brain activation during real life social contexts.

In another line of research, in the hyperscanning literature, the participants are often presented with a human and a non-human partner to be able to identify the differences between human communication and a pre-recorded speech or a non-coordinating computer to establish a contrasting example for human-human vs human-machine communication. In this regard, joint actions and coordinated behavior between people could be investigated in relation to human and machine interactions.

In conclusion, hyperscanning of joint actions in the context of social interactions among people are still a developing research field that would benefit from further research that investigate various aspects of human interactions.



REFERENCES

- Amodio, D. M., & Frith, C. D. (2006). Meeting of minds: the medial frontal cortex and social cognition. *Nature Reviews Neuroscience*, 7(4), 268-277.
- Amunts, K., Lenzen, M., Schleicher A., Morosan, P., Palomero-Gallagher. N. and Zilles, K. (2010). Broca's region: Novel organizational principles and multiple receptor mapping. *PLOS Biology*, 8(9).
- Ayaz, H. (2010). *Functional near infrared spectroscopy based brain computer interface*. PhD Thesis, Drexel University, Philadelphia, PA.
- Ayaz, H., Izzetoglu, M., Shewokis, P. A., & Onaral, B. (2010). Sliding-window motion artifact rejection for Functional Near-Infrared Spectroscopy. Conf Proc IEEE Eng Med Biol Soc, 2010, 6567-6570.
- Ayaz, H., Çakir, M. P., İzzetoğlu, K., Curtin, A., Shewokis, P. A., Bunce, S. C., & Onaral, B. (2012, March). Monitoring expertise development during simulated UAV piloting tasks using optical brain imaging. In *Aerospace Conference, 2012 IEEE* (pp. 1-11). IEEE.
- Ayaz, H., Shewokis, P.A., Curtin, A., Izzetoglu, M., Izzetoglu, K., & Onaral, B. (2011). Using MazeSuite and functional near infrared spectroscopy to study learning in spatial navigation. *Journal of Visualized Experiments*, 56, doi: 10.3791/3443.
- Ayaz, H., Shewokisa, P. A., Buncec, S., Izzetoglu, K., Willems, B., Onaral, B. (2012). Optical brain monitoring for operator training and mental workload assessment. *Neuroimage*, 59(1), 36-47.
- Baess, P., Zhdanov, A., Mandel, A., Parkkonen, L., Hirvenkari, L., Mäkelä, J. P., Jousmäki, V., & Hari, R. (2012). MEG dual scanning: A procedure to study real-time auditory interaction between two persons. *Frontiers in Human Neuroscience*, 6(83).
- Behrens, T. E., Hunt, L. T., Woolrich, M. W., & Rushworth, M. F. (2008). Associative learning of social value. *Nature*, 456(7219), 245-249.

- Belin, P., Fecteau, S., & Bedard, C. (2004). Thinking the voice: neural correlates of voice perception. *Trends in cognitive sciences*, 8(3), 129-135.
- Benjamini, Y., & Hochberg, Y. (1995). Controlling the false discovery rate: a practical and powerful approach to multiple testing. *Journal of the royal statistical society. Series B (Methodological)*, 289-300.
- Boersma, Paul (2001). Praat, a system for doing phonetics by computer. *Glott International* 5:9/10, 341-345.
- Bunce, S. C., Izzetoglu, M., Izzetoglu, K., Onaral, B., & Pourrezaei, K. (2006). Functional near-infrared spectroscopy. *IEEE engineering in medicine and biology magazine*, 25(4), 54-62.
- Cope, M., Delpy, D. T., Reynolds, E. O. R., Wray, S., Wyatt, J., & Van der Zee, P. (1988). Methods of quantitating cerebral near infrared spectroscopy data. In *Oxygen Transport to Tissue X* (pp. 183-189). NY: Springer.
- Cui, X., Bray, S., Bryant, D. M., Glover, G. H., & Reiss, A. L. (2011). A quantitative comparison of NIRS and fMRI across multiple cognitive tasks. *Neuroimage*, 54(4), 2808-2821.
- Cui, X., Bryant, D. M., & Reiss, A. L. (2012). NIRS-based hyperscanning reveals increased interpersonal coherence in superior frontal cortex during cooperation. *NeuroImage*, 59, 2430-2437.
- Cummins, F. (2007). The quantitative estimation of asynchrony among concurrent speakers. Technical Report UCD-CSI-2007-2, School of Computer Science and Informatics, University College Dublin.
- Cummins, F., Li, C., & Wang, B. (2013). Coupling among speakers during synchronous speaking in English and Mandarin. *Journal of Phonetics*, 41(6), 432-441.
- Doelling, K. B., Arnal, L. H., Ghitza, O., & Poeppel, D. (2014). Acoustic landmarks drive delta–theta oscillations to enable speech comprehension by facilitating perceptual parsing. *Neuroimage*, 85, 761-768.
- Dommer, L., Jäger, N., Scholkmann, F., Wolf, M., & Holper, L. (2012). Between-brain coherence during joint n-back task performance: A two-person

- functional near-infrared spectroscopy study. *Behavioral Brain Research*, 234(2), 212-222.
- Erten, B., Bozsahin, C., & Zeyrek, D. (2014). Turkish Resources for Visual Word Recognition. In *LREC* (pp. 2106-2110).
- Friederici, A. D. (2012). The cortical language circuit: from auditory perception to sentence comprehension. *Trends in cognitive sciences*, 16(5), 262-268.
- Funane, T., Kiguchi, M., Atsumori, H., Sato, H., Kubota, K., & Koizumi, H. (2011). Synchronous activity of two people's prefrontal cortices during a cooperative task measured by simultaneous near-infrared spectroscopy. *Journal of Biomedical Optics*, 16(7).
- Gagnon, L., Yücel M. A., Dehaes, M., Cooper, R. J., Perdue, K. L., Selb, J., Huppert, Hoge, R. D., & Boas, D. A. (2012). Quantification of the cortical contribution to the NIRS signal over the motor cortex using concurrent NIRS-fMRI measurements. *NeuroImage*, 59, 3933-3940.
- García, A. M., & Ibáñez, A. (2014). Two-person neuroscience and naturalistic social communication: The role of language and linguistic variables in brain-coupling research. *Frontiers in psychiatry*, 5.
- Golumbic, E. M. Z., Ding, N., Bickel, S., Lakatos, P., Schevon, C. A., McKhann, G. M., Goodman, R. R., Emerson, R., Mehta, A. D., Simon, J. Z., Poeppel, D., & Schroeder, C. E. (2013). Mechanisms underlying selective neuronal tracking of attended speech at a "cocktail party". *Neuron*, 77(5), 980-991.
- Grinsted A., Moore J., Jevrejeva S. (2004). Application of the cross wavelet transform and wavelet coherence to geophysical time series. *Nonlinear Processes in Geophysics*, 11, 561-566.
- Hasson, U., Yang, E., Vallines, I., Heeger, D. J., & Rubin, N. (2008). A hierarchy of temporal receptive windows in human cortex. *The Journal of Neuroscience*, 28 (10), 2539-2550.
- Hasson, U., Ghazanfar, A. A., Galantucci, B., Garrod, S., & Keysers, C. (2012). Brain-to-brain coupling: a mechanism for creating and sharing a social world. *Trends in Cognitive Science*, 16(2).

- Hayes, A. F., & Krippendorff, K. (2007). Answering the call for a standard reliability measure for coding data. *Communication methods and measures*, 1(1), 77-89.
- Hensel, L., Bzdok, D., Müller, V. I., Zilles, K., & Eickhoff, S. B. (2013). Neural correlates of explicit social judgments on vocal stimuli. *Cerebral cortex*, bht307.
- Hesse, W., Möller, E., Arnold, M., Schack, B. (2003). The use of time-variant EEG Granger causality for inspecting directed interdependencies of neural assemblies. *Journal of Neuroscience Methods*, 124, 27-44.
- Hickok, G., & Poeppel, D. (2007). The cortical organization of speech processing. *Nature Reviews Neuroscience*, 8(5), 393-402.
- Holper, L., Scholkmann, F., & Wolf, M. (2012). Between-brain connectivity during imitation measured by fNIRS. *NeuroImage*, 63, 212-222.
- Honey, C. J., Thesen, T., Donner, T. H., Silbert, L. J., Carlson, C. E., Devinsky, O., Doyle, W. K., Rubin, N., Heeger, D. J., & Hasson, U. (2012). Slow cortical dynamics and the accumulation of information over long timescales. *Neuron*, 76(2), 423-434.
- Izzetoglu, M., Izzetoglu, K., Bunce, S., Ayaz, H., Devaraj, A., Onaral, B., & Pourrezaei, K. Functional near-infrared neuroimaging. *Neural Systems and Rehabilitation Engineering*, IEEE Transactions on, 13(2), 153-159. (2005).
- Jaeggi S. M., Buschkuhl M., Jonides J., Perrig W. J. (2008). Improving fluid intelligence with training on working memory. In: *Proceedings of the National Academy of Sciences (PNAS)*. 2008. p. 6829–33.
- Jasmin, K. M., McGettigan, C., Agnew, Z. K., Lavan, N., Josephs, O., Cummins, F., & Scott, S. K. (2016). Cohesion and Joint Speech: Right Hemisphere Contributions to Synchronized Vocal Production. *The Journal of Neuroscience*, 36(17), 4669-4680.
- JASP Team (2016). JASP (Version 0.7.5.6) [Computer software]
- Jiang, J., Dai, B., Peng, D., Zhu, C., Liu, L., & Lu, C. (2012). Neural synchronization during face-to-face communication. *The Journal of Neuroscience*, 32(45), 16064-16069.

- Jobsis, F. F. (1977). Noninvasive, infrared monitoring of cerebral and myocardial oxygen sufficiency and circulatory parameters. *Science*, 198(4323), 1264-1267.
- Kemal Oflazer, Bilge Say, Dilek Zeynep Hakkani-Tür, Gökhan Tür, "Building a Turkish Treebank", Invited chapter in "Building and Exploiting Syntactically-annotated Corpora", Anne Abeille Editor, Kluwer Academic Publishers, 2003.
- Krippendorff, K. (2004). Reliability in content analysis. *Human communication research*, 30(3), 411-433.
- Lerner, Y., Honey, C. J., Silbert, L. J., & Hasson, U. (2011). Topographic mapping of a hierarchy of temporal receptive windows using a narrative story. *The Journal of Neuroscience*, 31(8), 2906-2915.
- Liu, T., & Pelowski, M. (2014). Clarifying the interaction types in two-person neuroscience research. *Frontiers in Human Neuroscience*, 8.
- Liu, N., Mok, C., Witt, E. E., Pradhan, A. H., Chen, J. E., & Reiss, A. L. (2016). NIRS-based hyperscanning reveals inter-brain neural synchronization during cooperative Jenga game with face-to-face communication. *Frontiers in human neuroscience*, 10.
- Mathôt, S., Schreij, D., & Theeuwes, J. (2012). OpenSesame: An open-source, graphical experiment builder for the social sciences. *Behavior Research Methods*, 44(2), 314-324. doi:10.3758/s13428-011-0168-7
- Montague, P. R., Berns, G. S., Cohen, J. D., McClure, S. M., Pagnoni, G., Dhamala, M., Wiest, M. C., Karpov, I., King, R. D., Apple, N., & Fisher, R. E. (2002). Hyperscanning: Simultaneous fMRI during linked social interactions. *NeuroImage*, 16, 1159-1164.
- Nart B. Atalay, Kemal Oflazer, Bilge Say, "The Annotation Process in the Turkish Treebank", in "Proceedings of the EACL Workshop on Linguistically Interpreted Corpora - LINC", April 13-14, 2003, Budapest, Hungary
- Nishitani, N., Schürmann, M., Amunts, K., & Hari, R. (2005). Broca's region: from action to language. *Physiology*, 20(1), 60-69.
- Nozawa, T., Sasaki, Y., Sakaki, K., Yokoyama, R., & Kawashima, R. (2016). Interpersonal frontopolar neural synchronization in group communication: An

- exploration toward fNIRS hyperscanning of natural interactions. *NeuroImage*, 133, 484-497.
- Obrig, H., Wenzel, R., Kohl, M., Horst, S., Wobst, P., Steinbrink, J. & Villringer, A. (2000). Near-infrared spectroscopy: does it function in functional activation studies of the adult brain? *International Journal of Psychophysiology*, 35(2), 125-142.
- Oldfield, R. C. (1971). The assessment and analysis of handedness: The Edinburgh inventory. *Neuropsychologia*, 9(1), 97-113.
- Osaka, N., Minamoto, T., Yaoi, K., Azuma, M., Shimada, Y. M., & Osaka, M. (2015). How Two Brains Make One Synchronized Mind in the Inferior Frontal Cortex: fNIRS-Based hyperscanning during cooperative singing. *Frontiers in psychology*, 6.
- Poeppel, D. (2014). The neuroanatomic and neurophysiological infrastructure for speech and language. *Current Opinion in Neurobiology*, 28, 142-149.
- Sakoe, H. and Chiba, S. *Dynamic programming algorithm optimization for spoken word recognition*. IEEE Transactions on Acoustics, Speech, and Signal Processing, ASSP 26, 43-49 (1978).
- Sato, H., Yahata, N., Funane, T., Takizawa, R., Katura, T., Atsumori, H., & Fukuda, M. (2013). A NIRS-fMRI investigation of prefrontal cortex activity during a working memory task. *Neuroimage*, 83, 158-173.
- Say, B., Zeyrek, D., Oflazer, K., & Özge, U. (2004) "Development of a Corpus and a Treebank for Presentday Written Turkish", (Proceedings of the Eleventh International Conference of Turkish Linguistics, August, 2002) İmer, Kamile and Gürkan Doğan (eds), Current Research in Turkish Linguistics, pp.183-192, Eastern Mediterranean University Press, 2004.
- Schilbach, L., Timmermans, B., Reddy, V., Costall, A., Bente, G., Schlicht, T., & Vogeley, K. (2013). Toward a second-person neuroscience. *Behavioral and Brain Sciences*, 36(04), 393-414.
- Schippers, M. B., Roebroek, A., Renken, R., Nanetti, L., & Keysers, C. (2010). Mapping the information flow from one brain to another during gestural communication. *Proceedings of the National Academy of Sciences of the United States of America*. 107(20), 9388-9393.

- Scott, S. K., & Johnsrude, I. S. (2003). The neuroanatomical and functional organization of speech perception. *Trends in neurosciences*, 26(2), 100-107.
- Silbert, L. J., Honey, C. J., Simony, E., Poeppel, D., & Hasson, U. (2014). Coupled neural systems underlie the production and comprehension of naturalistic narrative speech. *Proceedings of the National Academy of Sciences*, 111(43), E4687-E4696.
- Spiegelhalder, K., Ohlendorf, S., Regen, W., Feige, B., Tebartz van Elst, L., Weiller, C., Hennig, J., Berger, M., & Tüscher, O. (2014). Interindividual synchronization of brain activity during live verbal communication. *Behavioural Brain Research*, 258, 75-79.
- IBM Corp. Released 2013. IBM SPSS Statistics for Windows, Version 23.0.0. Armonk, NY: IBM Corp.
- Stephens, G. J., Silbert, L. J., & Hasson, U. (2010). Speaker-listener neural coupling underlies successful communication. *Proc. Natl. Acad. Sci. U.S.A.* 107, 14425–14430.
- Strangman, G., Boas, D. A., & Sutton, J. P. (2002). Non-invasive neuroimaging using near-infrared light. *Biological Psychiatry*, 52, 679-693.
- Suda, M., Takei, Y., Aoyama, Y., Narita, K., Sato, T., Fukuda, M., & Mikuni, M. (2010). Frontopolar activation during face-to-face conversation: An *in situ* study using near-infrared spectroscopy. *Neuropsychologia*, 48(2), 441-447.
- Tang, H., Mai, X., Wang, S., Zhu, C., Krueger, F., & Liu, C. (2015). Interpersonal brain synchronization in the right temporo-parietal junction during face-to-face economic exchange. *Social cognitive and affective neuroscience*, nsv092.
- Torrence, C., Compo, G.P. (1998) A practical guide to wavelet analysis, *Bulletin of the American Meteorological Society*, 79, 61–78.
- Whitaker, H. A., & Stemmer, B. (Eds.). (1998). *Handbook of Neurolinguistics*. Academic Press.
- Yamamoto, T., & Kato, T. (2002). Paradoxical correlation between signal in functional magnetic resonance imaging and deoxygenated haemoglobin content in capillaries: a new theoretical explanation. *Physics in medicine and biology*, 47(7), 1121.

Zhang, X., Yu, J., Zhao, R., Xu, W., Niu, H., Zhang, Y., Zuo, N., & Jiang, T. (2015). Activation detection in functional near-infrared spectroscopy by wavelet coherence. *Journal of biomedical optics*, 20(1), 016004-016004.



APPENDICES

APPENDIX A - JOINT SENTENCE READING TASK BLOCKS

(x2) at the end of the sentences indicate those sentences were read twice by the participants in the pair.

.xml references at the end of the sentences indicate METU Turkish Tree Bank XML file references of the sentences.

Silent reading – practice

Arjantin'den Yunanistan'a, darbe depremleriyle sarsılmış pek çok ülke, enkaz kaldırma çalışmaları sırasında mahkemeler kurdu.

Ülke ekonomisiyle kişisel hayatların girdabından çıkış arasındaki denklemin çözümü uykularımı bölüyor.

Roman, bir kasabaya atanan genç ve deneyimsiz bir kaymakamla çeltikçiler arasındaki çekişmeleri anlatır.

Silent Reading

Ücretlerin yüksek olması nedeniyle bu kuruluşların verimli işletmecilik anlayışının dışına çıktığı da doğrudur.

Geride bırakılan birkaç genç ve yolculuğa dayanma gücü olmayan bir yaşlı kadın dışında tüm çobanlar kervanla yola çıkıyorlar. (00220160-20.xml)
(x2)

Çocuk annesinin kendisini tutsaklaştıran bu aşırı ilgisiyle [**duygusal (W) – dülyusal (NW)**] ve ruhsal olarak gelişmeden, sorumluluk üstlenmeyi öğrenmeden büyüyordu.

Dere yatağından getirilip köpeklerin erişemeyeceği bir yükseklikteki kütük setin üstüne istiflenmiş buz bloklarından bıçağıyla kopardığı parçaları kovaya dolduruyor. (x2)

Çeyiz olarak bölüp dağıtsan birkaç kız evlendirmeye yetecek kadar gümüş kabın yığılmış olduğu tepsiyle uşak geldi. (00105133-33.xml)

Practice Sentences

AB'ye uyum süreci nedeniyle hazırlanan azınlık cemaatleri vakıflarının mal edinmelerini düzenleyen yönetmelik kapsamına alınmayan Süryani ve Protestanlar isyan etti. (20200000-11.xml)

Harekatın çeşitli nedenlerle ertelenmesinin kısa vade için piyasaları olumlu etkileyeceği düşünülebilir. (21040000-13.xml)

Bu arada Şelaleevleri'ne kaçırdığını sandığı yedi'deki İstanbul-Diyarbakır seferi, iki saat kırkbeş dakika gecikmeyle dokuzkırkbeş'te kalkmıştı. (20710000-28.xml)

Tedbirler paketinde, sürekli ve geçici işçilerin memuriyete kaydırılması yöntemiyle ikibinüç yılında yüzdoksanbeş trilyon lira tasarruf sağlanması da hedefleniyor. (20970000-37.xml)

Irak'ta savaş tehdidi yanısıra, Amerika'nın baskısına rağmen AB için Türkiye'ye müzakere tarihi verilmeyeceği yönündeki sinyaller piyasada moral bozdu. (20210000-18.xml)

Block 1 Sentences

Yıllar yılı içi boş bir profesyonellik anlayışı içinde gelişmesi engellenen futbol artık zincirlerinden boşalıyor. (x2)

Ormandaki uzun yürüyüşlerim sırasında kuşların sesine, ağaçların hışırtısına, bir ağaçkakanın gaga vuruşuna, ıslığımla katılmaya çalışırım.

Yaklaşık otuz yıldan beri şehirleşme sürecine paralel olarak modernizm ile karşılaşmak toplumda sarsıntı yaratmaktadır.

Bu tür karşılaştırmaların bilgisayar teknolojisindeki gelişmeleri iyiden iyiye çarpıcı hale getirdiğini de biliyorsunuzdur. (x2)

İki yaşlı çift ve torunlarının yaşadığı bu alan kasabaya yakınlığından dolayı daha sık ziyaret ediliyor. (00220160-21.xml)

Block 2 Sentences

Yaklaşık otuz yıldan beri şehirleşme sürecine paralel olarak modernizm ile karşılaşmak toplumda sarsıntı yaratmaktadır.

Defalarca tırmanılan, sonra kayarak inilen [tepeler (W) – meceler (NW)] bir anda yerlerini geniş bir düzlüğe bıraktı.

Yüksek teknolojinin yetersiz kaldığı bu havanın, bu iklimin içinde yetişen canlılar, birbirlerine ilaç, barınak, korunak oluyordu. (x2)

İki yaşlı çift ve torunlarının yaşadığı bu alan kasabaya yakınlığından dolayı daha sık ziyaret ediliyor. (00220160-21.xml)

Kervan evlere yaklaşırken kasabaya doğru yola çıkan iki kar motosikletinin uzaklaşan gürültüsü geyikleri ürkütüyor. (x2)

Block 3 Sentences

Geçenlerde anneannemin komşuları babamın hemen evlenebileceğini, belki de başka bir kadın yüzünden evi terk ettiğini konuşuyorlardı. (x2)

İki yaşlı çift ve torunlarının yaşadığı bu alan kasabaya yakınlığından dolayı daha sık ziyaret ediliyor. (00220160-21.xml)

Kaldırımında küçük süt ve yoğurt kutularından bir iki tane, üzerinden kavun kabukları dökülmüş bir iki çöp poşeti ve izmaritler vardı. (x2) (00105133-15.xml)

Yaklaşık otuz yıldan beri şehirleşme sürecine paralel olarak modernizm ile karşılaşmak toplumda sarsıntı yaratmaktadır.

Borsada yönün yukarı dönmesi durumunda likit [**enstrümanlarda (W) – enstrokenlerde (NW)**] bekleyen paranın hisse senedine kayacağı söylenebilir. (20210000-14.xml)

Block 4 Sentences

Hat boyundaki köylerde halk, terkedilmiş, para etmeyen arazilerini boru hattı için yapılacak kamulaştırmada devlete satacak. (x2) (20200000-46.xml)

İnşaatta çalışacak vasıfsız işçilerin alımında [**sözleşme (W) – sutleşme (NW)**] gereği güzergah boyundaki köylerine öncelik verilecek. (20200000-46.xml)

İki yaşlı çift ve torunlarının yaşadığı bu alan kasabaya yakınlığından dolayı daha sık ziyaret ediliyor. (00220160-21.xml)

Yaklaşık otuz yıldan beri şehirleşme sürecine paralel olarak modernizm ile karşılaşmak toplumda sarsıntı yaratmaktadır.

Tarihi, içinden dersler çıkarılacak cep kılavuzu olmaktan çıkarıp kültür boyutuna taşımak gerekiyor. (x2) (00009120127.xml)

Block 5 Sentences

Dünyada düşünülecek onca güzel şey varken, senin kuruntular yaratman ve onların içinde bunalman akıl alacak gibi değil. (x2) (00172170-51.xml)

Yaklaşık otuz yıldan beri şehirleşme sürecine paralel olarak modernizm ile karşılaşmak toplumda sarsıntı yaratmaktadır.

Alışveriş bilimi bize ikna etmekle kararlılık arasında çok karmaşık ve ayrılmaz bir bağlantının olduğunu gösterir. (20200000-62.xml)

İki yaşlı çift ve torunlarının yaşadığı bu alan kasabaya yakınlığından dolayı daha sık ziyaret ediliyor. (00220160-21.xml)

Bakanlık, davaya müdahil olacak şehit ve yaralı diplomat ailelerine ise maddi ve manevi destek sağlayacak. (x2) (20200000-30.xml)

Block 6 Sentences

Yaklaşık otuz yıldan beri şehirleşme sürecine paralel olarak modernizm ile karşılaşmak toplumda sarsıntı yaratmaktadır.

Kız bütün gün çalışıp yorgunluktan adım atacak hali kalmayınca, adam para yerine kıza bir bardak pekmez vermiş. (x2) (00172170-31.xml)

Çeyrek asırdır, milyonlarca insanın ve üç kuşak nüfusun [**kaderini (W) – kamirini (NW)**] terk ve teslim ettiği liderlik kadroları güçlerini nereden alıyordu. (00009120233.xml)

İki yaşlı çift ve torunlarının yaşadığı bu alan kasabaya yakınlığından dolayı daha sık ziyaret ediliyor. (00220160-21.xml)

Çinliler Avrupa’da kendi vatandaşlarına sadece Almanya, Türkiye ve Malta için vize veriyor. (x2) (20970000-30.xml)

Block 7 Sentences

İstatistiklere baktığımızda bu seviyenin mevcut belirsizlik unsurlarının ortadan kalkması durumunda ikibinüç [**yılında (W) – pılında (NW)**] da büyük bir olasılıkla test edilebileceğini tahmin edebiliriz. (21040000-37.xml)

İki yaşlı çift ve torunlarının yaşadığı bu alan kasabaya yakınlığından dolayı daha sık ziyaret ediliyor. (00220160-21.xml)

Bugün yeni teknolojiler ancak bütünüyle bilimsel bilgiler temelinde üretilebilir hale gelmiştir. (x2) (00016112330.xml)

Yaklaşık otuz yıldan beri şehirleşme sürecine paralel olarak modernizm ile karşılaşmak toplumda sarsıntı yaratmaktadır.

Geceyarısından sonra biten işimden çıktığımda, o zamanların Beyoğlu'sunda varolan, kendine özgü, sabaha kadar açık kulüplere dadandım. (x2) (0000613020.xml)

Block 8 Sentences

Yaklaşık otuz yıldan beri şehirleşme sürecine paralel olarak modernizm ile karşılaşmak toplumda sarsıntı yaratmaktadır.

Güneş bulutların arkasından çıkmak istiyor, mat bir ışık olarak aydınlığını kentin üzerine vuruyordu. (x2) (0000613062.xml)

İki yaşlı çift ve torunlarının yaşadığı bu alan kasabaya yakınlığından dolayı daha sık ziyaret ediliyor. (00220160-21.xml)

Müşterilerin özel ihtiyaçlarına cevap verebilecek bir perakende ortamı [inşa (W) – ilça (NW)] etmeniz ve işletmeniz halinde, başarılı bir mağaza yaratırsınız. (20200000-62.xml)

Memur zammı geçmiş enflasyona göre yapılırsa, yıl sonu gerçekleşme beklentisine göre yüzde otuzun altında olmayacak. (x2) (20580000-64.xml)

Block 9 Sentences

İki yaşlı çift ve torunlarının yaşadığı bu alan kasabaya yakınlığından dolayı daha sık ziyaret ediliyor. (00220160-21.xml)

Teknoloji, bilginin üretimde kullanılabilir hale getirilmesi amacıyla birtakım düzeneklerin tasarlanıp oluşturulmasıdır. (x2) (00009120280.xml)

Yavaş yavaş çevremdeki karmakarışık dünyanın bilincine varıyordum.

İhtiyaç olabileceği düşüncesiyle evin etrafında gün boyu bekleyecek on kadar geyik seçildikten sonra diğerleri serbest bırakıldı. (x2) (00220160-16.xml)

Yaklaşık otuz yıldan beri şehirleşme sürecine paralel olarak modernizm ile karşılaşmak toplumda sarsıntı yaratmaktadır.



APPENDIX B - ONE SAMPLE T-TESTS FOR HbR AND HbO COHERENCE INCREASE

One sample t-tests were conducted for each condition (i.e., self, both, other, silent, random control and match, mismatch sentences) to detect optodes that exhibit non-zero HbR and HbO coherence increase values. A False Discovery Rate (FDR) correction (Benjamini & Hochberg, 1995) was applied to the t-values.

One sample t-Tests for HbO Coherence Increase

Table 4. One-sample t-test for HbO in Both condition

	Test Value = 0		Sig. (2-tailed)
	t	df	
Optode 2	-0.149	24	0.883
Optode 3	-0.337	28	0.739
Optode 4	0.05	23	0.961
Optode 5	0.142	22	0.888
Optode 6	0.348	23	0.731
Optode 7	-0.367	16	0.718
Optode 8	0.615	14	0.548
Optode 9	0.288	13	0.778
Optode 10	-0.608	13	0.553
Optode 11	0.769	18	0.452
Optode 12	-0.688	19	0.500
Optode 13	2.255	18	0.037*
Optode 14	0.892	19	0.383
Optode 15	0.218	29	0.829
Optode 16	1.822	22	0.082

Type = BOTH

Table 5. One-sample t-test for HbO in Other condition

	Test Value = 0		Sig. (2-tailed)
	t	df	
Optode 2	-0.149	24	0.883
Optode 3	-0.337	28	0.739
Optode 4	0.05	23	0.961
Optode 5	0.142	22	0.888
Optode 6	0.348	23	0.731
Optode 7	-0.367	16	0.718
Optode 8	0.615	14	0.548
Optode 9	0.288	13	0.778
Optode 10	-0.608	13	0.553
Optode 11	0.769	18	0.452
Optode 12	-0.688	19	0.500
Optode 13	2.255	18	0.037
Optode 14	0.892	19	0.383
Optode 15	0.218	29	0.829
Optode 16	1.822	22	0.082
Type = OTHER			

Table 6. One-sample t-test for HbO in Self condition

	Test Value = 0		Sig. (2-tailed)
	t	df	
Optode 2	-0.382	24	0.706
Optode 3	0.365	28	0.718
Optode 4	-0.404	23	0.690
Optode 5	-0.241	22	0.811
Optode 6	0.851	23	0.403
Optode 7	0.404	16	0.691
Optode 8	0.396	14	0.698
Optode 9	-0.022	13	0.983
Optode 10	-0.832	13	0.420
Optode 11	0.3	18	0.768
Optode 12	-0.728	19	0.475
Optode 13	0.933	18	0.363
Optode 14	0.434	19	0.669
Optode 15	-0.795	29	0.433
Optode 16	2.544	22	0.018*
Type = SELF			

Table 7. One-sample t-test for HbO in Silent condition

	Test Value = 0		Sig. (2-tailed)
	t	df	
Optode 2	-0.983	24	0.335
Optode 3	-1.28	28	0.211
Optode 4	-0.398	23	0.694
Optode 5	0.02	22	0.985
Optode 6	-0.044	23	0.965
Optode 7	-0.714	16	0.485
Optode 8	-0.257	14	0.801
Optode 9	-1.38	13	0.191
Optode 10	-0.56	13	0.585
Optode 11	-0.776	18	0.448
Optode 12	-0.628	19	0.538
Optode 13	0.089	18	0.930
Optode 14	-0.294	19	0.772
Optode 15	-0.855	29	0.399
Optode 16	1.062	22	0.300
Type = SILENT			

Table 8. One-sample t-test for HbO in Both-Match condition

	Test Value = 0		Sig. (2-tailed)
	t	df	
Optode 2	0.109	24	0.914
Optode 3	0.272	27	0.788
Optode 4	-0.166	22	0.870
Optode 5	-0.418	22	0.680
Optode 6	0.021	22	0.984
Optode 7	-0.877	16	0.394
Optode 8	0.956	13	0.356
Optode 9	-0.04	13	0.969
Optode 10	-0.483	12	0.638
Optode 11	1.041	17	0.313
Optode 12	-0.696	18	0.495
Optode 13	2.077	17	0.053
Optode 14	-0.129	19	0.899
Optode 15	0.179	28	0.860
Optode 16	2.06	22	0.051
Type = BOTH Match = MATCH			

Table 9. One-sample t-test for HbO in Both-Mismatch condition

	Test Value = 0		Sig. (2-tailed)
	t	df	
Optode 2	-0.312	24	0.758
Optode 3	-0.7	27	0.490
Optode 4	0.058	23	0.955
Optode 5	0.479	22	0.637
Optode 6	0.497	23	0.624
Optode 7	-0.118	15	0.907
Optode 8	0.687	14	0.503
Optode 9	0.455	13	0.657
Optode 10	-0.387	13	0.705
Optode 11	0.64	18	0.530
Optode 12	-0.582	18	0.568
Optode 13	2.385	18	0.028*
Optode 14	1.175	18	0.255
Optode 15	0.259	28	0.798
Optode 16	1.596	21	0.125

Type = BOTH Match = MISMATCH

Table 10. One-sample t-test for HbO in Other-Match condition

	Test Value = 0		Sig. (2-tailed)
	t	df	
Optode 2	-1.549	21	0.136
Optode 3	1.138	25	0.266
Optode 4	-0.561	20	0.581
Optode 5	-0.154	19	0.879
Optode 6	0.927	21	0.364
Optode 7	0.676	14	0.510
Optode 8	2.244	12	0.045*
Optode 9	-0.338	11	0.742
Optode 10	1.413	11	0.185
Optode 11	0.426	16	0.676
Optode 12	-0.249	17	0.806
Optode 13	1.44	16	0.169
Optode 14	1.295	17	0.213
Optode 15	-0.195	26	0.847
Optode 16	1.248	19	0.227

Type = OTHER Match = MATCH

Table 11. One-sample t-test for HbO in Other-Mismatch condition

	Test Value = 0		Sig. (2-tailed)
	t	df	
Optode 2	-0.104	24	0.918
Optode 3	-0.439	27	0.664
Optode 4	-0.345	23	0.733
Optode 5	-0.905	22	0.375
Optode 6	-0.448	23	0.658
Optode 7	-0.773	15	0.451
Optode 8	-0.493	14	0.629
Optode 9	0.381	13	0.709
Optode 10	-1.088	13	0.297
Optode 11	0.362	18	0.721
Optode 12	-0.939	18	0.360
Optode 13	0.141	18	0.890
Optode 14	-0.444	18	0.662
Optode 15	-0.92	28	0.365
Optode 16	1.323	21	0.200

Type = OTHER Match = MISMATCH

Table 12. One-sample t-test for HbO in Self-Match condition

	Test Value = 0		Sig. (2-tailed)
	t	df	
Optode 2	-0.062	19	0.952
Optode 3	-0.711	23	0.484
Optode 4	-0.483	19	0.635
Optode 5	-0.86	20	0.400
Optode 6	0.359	18	0.724
Optode 7	0.25	16	0.806
Optode 8	-0.343	13	0.737
Optode 9	-0.102	13	0.920
Optode 10	-1.34	12	0.205
Optode 11	-0.425	14	0.677
Optode 12	-1.333	14	0.204
Optode 13	0.289	14	0.777
Optode 14	-0.377	16	0.711
Optode 15	-0.662	24	0.514
Optode 16	1.737	17	0.100

Type = SELF Match = MATCH

Table 13. One-sample t-test for HbO in Self-Mismatch condition

	Test Value = 0		Sig. (2-tailed)
	t	df	
Optode 2	-0.28	24	0.782
Optode 3	0.777	28	0.444
Optode 4	-0.282	23	0.780
Optode 5	0.481	22	0.636
Optode 6	0.907	23	0.374
Optode 7	0.476	16	0.640
Optode 8	0.898	14	0.384
Optode 9	0.052	13	0.960
Optode 10	-0.468	13	0.647
Optode 11	0.576	18	0.572
Optode 12	-0.41	19	0.687
Optode 13	0.918	18	0.371
Optode 14	0.723	19	0.478
Optode 15	-0.834	29	0.411
Optode 16	2.492	22	0.021*

Type = SELF Match = MISMATCH

One sample t-Tests for HbR Coherence Increase

Table 14. One-sample t-test for HbR in Both condition

	Test Value = 0		
	t	df	Sig. (2-tailed)
Optode 2	2.754	24	0.011*
Optode 3	1.767	28	0.088
Optode 4	1.846	23	0.078
Optode 5	2.07	22	0.050*
Optode 6	2.315	23	0.030*
Optode 7	1.588	16	0.132
Optode 8	0.207	14	0.839
Optode 9	1.94	13	0.074
Optode 10	0.355	13	0.728
Optode 11	1.87	18	0.078
Optode 12	2.723	19	0.013*
Optode 13	2.098	18	0.050*
Optode 14	3.535	19	0.002*
Optode 15	3.141	29	0.004*
Optode 16	1.499	22	0.148

Type = BOTH

Table 15. One-sample t-test for HbR in Other condition

	Test Value = 0		
	t	df	Sig. (2-tailed)
Optode 2	2.623	24	0.015*
Optode 3	1.777	28	0.086
Optode 4	1.603	23	0.123
Optode 5	1.964	22	0.062
Optode 6	2.158	23	0.042*
Optode 7	1.816	16	0.088
Optode 8	0.464	14	0.650
Optode 9	1.518	13	0.153
Optode 10	1.315	13	0.211
Optode 11	1.783	18	0.092
Optode 12	2.651	19	0.016*
Optode 13	2.424	18	0.026*
Optode 14	3.259	19	0.004*
Optode 15	3.248	29	0.003*
Optode 16	1.036	22	0.312

Type = OTHER

Table 16. One-sample t-test for HbR in Self condition

	Test Value = 0		Sig. (2-tailed)
	t	df	
Optode 2	3.209	24	0.004*
Optode 3	2.177	28	0.038*
Optode 4	1.718	23	0.099
Optode 5	2.118	22	0.046*
Optode 6	2.457	23	0.022*
Optode 7	1.574	16	0.135
Optode 8	-0.08	14	0.937
Optode 9	1.251	13	0.233
Optode 10	0.445	13	0.664
Optode 11	1.732	18	0.100
Optode 12	2.578	19	0.018*
Optode 13	2.124	18	0.048*
Optode 14	3.173	19	0.005*
Optode 15	3.308	29	0.003*
Optode 16	1.127	22	0.272
Type = SELF			

Table 17. One-sample t-test for HbR in Silent condition

	Test Value = 0		Sig. (2-tailed)
	t	df	
Optode 2	2.1	24	0.046*
Optode 3	0.852	28	0.401
Optode 4	1.141	23	0.265
Optode 5	1.399	22	0.176
Optode 6	0.929	23	0.363
Optode 7	0.61	16	0.550
Optode 8	-0.29	14	0.776
Optode 9	0.286	13	0.780
Optode 10	-0.124	13	0.903
Optode 11	2.004	18	0.060
Optode 12	1.189	19	0.249
Optode 13	0.114	18	0.910
Optode 14	1.98	19	0.062
Optode 15	3.044	29	0.005*
Optode 16	0.97	22	0.343
Type = SILENT			

Table 18. One-sample t-test for HbR in Both-Match condition

	Test Value = 0		Sig. (2-tailed)
	t	df	
Optode 2	2.861	24	0.009*
Optode 3	1.727	27	0.096
Optode 4	1.872	22	0.075
Optode 5	2.249	22	0.035*
Optode 6	3.109	22	0.005*
Optode 7	1.408	16	0.178
Optode 8	0.873	13	0.398
Optode 9	2.387	13	0.033*
Optode 10	0.381	12	0.710
Optode 11	3.026	17	0.008*
Optode 12	2.361	18	0.030*
Optode 13	1.055	17	0.306
Optode 14	3.201	19	0.005*
Optode 15	2.874	28	0.008*
Optode 16	1.695	22	0.104

Type = BOTH Match = MATCH

Table 19. One-sample t-test for HbR in Both-Mismatch condition

	Test Value = 0		Sig. (2-tailed)
	t	df	
Optode 2	2.574	24	0.017*
Optode 3	1.698	27	0.101
Optode 4	1.747	23	0.094
Optode 5	1.848	22	0.078
Optode 6	2.049	23	0.052
Optode 7	1.331	15	0.203
Optode 8	0.242	14	0.812
Optode 9	1.581	13	0.138
Optode 10	0.537	13	0.600
Optode 11	1.166	18	0.259
Optode 12	2.207	18	0.041*
Optode 13	2.63	18	0.017*
Optode 14	3.267	18	0.004*
Optode 15	2.942	28	0.006*
Optode 16	1.027	21	0.316

Type = BOTH Match = MISMATCH

Table 20. One-sample t-test for HbR in Other-Match condition

	Test Value = 0		Sig. (2-tailed)
	t	df	
Optode 2	1.265	21	0.220
Optode 3	1.908	25	0.068
Optode 4	1.46	20	0.160
Optode 5	2.123	19	0.047*
Optode 6	1.752	21	0.094
Optode 7	1.596	14	0.133
Optode 8	2.503	12	0.028*
Optode 9	0.248	11	0.809
Optode 10	2.192	11	0.051
Optode 11	0.617	16	0.546
Optode 12	1.321	17	0.204
Optode 13	1.961	16	0.068
Optode 14	2.543	17	0.021*
Optode 15	2.691	26	0.012*
Optode 16	0.669	19	0.512

Type = OTHER Match = MATCH

Table 21. One-sample t-test for HbR in Other-Mismatch condition

	Test Value = 0		Sig. (2-tailed)
	t	df	
Optode 2	3.452	24	0.002*
Optode 3	1.384	27	0.178
Optode 4	1.737	23	0.096
Optode 5	1.8	22	0.086
Optode 6	2.353	23	0.028*
Optode 7	1.536	15	0.145
Optode 8	-0.176	14	0.863
Optode 9	1.829	13	0.090
Optode 10	0.744	13	0.470
Optode 11	2.337	18	0.031*
Optode 12	3.126	18	0.006*
Optode 13	2.173	18	0.043*
Optode 14	2.982	18	0.008*
Optode 15	2.9	28	0.007*
Optode 16	0.646	21	0.526

Type = OTHER Match = MISMATCH

Table 22. One-sample t-test for HbR in Self-Match condition

	Test Value = 0		Sig. (2-tailed)
	t	df	
Optode 2	3.063	19	0.006*
Optode 3	1.499	23	0.148
Optode 4	1.462	19	0.160
Optode 5	1.124	20	0.274
Optode 6	2.301	18	0.034*
Optode 7	1.83	16	0.086
Optode 8	-0.861	13	0.405
Optode 9	1.091	13	0.295
Optode 10	-0.335	12	0.743
Optode 11	1.615	14	0.129
Optode 12	2.973	14	0.010*
Optode 13	2.403	14	0.031*
Optode 14	2.352	16	0.032*
Optode 15	3.008	24	0.006*
Optode 16	1.143	17	0.269

Type = SELF Match = MATCH

Table 23. One-sample t-test for HbR in Both-Match condition

	Test Value = 0		Sig. (2-tailed)
	t	df	
Optode 2	3	24	0.006*
Optode 3	2.354	28	0.026*
Optode 4	1.763	23	0.091
Optode 5	2.482	22	0.021*
Optode 6	2.481	23	0.021*
Optode 7	1.34	16	0.199
Optode 8	0.262	14	0.797
Optode 9	1.195	13	0.253
Optode 10	0.845	13	0.414
Optode 11	1.886	18	0.076
Optode 12	2.64	19	0.016*
Optode 13	2.056	18	0.055
Optode 14	3.249	19	0.004*
Optode 15	3.353	29	0.002*
Optode 16	1.147	22	0.264

Type = SELF Match = MISMATCH

One sample t-Tests for HbO Random Matching Coherence Increase

Table 24. One-sample t-test for HbO in Random Both condition

	Test Value = 0		Sig. (2-tailed)
	t	df	
Optode 2	1.452	24	0.160
Optode 3	0.111	28	0.912
Optode 4	0.671	23	0.509
Optode 5	1.511	22	0.145
Optode 6	-0.108	23	0.915
Optode 7	0.54	16	0.596
Optode 8	0.33	14	0.746
Optode 9	0.34	13	0.739
Optode 10	1.336	13	0.204
Optode 11	2.112	18	0.049*
Optode 12	-0.273	19	0.788
Optode 13	1.913	18	0.072
Optode 14	0.363	19	0.721
Optode 15	0.326	29	0.747
Optode 16	0.369	31	0.715

Type = BOTH

Table 25. One-sample t-test for HbO in Random Other condition

	Test Value = 0		Sig. (2-tailed)
	t	df	
Optode 2	0.13	24	0.898
Optode 3	-0.495	28	0.625
Optode 4	0.589	23	0.562
Optode 5	1.343	22	0.193
Optode 6	-1.286	23	0.211
Optode 7	-0.389	16	0.702
Optode 8	0.244	14	0.811
Optode 9	0.377	13	0.713
Optode 10	0.437	13	0.669
Optode 11	0.863	18	0.399
Optode 12	-0.858	19	0.402
Optode 13	1.221	18	0.238
Optode 14	0.063	19	0.950
Optode 15	-0.412	29	0.683
Optode 16	-0.115	31	0.909

Type = OTHER

Table 26. One-sample t-test for HbO in Random Self condition

	Test Value = 0		Sig. (2-tailed)
	t	df	
Optode 2	0.403	24	0.691
Optode 3	-0.088	28	0.930
Optode 4	0.788	23	0.439
Optode 5	1.523	22	0.142
Optode 6	-0.759	23	0.456
Optode 7	0.37	16	0.716
Optode 8	0.549	14	0.591
Optode 9	-0.039	13	0.969
Optode 10	1.027	13	0.323
Optode 11	1.537	18	0.142
Optode 12	-1.122	19	0.276
Optode 13	1.296	18	0.211
Optode 14	0.165	19	0.870
Optode 15	-0.045	29	0.965
Optode 16	0.879	31	0.386

Type = SELF

Table 27. One-sample t-test for HbO in Random Silent condition

	Test Value = 0		Sig. (2-tailed)
	t	df	
Optode 2	0.814	24	0.423
Optode 3	-0.391	28	0.699
Optode 4	0.694	23	0.495
Optode 5	0.127	22	0.900
Optode 6	-1.775	23	0.089
Optode 7	0.429	17	0.674
Optode 8	-1.312	15	0.209
Optode 9	0.635	14	0.536
Optode 10	-0.017	14	0.987
Optode 11	1.477	18	0.157
Optode 12	-0.683	19	0.503
Optode 13	1.088	18	0.291
Optode 14	-0.154	19	0.879
Optode 15	-0.067	29	0.947
Optode 16	-0.594	31	0.557

Type = SILENT

Table 28. One-sample t-test for HbO in Random Both-Match condition

	Test Value = 0		Sig. (2-tailed)
	t	df	
Optode 2	0.328	24	0.745
Optode 3	-0.133	27	0.895
Optode 4	-0.587	22	0.563
Optode 5	1.37	22	0.185
Optode 6	-0.176	22	0.862
Optode 7	-0.042	16	0.967
Optode 8	-0.163	13	0.873
Optode 9	0.062	13	0.951
Optode 10	0.863	12	0.405
Optode 11	1.699	17	0.108
Optode 12	-1.172	18	0.256
Optode 13	0.723	17	0.480
Optode 14	-0.452	19	0.656
Optode 15	-0.162	28	0.872
Optode 16	0.157	22	0.877

Type = BOTH Match = MATCH

Table 29. One-sample t-test for HbO in Random Both-Mismatch condition

	Test Value = 0		Sig. (2-tailed)
	t	df	
Optode 2	1.74	24	0.095
Optode 3	0.3	27	0.767
Optode 4	1.346	23	0.191
Optode 5	1.339	22	0.194
Optode 6	0.09	23	0.929
Optode 7	0.76	15	0.459
Optode 8	0.705	14	0.492
Optode 9	0.466	13	0.649
Optode 10	1.537	13	0.148
Optode 11	1.627	18	0.121
Optode 12	0.357	18	0.726
Optode 13	2.104	18	0.050*
Optode 14	0.771	18	0.451
Optode 15	0.992	28	0.330
Optode 16	0.36	21	0.722

Type = BOTH Match = MISMATCH

Table 30. One-sample t-test for HbO in Random Other-Match condition

	Test Value = 0		Sig. (2-tailed)
	t	df	
Optode 2	-0.414	21	0.683
Optode 3	0.154	25	0.879
Optode 4	1.352	20	0.192
Optode 5	1.541	19	0.140
Optode 6	-0.756	21	0.458
Optode 7	-0.504	14	0.622
Optode 8	0.142	12	0.890
Optode 9	0.083	11	0.936
Optode 10	0.897	11	0.389
Optode 11	0.666	16	0.515
Optode 12	-1.11	17	0.282
Optode 13	2.464	16	0.025*
Optode 14	0.732	17	0.474
Optode 15	-0.191	26	0.850
Optode 16	-0.78	19	0.445

Type = OTHER Match = MATCH

Table 31. One-sample t-test for HbO in Random Other-Mismatch condition

	Test Value = 0		Sig. (2-tailed)
	t	df	
Optode 2	0.442	24	0.663
Optode 3	-0.082	27	0.935
Optode 4	0.412	23	0.684
Optode 5	1.556	22	0.134
Optode 6	-1.122	23	0.273
Optode 7	0.043	15	0.966
Optode 8	0.356	14	0.727
Optode 9	0.889	13	0.390
Optode 10	0.576	13	0.575
Optode 11	0.913	18	0.373
Optode 12	-0.115	18	0.910
Optode 13	0.66	18	0.518
Optode 14	0.176	18	0.862
Optode 15	0.411	28	0.684
Optode 16	0.003	21	0.998

Type = OTHER Match = MISMATCH

Table 32. One-sample t-test for HbO in Random Self-Match condition

	Test Value = 0		Sig. (2-tailed)
	t	df	
Optode 2	-0.411	19	0.686
Optode 3	-0.331	23	0.743
Optode 4	0.079	19	0.938
Optode 5	0.248	20	0.807
Optode 6	-0.49	18	0.630
Optode 7	-0.3	16	0.768
Optode 8	-0.194	13	0.850
Optode 9	-0.572	13	0.577
Optode 10	0.725	12	0.482
Optode 11	2.585	14	0.022*
Optode 12	-1.017	14	0.326
Optode 13	1.768	14	0.099
Optode 14	0.102	16	0.920
Optode 15	0.136	24	0.893
Optode 16	1.246	17	0.230

Type = SELF Match = MATCH

Table 33. One-sample t-test for HbO in Random Self-Mismatch condition

	Test Value = 0		Sig. (2-tailed)
	t	df	
Optode 2	0.53	24	0.601
Optode 3	0.197	28	0.845
Optode 4	1.128	23	0.271
Optode 5	1.98	22	0.060
Optode 6	-0.456	23	0.653
Optode 7	0.674	16	0.510
Optode 8	0.901	14	0.383
Optode 9	0.296	13	0.772
Optode 10	1.038	13	0.318
Optode 11	1.325	18	0.202
Optode 12	-0.847	19	0.408
Optode 13	1.057	18	0.304
Optode 14	0.235	19	0.816
Optode 15	0.13	29	0.898
Optode 16	0.728	22	0.474

Type = SELF Match = MISMATCH

One sample t-Tests for HbR Random Matching Coherence Increase

Table 34. One-sample t-test for HbR in Random Both condition

	Test Value = 0		Sig. (2-tailed)
	t	df	
Optode 2	-0.131	24	0.897
Optode 3	0.779	28	0.442
Optode 4	-0.199	23	0.844
Optode 5	0.397	22	0.695
Optode 6	-0.977	23	0.339
Optode 7	-0.072	16	0.943
Optode 8	0.482	14	0.637
Optode 9	1.738	13	0.106
Optode 10	1.809	13	0.094
Optode 11	1.284	18	0.215
Optode 12	0.743	19	0.466
Optode 13	1.063	18	0.302
Optode 14	2.782	17	0.013*
Optode 15	1.342	29	0.190
Optode 16	1.164	22	0.257

Type = BOTH

Table 35. One-sample t-test for HbR in Random Other condition

	Test Value = 0		Sig. (2-tailed)
	t	df	
Optode 2	-0.55	24	0.588
Optode 3	-0.308	28	0.760
Optode 4	-0.441	23	0.663
Optode 5	-0.64	22	0.529
Optode 6	-1.351	23	0.190
Optode 7	-1.02	16	0.323
Optode 8	0.051	14	0.960
Optode 9	0.364	13	0.722
Optode 10	0.403	13	0.693
Optode 11	0.692	18	0.498
Optode 12	0.457	19	0.653
Optode 13	-0.045	18	0.965
Optode 14	1.411	19	0.174
Optode 15	0.355	29	0.725
Optode 16	1.579	22	0.129

Type = OTHER

Table 36. One-sample t-test for HbR in Random Self condition

	Test Value = 0		Sig. (2-tailed)
	t	df	
Optode 2	-0.101	24	0.921
Optode 3	0.399	28	0.693
Optode 4	0.093	23	0.927
Optode 5	0.584	22	0.565
Optode 6	-1.084	23	0.290
Optode 7	-0.155	16	0.879
Optode 8	0.168	14	0.869
Optode 9	0.755	13	0.463
Optode 10	1.167	13	0.264
Optode 11	1.356	18	0.192
Optode 12	0.063	19	0.950
Optode 13	1.436	18	0.168
Optode 14	1.043	19	0.310
Optode 15	0.529	29	0.601
Optode 16	1.828	21	0.082
Type = SELF			

Table 37. One-sample t-test for HbR in Random Silent condition

	Test Value = 0		Sig. (2-tailed)
	t	df	
Optode 2	-1.052	24	0.303
Optode 3	0.577	28	0.569
Optode 4	-0.057	23	0.955
Optode 5	-0.955	22	0.350
Optode 6	-1.177	23	0.251
Optode 7	-0.172	17	0.866
Optode 8	-0.965	15	0.350
Optode 9	1.354	14	0.197
Optode 10	0.327	14	0.749
Optode 11	1.156	18	0.263
Optode 12	1.071	19	0.297
Optode 13	-0.617	18	0.545
Optode 14	1.078	19	0.294
Optode 15	-0.023	29	0.982
Optode 16	1.333	22	0.196
Type = SILENT			

Table 38. One-sample t-test for HbR in Random Both-Match condition

	Test Value = 0		Sig. (2-tailed)
	t	df	
Optode 2	-0.72	24	0.478
Optode 3	0.56	27	0.580
Optode 4	0.333	22	0.742
Optode 5	0.278	22	0.784
Optode 6	-1.182	22	0.250
Optode 7	-0.529	16	0.604
Optode 8	0.197	13	0.847
Optode 9	1.472	13	0.165
Optode 10	1.063	12	0.309
Optode 11	0.694	17	0.497
Optode 12	-1.001	18	0.330
Optode 13	0.367	17	0.718
Optode 14	0.756	15	0.461
Optode 15	0.37	28	0.714
Optode 16	0.89	22	0.383

Type = BOTH Match = MATCH

Table 39. One-sample t-test for HbR in Random Both-Mismatch condition

	Test Value = 0		Sig. (2-tailed)
	t	df	
Optode 2	0.108	24	0.915
Optode 3	1.062	27	0.298
Optode 4	-0.581	23	0.567
Optode 5	0.407	22	0.688
Optode 6	-0.697	23	0.492
Optode 7	0.482	15	0.637
Optode 8	0.659	14	0.521
Optode 9	1.599	13	0.134
Optode 10	1.773	13	0.100
Optode 11	1.46	18	0.161
Optode 12	1.672	16	0.114
Optode 13	1.429	18	0.170
Optode 14	1.915	12	0.080
Optode 15	1.63	28	0.114
Optode 16	1.048	21	0.307

Type = BOTH Match = MISMATCH

Table 40. One-sample t-test for HbR in Random Other-Match condition

	Test Value = 0		Sig. (2-tailed)
	t	df	
Optode 2	-0.949	21	0.353
Optode 3	-0.24	25	0.812
Optode 4	-0.85	20	0.405
Optode 5	-0.37	19	0.716
Optode 6	-0.297	21	0.769
Optode 7	-1.174	14	0.260
Optode 8	0.378	12	0.712
Optode 9	0.052	11	0.960
Optode 10	0.315	11	0.759
Optode 11	0.396	16	0.697
Optode 12	0.4	17	0.694
Optode 13	-0.312	16	0.759
Optode 14	0.648	17	0.526
Optode 15	0.067	26	0.947
Optode 16	1.346	19	0.194

Type = OTHER Match = MATCH

Table 41. One-sample t-test for HbR in Random Other-Mismatch condition

	Test Value = 0		Sig. (2-tailed)
	t	df	
Optode 2	-0.414	24	0.683
Optode 3	0.223	27	0.825
Optode 4	-0.085	23	0.933
Optode 5	-0.618	22	0.543
Optode 6	-1.644	23	0.114
Optode 7	-0.269	15	0.791
Optode 8	-0.024	14	0.981
Optode 9	0.808	13	0.434
Optode 10	0.689	13	0.503
Optode 11	0.634	18	0.534
Optode 12	1.11	18	0.282
Optode 13	0.023	18	0.982
Optode 14	1.567	17	0.136
Optode 15	0.618	28	0.542
Optode 16	1.339	21	0.195

Type = OTHER Match = MISMATCH

Table 42. One-sample t-test for HbR in Random Self-Match condition

	Test Value = 0		Sig. (2-tailed)
	t	df	
Optode 2	-0.241	19	0.812
Optode 3	-0.448	23	0.658
Optode 4	-0.496	19	0.626
Optode 5	-0.609	20	0.549
Optode 6	-1.698	18	0.107
Optode 7	-0.863	16	0.401
Optode 8	0.452	13	0.658
Optode 9	0.229	13	0.822
Optode 10	1.311	12	0.214
Optode 11	1.991	13	0.068
Optode 12	0.167	14	0.869
Optode 13	2.004	10	0.073
Optode 14	-0.349	16	0.732
Optode 15	0.619	24	0.542
Optode 16	0.908	17	0.377

Type = SELF Match = MATCH

Table 43. One-sample t-test for HbR in Random Self-Mismatch condition


	Test Value = 0		Sig. (2-tailed)
	t	df	
Optode 2	-0.27	24	0.789
Optode 3	0.631	28	0.533
Optode 4	0.145	23	0.886
Optode 5	1.28	22	0.214
Optode 6	-0.561	23	0.581
Optode 7	0.347	16	0.733
Optode 8	0.239	14	0.814
Optode 9	1.05	13	0.313
Optode 10	0.987	13	0.342
Optode 11	0.228	17	0.822
Optode 12	0.213	19	0.834
Optode 13	1.13	18	0.273
Optode 14	1.416	19	0.173
Optode 15	0.591	29	0.559
Optode 16	1.879	20	0.075

Type = SELF Match = MISMATCH



APPENDIX C - ETHICAL APPROVAL FORM

UYGULAMALI ETİK ARASTIRMA MERKEZİ
APPLIED ETHICS RESEARCH CENTER

 ORTA DOĞU TEKNİK ÜNİVERSİTESİ
MIDDLE EAST TECHNICAL UNIVERSITY

DUNLUPINAR BULVARI 06800
ÇANKAYA ANKARA/TURKEY
T: +90 312 210 22 91
F: +90 312 210 79 59
ueam@metu.edu.tr
www.ueam.metu.edu.tr

Sayı: 28620816/

06 Şubat 2014

Gönderilen: Y.Doç.Dr. Murat Perit Çakır
Bilişsel Bilimler

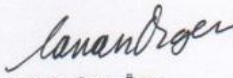
Gönderen : Prof. Dr. Canan Özgen
Uygulamalı Etik Araştırma Merkezi Başkanı



İlgi : Etik Onayı.

Etik Kurul izni için sunmuş olduğunuz " Sosyal Etkileşim Süreçlerinin Sinirsel İzdüşümlerinin Çok Kipli İncelemesi." isimli Tübitak projesi başvurunuz ODTÜ "İnsan Araştırmaları Etik Komitesi" tarafından uygun görülerek etik onayı verilmiştir.

Bilgilerinize saygılarımla sunarım.



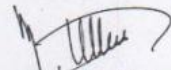
Prof. Dr. Canan Özgen
UEAM Başkanı



Prof. Dr. Canan Sümer
Etik Komitesi Üyesi



Prof. Dr. Aydan Balamir
Etik Komitesi Üyesi



Prof. Dr. Mehmet Utku
Etik Komitesi Üyesi

KATILAMADI

Prof. Dr. Ayhan Sol
Etik Komitesi Üyesi



APPENDIX D - CURRICULUM VITAE

PERSONAL INFORMATION

Surname, Name: İşbilir, Erdinç

Nationality: Turkish

Date and Place of Birth: 27.01.1985 Karabük, TÜRKİYE

email: erdincisbilir@gmail.com

EDUCATION

Degree	Institution	Year of Graduation
PhD	Middle East Technical University	2016
MS	Middle East Technical University	2010
BS	Middle East Technical University	2008

WORK EXPERIENCE

Year	Place	Enrollment
2008-2016	Middle East Technical University	Research Assistant

SCHOLARSHIP AND AWARDS

TÜBİTAK (The Scientific and Technological Research Council of Turkey)
National Graduate Scholarship

September, 2008 – June, 2010, 300-TL/month - June 2010

PROGRAM(S) / SKILL(S)

MATLAB, SPSS, MS Office Programs

FOREIGN LANGUAGES

Native Turkish, Advanced English

TOEFL IBT 2011 Score: 111/120

Reading	Listening	Speaking	Writing
29	28	23	28

TOEFL IBT 2014 Score: 109/120

Reading	Listening	Speaking	Writing
28	29	24	28

PUBLICATION LIST

Conferences

Cognitive Science'11 Participant. Boston, MA, USA.

ESERA'11 Isbilir, E., Ertepinar, H., Cakiroglu, J. (2011). Variation of pre-service science teachers' argumentation levels across socio-scientific issues. Paper presented at European Science Education Research Association (ESERA), Lyon, FRANCE.

NARST'11 Isbilir, E., Ertepinar, H., & Cakiroglu, J. (2011). Relationship between pre-service elementary science teachers' argumentation quality about climate change and epistemic belief levels. Paper presented at National Association for Research in Science Teaching (NARST), Orlando, FL.

CogInfoCom'12 Gokcay, D., Isbilir, E., & Yildirim, G. (2012). Predicting the sentiment in sentences based on words: An exploratory study in ANEW and ANET. Paper accepted for IEEE Internal Conference on Cognitive Infocommunications, Kosice, Slovakia.

Journal Article(s)

Isbilir, E., & Cakir, M. P. (2016). An fNIR hyperscanning study on brain-brain interactions of a dyad during a joint sentence reading task. *International Journal of Experimental and Clinical Anatomy*. doi: 10.2399/ana.16.001s.

Isbilir, E., Cakiroglu, J., & Ertepinar, H. (2014). Pre-service science teachers' witten argumentation qualities: From the perspectives of socio-scientific issues, epistemic belief levels and online discussion environment.

Eurasia Journal of Science and Technology Education. doi:
10.12973/eurasia.2014.1110a

Poster Presentation(s)

Isbilir, E., Cakir, M. P., Cummins, F., & Ayaz, H. (2016). *Investigating brain-brain interactions of a dyad using fNIR hyperscanning during joint sentence reading task.* Poster presented at International Symposium on Brain and Cognitive Science, Yeditepe, İstanbul.

Isbilir, E., & Cakir, M. P. (2014). *Brain-brain coupling: fNIRS hyperscanning of pairs in a sentence repetition task.* Poster presented at German-Turkish Workshop on Cognitive Science, Ankara.

Summer School(s)

Summer School NN2012: Neural Networks in classification, regression and data mining. Porto, PORTUGAL

2nd International Summer School and Workshop on Brain Dynamics: Connectivity & Cognition, 2013. Turunc, Marmaris, TURKEY

3rd International Summer School and Workshop on Brain Dynamics: Connectivity & Cognition, 2014. Turunc, Marmaris, TURKEY



APPENDIX E - TEZ FOTOKOPİ İZİN FORMU

ENSTİTÜ

Fen Bilimleri Enstitüsü

Sosyal Bilimler Enstitüsü

Uygulamalı Matematik Enstitüsü

Enformatik Enstitüsü

Deniz Bilimleri Enstitüsü

YAZARIN

Soyadı : İŞBİLİR

Adı : Erdinç

Bölümü : Bilişsel Bilimler (COGS)

TEZİN ADI (İngilizce) : HYPERSCANNING OF BRAIN-TO-BRAIN INTERACTIONS IN THE PREFRONTAL CORTEX DURING A JOINT SENTENCE READING TASK: AN OPTICAL BRAIN IMAGING STUDY

TEZİN TÜRÜ : Yüksek Lisans

Doktora

1. Tezimin tamamı dünya çapında erişime açılsın ve kaynak gösterilmek şartıyla tezimin bir kısmı veya tamamının fotokopisi alınsın.
2. Tezimin tamamı yalnızca Orta Doğu Teknik Üniversitesi kullanıcılarının erişimine açılsın. (Bu seçenekle tezinizin fotokopisi ya da elektronik kopyası Kütüphane aracılığı ile ODTÜ dışına dağıtılmayacaktır.)
3. Tezim bir (1) yıl süreyle erişime kapalı olsun. (Bu seçenekle tezinizin fotokopisi ya da elektronik kopyası Kütüphane aracılığı ile ODTÜ dışına dağıtılmayacaktır.)

Yazarın imzası

Tarih